University of Kentucky
UKnowledge

Theses and Dissertations--Pharmacy | College of Pharmacy

2015

ROLES OF ABCG5 ABCG8 CHOLESTEROL TRANSPORTER IN LIPID HOMEOSTASIS

Yuhuan Wang
University of Kentucky, yuhuan.wangpharm@gmail.com

Click here to let us know how access to this document benefits you.

Recommended Citation
Wang, Yuhuan, "ROLES OF ABCG5 ABCG8 CHOLESTEROL TRANSPORTER IN LIPID HOMEOSTASIS" (2015). *Theses and Dissertations--Pharmacy*. 50.
https://uknowledge.uky.edu/pharmacy_etds/50

This Doctoral Dissertation is brought to you for free and open access by the College of Pharmacy at UKnowledge. It has been accepted for inclusion in Theses and Dissertations--Pharmacy by an authorized administrator of UKnowledge. For more information, please contact UKnowledge@lsv.uky.edu.

STUDENT AGREEMENT:

I represent that my thesis or dissertation and abstract are my original work. Proper attribution has been given to all outside sources. I understand that I am solely responsible for obtaining any needed copyright permissions. I have obtained needed written permission statement(s) from the owner(s) of each third-party copyrighted matter to be included in my work, allowing electronic distribution (if such use is not permitted by the fair use doctrine) which will be submitted to UKnowledge as Additional File.

I hereby grant to The University of Kentucky and its agents the irrevocable, non-exclusive, and royalty-free license to archive and make accessible my work in whole or in part in all forms of media, now or hereafter known. I agree that the document mentioned above may be made available immediately for worldwide access unless an embargo applies.

I retain all other ownership rights to the copyright of my work. I also retain the right to use in future works (such as articles or books) all or part of my work. I understand that I am free to register the copyright to my work.

REVIEW, APPROVAL AND ACCEPTANCE

The document mentioned above has been reviewed and accepted by the student's advisor, on behalf of the advisory committee, and by the Director of Graduate Studies (DGS), on behalf of the program; we verify that this is the final, approved version of the student's thesis including all changes required by the advisory committee. The undersigned agree to abide by the statements above.

Yuhuan Wang, Student

Dr. Gregory A. Graf, Major Professor

Dr. Jim Pauly, Director of Graduate Studies

ROLES OF ABCG5 ABCG8 CHOLESTEROL TRANSPORTER IN LIPID HOMEOSTASIS

DISSERTATION

A dissertation submitted in partial fulfillment of the requirements for the degree of Doctor of Philosophy in the Graduate School at the University of Kentucky

By

Yuhuan Wang

Lexington, Kentucky

Director: Dr. Gregory A. Graf, Associate Professor,

Pharmaceutical Sciences

Lexington, KY

2015

Copyright © Yuhuan Wang 2015

ABSTRACT OF DISSERTATION

ROLES OF ABCG5 ABCG8 CHOLESTEROL TRANSPORTER IN LIPID HOMEOSTASIS

The ABCG5 ABCG8 (G5G8) sterol transporter promotes cholesterol secretion into bile and opposes dietary sterol absorption in the small intestine. An emerging body of literature suggests that G5G8 links sterol flux to various risk factors for metabolic syndrome (MetS) and nonalcoholic fatty liver disease (NAFLD). Therapeutic approaches that accelerate G5G8 activity may augment reverse cholesterol transport (RCT) and provide beneficial effects in the prevention and treatment of cardiovascular and liver disease.

Mice lacking leptin (*ob/ob*) or its receptor (*db/db*) are obese, insulin resistant in part due to the reduced levels of hepatic G5G8 and biliary cholesterol. The underlying mechanisms responsible for the reduced G5G8 protein expression in these mice may provide a clue to the drug development for this target. My studies show that neither acute leptin replacement nor liver-specific deletion of leptin receptor alters G5G8 abundance or biliary cholesterol. Similarly, hepatic vagotomy has no effect on G5G8 expression. Conversely, expression of the ER chaperone, GRP78, rescues G5G8 in *db/db* mice.

Previous studies suggest an interdependent relationship between liver and intestine for cholesterol elimination. A combination therapy that increases G5G8-mediated biliary cholesterol secretion and simultaneously reduces intestinal absorption is likely to act additively in cholesterol elimination. My studies show that treatment with ursodiol (Urso) increases hepatic G5G8 protein and both biliary and fecal sterols in a dose-dependent manner. Ezetimibe (EZ), a potent inhibitor of intestinal cholesterol absorption, produces an additive and dose-dependent increase in fecal sterol excretion in the presence of Urso. However, the stimulatory effects of both Urso and Urso-EZ are not G5G8-dependent.

Beyond increasing G5G8 protein expression and biliary cholesterol secretion, my studies also show that Urso stimulates ileal FGF15 expression in mice. Our data of the stimulated ileal FGF15 expression in LIRKO and reduced hepatic G5G8 protein levels in Atsb KO mice both indicate the previous unrecognized role of FGF15/19 in the regulation of G5G8 and its activity. Indeed, this is subsequently confirmed by our results from the direct test of recombinant human FGF19 on G5G8. Thus, FGF15/19 may provide an alternative strategy in drug development to target G5G8 activity and accelerate cholesterol elimination.

KEYWORDS: Reverse cholesterol transport, G5G8, GRP78, Ursodiol, Ezetimibe, FGF15/19

Yuhuan Wang
Student's Signature

August 19th, 2015
Date

ROLES OF ABCG5 ABCG8 CHOLESTEROL TRANSPORTER IN LIPID HOMEOSTASIS

By

Yuhuan Wang

Gregory A. Graf, Ph.D.
Director of Dissertation

Jim Pauly, Ph.D.
Director of Graduate Studies

August 19th, 2015
Date

ACKNOWLEDMENTS

First and foremost, I would like to thank my mentor Dr. Gregory A. Graf for his limitless support and encouragement. I am deeply grateful to him for his patient guidance, invaluable feedback, and insightful advice that inspired me to do scientific research and complete my projects. I am also thankful to him for helping me improve my scientific writing, communication and presentation skills that will be very instrumental for my future career development.

I sincerely thank my committee members, Dr. Mary Vore, Dr. Deneys R. van der Westhuyzen, Dr. Markos Leggas, and Dr. Penni Black, who have provided helpful suggestions and feedbacks that accelerated the progress of my projects.

I would like to thank all my current and previous lab members for their help, suggestions, and support.

Lastly but not least, I would like to thank my loving boyfriend Xiaoxi Liu, for sharing the happiest moments in my life, and for his love, support and accompany over the most difficult times in my career. I also thank my family and friends for their limitless support, especially my beloved grandfather who was always my great supporter. But unfortunately he couldn't make to see my graduation. May he rest in peace and love.

TABLE OF CONTENTS

LIST OF FIGURES

CHAPTER 1: INTRODUCTION

The metabolic syndrome (MetS) is a constellation of interrelated risk factors including obesity, atherogenic dyslipidemia, and elevated blood glucose and pressure with insulin resistance as the central source of pathogenesis. This symptom identifies individuals at an increased risk for developing type II diabetes and cardiovascular disease (CVD), the number one cause of global mortality. Patients with MetS have 50-60% higher risk for CVD than those without [1]. Thus, MetS is an important risk factor for the incidence and mortality of CVD.

MetS has deleterious effects on many organs, the liver being one of them. There is increased evidence that NAFLD is now considered the hepatic manifestation of MetS and has been identified as a common feature in patients with the MetS. NAFLD involves a spectrum of liver-related disorders that range from simple steatosis to steatohepatitis (NASH), fibrosis, and cirrhosis. It is the most common liver disease that affects 20%-30% of the US population and hence is increasingly recognized as a major contributor to the burden of chronic liver disease world-wide. MetS and NAFLD appear to have a common pathogenesis, arising from insulin resistance and abdominal obesity. Treatment of MetS may have a significant impact on progression of NAFLD, and therapeutic approaches treating the underlying risk factors of MetS appear to be valid options in treating NAFLD/NASH.

Given the progressively increasing prevalence and incidence of MetS and NAFLD, such conditions have gained worldwide attention and become major public health problems that are approaching epidemic proportions globally. The general lack of knowledge of pathogenesis prevents us from refining the most efficient therapies for individuals with MetS and NAFLD. The major goal of clinical management is to reduce the risks for CVD. The prime emphasis is given to the effective lifestyle interventions. If lifestyle change is not sufficient, pharmacological therapies are incorporated to the regimen. For example, statins and ezetimibe (EZ) have been used to target cholesterol synthesis and absorption, respectively, to reduce plasma low-density lipoprotein cholesterol (LDL-C) and lower the risk of CVD. However, an emerging body of work suggests that the flux of cholesterol through lipoproteins is more relevant to CVD than their absolute levels in plasma. Consequently, there has been intensely increased interest in strategies aimed at enhancing sterol flux from peripheral tissues to liver for ultimate excretion into feces, a process termed reverse cholesterol transport (RCT).

A substantial amount of work has been devoted to the conceptual approaches to augment RCT by improving cellular cholesterol efflux from peripheral cells, enhancing the functionality of circulating high-density lipoprotein (HDL), and increasing hepatic uptake of returned cholesterol. Relatively little effort has been geared at developing therapeutic approaches to target the final step of RCT.

Recent studies suggest that cholesterol taken up by hepatocytes is secreted into bile via the apical membrane sterol transporters ABCG5 and ABCG8 (G5G8), which form a functional heterodimeric complex that ties the link of sterol flux to metabolic disease [2-4]. The goal of this dissertation thesis is to understand the mechanisms responsible for the post-transcriptional regulation of G5G8 in vivo such that appropriate therapeutics could be employed to accelerate cholesterol elimination in the treatment of liver and cardiovascular disease.

Overview of the metabolic syndrome (MetS) and its hepatic manifestation: nonalcoholic fatty liver disease (NAFLD)

The clustering of several metabolic and pathophysiological cardiovascular risk factors (e.g., insulin resistance, abdominal obesity, dyslipidemia, impaired glucose tolerance, hypertension) was firstly discussed by Dr. Reaven in his Banting lecture in 1998 [5]. He named this clustering Syndrome X and recognized it as a multidimensional risk factor for CVD. Since then, this clinical symptom has been given different names (e.g., insulin resistance syndrome, metabolic syndrome X). It is now widely referred to as MetS in clinical practice.

The prevalence of MetS ranges largely from less than 10% to 84%, depending on the region, composition (e.g., age, sex, and race) of the population studied, and the definition and criteria of the syndrome used [6, 7]. But in general, the International Diabetes Federation (IDF) estimates that approximately 25% of the world's adult population has MetS [8]. The increasing prevalence of MetS is also

associated with the substantial progression of diabetes and CVD. Thus, MetS has received a lot of focused attention as a major public health concern.

Components of metabolic syndrome: underlying and metabolic risk factors

The MetS encompasses a group of interrelated risk factors that together confers an increased risk of type II diabetes and CVD. The components of MetS include both underlying and metabolic risk factors [9, 10]. The predominant underlying risk factors, which provoke the metabolic risk factors, are thought to be abdominal obesity and insulin resistance [5, 11-14]. The major metabolic risk factors are mostly widely recognized as atherogenic dyslipidemia, raised plasma glucose, and hypertension [9].

Underlying risk factors: abdominal obesity and insulin resistance

The enormous scope of epidemiological research has shed light on the positive relationship between obesity and MetS. This is largely based on the possible ability of obesity to engender insulin resistance. One theory postulated by Reaven and others holds that insulin resistance is the core cause of MetS. Hence, this symptom was also widely known as insulin resistance syndrome. However, many details of the mechanisms, by which obesity causes systemic insulin resistance, have not been adequately elucidated. There is also an explosive increase in evidence supporting that insulin resistance is an etiological aspect of

obesity. Therefore, the unraveled cause-and-effect relationship between obesity and insulin resistance renders both of them the underlying risk factors for MetS.

Abdominal obesity

The National Cholesterol Education Program's Adult Treatment Panel III report (ATP III) considered the "obesity epidemic" as the driving force that underlies the rising prevalence of MetS and defined MetS as a clustering of metabolic complications of obesity, especially abdominal obesity [14-17]. This statement needs to be in agreement with the insulin resistance theory. Abdominal obesity (or central obesity, upper-body obesity) is the form of obesity most likely to be associated with MetS and contribute to the increased risk of type II diabetes and CVD [17-21]. It presents as increased waist circumference in clinical practice. The ATP III defined the thresholds of waist circumference for the identification of MetS to be 102 cm for men and 88 cm for women, respectively [15].

The abdominal obesity strongly correlates with insulin resistance. This positive correlation is largely due to the dysfunctional adipose tissues. However, the underlying mechanisms about fat and insulin resistance in abdominal obesity have not been sufficiently articulated. One theory is that the excess upper-body fat releases elevated levels of nonesterified fatty acids (NEFA) [22]. The acute exposure to unusual high levels of NEFA overloads liver and skeletal muscles with lipids [23-25]. This ectopic lipid accumulation in sites other than adipose

tissue seemingly supports abdominal obesity as a causal factor for developing insulin resistance and increased risk of MetS.

The adipocyte is now recognized as a secretory cell that has a major endocrine function [26, 27]. The adipokine is a collective name given to various peptide hormones and protein factors including leptin, adiponectin, tumor necrosis factor-alpha (TNFα), interleukin-6 (IL-6), C-reactive protein (CRP), plasminogen activator inhibitor-1 (PAI-1), and others that are secreted or synthesized by the adipocyte [28-31]. An alternative hypothesized mechanism is that in abdominal obesity, the abnormal production of several adipokines by the intra-abdominal adipocytes may exert harmful effects to insulin sensitivity and modify risks for MetS and CVD. The abnormalities may include increased production of TNFα, IL-6, CRP, PAI-1, and at the same time reduced adiponectin levels [32-34].

Insulin resistance

Insulin is a critical hormonal regulator of glucose and lipid homeostasis among the major insulin-responsive organs including liver, fat, and muscle. It binds to and activates the insulin receptor tyrosine kinase, which in turn phosphorylates insulin receptor substrate (IRS) proteins (Irs1 and 2) and initiates two branches of insulin signaling events [35]. One is the activation of phosphatidylinositol 3-kinase (PI3K), which mediates insulin's metabolic effects. The other one is the activation of mitogen activated protein (MAP) kinase, which is primarily associated with the mitogenic effects of insulin.

The action of insulin to reduce plasma glucose results from the suppression of gluconeogenesis in liver and the increase of glucose uptake into fat and muscle [36, 37]. The phosphorylation of forkhead box protein O1 (FOXO1), a transcription factor that mediates insulin actions through PI3K pathway, diminishes gluconeogenesis [36]. The action of insulin to promote TG storage is derived from multiple mechanisms. In liver, insulin activates the sterol regulatory element binding protein (SREBP)-1c, a transcription factor which enhances the transcription of genes involved in fatty acid and TG synthesis (lipogenesis) [37-40]. The newly synthesized TGs are secreted from liver via very low density lipoprotein (VLDL), a lipoprotein that delivers TGs to fat for storage and muscle for energy expenditure. In fat, insulin stimulates the differentiation of preadipocytes to adipocytes. In mature adipocytes, insulin facilitates the uptake of VLDL-derived fatty acids, promotes lipogenesis, and inhibits lipolysis [41].

Insulin resistance usually refers to a state of reduced responsiveness to the action of insulin on glucose uptake, metabolism, or storage. It is not established that insulin resistance per se plays a causal role in MetS due to the fact that it is difficult to identify a unique role of insulin resistance from a complex interaction of many factors. But it is well accepted that insulin resistance in obesity is the underlying cause for MetS [42]. Although insulin resistance is pronounced in obesity, MetS, and type II diabetes, it is not to say that all of the insulin actions

are diminished in individuals with such conditions. For example, while insulin-stimulated glucose transport and metabolism are decreased in fat and muscle and the suppression of gluconeogenesis in liver is impaired, hepatic lipogenesis is still sensitive to insulin and is driven to excess by the commentary hyperinsulinemia [37]. To dissect the role of insulin resistance in the molecular and pathophysiological basis of MetS, Kahn and colleagues generated the liver-specific insulin receptor knockout (LIKRO) micel, which initiated a discussion about the pathogenic paradox in selective versus total insulin resistance in liver.

Selective insulin resistance is the typical insulin resistance defined clinically in terms of the failure of insulin to maintain glucose homeostasis. However, insulin continues to activate lipogenesis, producing a combination of hyperglycemia and hypertriglyceridemia. These are characteristic features of humans and mice with MetS and type II diabetes. The extensively used mouse models of MetS and insulin-resistant type II diabetes are *ob/ob* and *db/db* mice, due to the lack of leptin or its receptor, respectively. Both strains of mice have increased food intake attributed to the deficiency of leptin, a neutral hunger suppressant. They are massively obese and hyperphagic and exhibit a triad of hyperglycemia, hyperinsulinemia, and hypertriglyceridemia [43, 44].

Total hepatic insulin resistance refers to a defect in hepatic insulin signaling due to the ablation of the hepatic insulin receptor gene. It implies that all processes regulated by hepatic insulin signaling become resistance to insulin in parallel

with glucose metabolism. Paradoxically, despite hyperglycemia, neither humans with insulin receptor mutations nor LIRKO mice manifest hypertriglyceridemia or hepatic steatosis [45-48]. This is largely due to that insulin fails to stimulate lipogenesis. Based on this paradox, Biddinger and colleagues concluded that hepatic steatosis and hypertriglyceridemia are not directly attributed to insulin resistance, and should be considered as distinct features contributing to the pathogenesis of MetS [49]. However, due to the complex interplay among insulin resistance, steatosis, and hypertriglyceridemia, it remains uncertain whether this argument is true.

Another paradox is also associated with the two stages of insulin resistance. The complete hepatic insulin resistance in LIRKO mice produces increased biliary cholesterol secretion and cholesterol gallstones. This links insulin resistance to biliary lipid metabolism. Various features of the selective insulin resistant *ob/ob* and *db/db* mice also potentiate the risk of gallstone formation. However, they manifest paradoxically low biliary cholesterol saturation. This puzzle will be particularly addressed in the Chapter 2 of this dissertation.

Metabolic risk factors

As stated earlier, the major metabolic risk factors comprise atherogenic dyslipidemia, elevated plasma glucose, and hypertension. Each of them conveys increased risk of MetS even when only marginally abnormal. Atherogenic dyslipidemia consists of a triad of lipoprotein abnormalities implicated as

independent atherogenic factors. These abnormalities include increased plasma concentrations of TG and small, dense LDL particles, and decreased high-density lipoprotein cholesterol (HDL-C) [50]. The LDL particle size is not corrected with the LDL-C, but it shows striking correlations with the TG and HDL-C concentrations [51]. Thus, the TG/HDL-C ratio is beneficial for assessing the presence of small LDL [51]. As a characteristic feature of obesity and insulin resistance, atherogenic dyslipidemia has emerged as a critical risk factor for MetS and CVD. Other well established metabolic risk factors are elevated plasma glucose and hypertension. Multiple mechanisms have been postulated to explain how increased plasma glucose may promote atherosclerosis, but none is particularly well established. Regardless, once MetS compounds type II diabetes, risk and incidence for CVD events increase further more.

Clinical outcomes of MetS

The major clinical outcome of MetS is CVD, the most dreaded complication of this disease [1, 52-55]. Reaven and others postulated that insulin resistance is the essential cause of MetS [5, 56]. Hence, insulin resistance syndrome was also commonly used to name the clustering of risk factors. The majority of people with MetS have insulin resistance. Insulin resistance and the compensatory hyperinsulinemia predispose to type II diabetes. Thus, individuals with MetS are also susceptible to type II diabetes, another major risk factor for CVD [57-59]. When type II diabetes emerges, CVD risk rises even more [60]. Beyond CVD and

type II diabetes, a variety of other conditions are notably present in individuals with MetS; one of them is NAFLD [61-65]. There is increased evidence that NAFLD is now considered the hepatic manifestation of MetS and has been identified as a common feature in patients with the MetS [63, 64]. Recent studies have indicated that NAFLD is also intensely associated with increased risk of CVD [66, 67].

Nonalcoholic fatty liver disease (NAFLD)

NAFLD involves a wide spectrum of fat-induced liver-related disorders that range from relatively benign simple steatosis to NASH with fibrosis and scarring, which can further progress to the devastating conditions like cirrhosis or eventually hepatocellular carcinoma (HCC) [68]. Steatosis is defined as the presence of fat in more than 5%-10% of liver weight. It is usually considered benign and reversible, but can progress to NASH. NASH, the most extreme stage of NAFLD, is distinguished from steatosis by the features including hepatocyte injury, inflammation, and fibrosis [68]. Between 10-29% of individuals diagnosed with NASH may develop cirrhosis within 10 years and 4-27% among them may develop HCC eventually [68]. NAFLD is a growing health problem with an incidence ranging from 17-33% and 5-17% for its more severe expression, NASH [69]. It is estimated that NAFLD/NASH will increase medical costs by 26% [70].

Available data from epidemiological, experimental, and clinical studies support a close association between NAFLD and MetS. For example, 90% of subjects with

NAFLD have at least one risk factor of MetS, and 33% of them have all the features of MetS. In 271 nondiabetic subjects, liver fat content is significantly increased in subjects with MetS as compared with those without the syndrome [71]. In a prospective observational study containing 4401 apparently healthy Japanese, participants diagnosed with MetS have 4 to 11 folds higher risk for future NAFLD [72]. Additionally, if NAFLD and MetS coexist, disease regression is less likely [72]. In another study containing 16,486 Taiwanese NAFLD patients, the presence of severe fatty liver is significantly correlated with the prevalence and degree of hypertension, abnormal TG and glucose metabolism, all of which are metabolic risk factors for MetS [73]. NAFLD ranging from steatosis to NASH might represent another characteristic feature of MetS. Accumulating data suggest that MetS and NAFLD seem to share common pathophysiological mechanisms, with abdominal obesity and insulin resistance as the key pathogenic factors.

Pathogenesis of NAFLD/NASH

The majority of NAFLD subjects are obese and insulin resistant. The regulation of glucose and lipid metabolism involves a complicated interplay among the major metabolic tissues including liver, fat, and muscle. Obesity, insulin resistance, inflammation, genetic factors, over-nutrients, and unhealthy lifestyle may all paly essential roles in the development of NAFLD. While our knowledge

of the pathogenesis of NAFLD has extensively increased over the past two decades, many uncertainties remain to be intensely investigated.

The central mechanisms responsible for NAFLD similar to MetS are thought to be abdominal obesity and insulin resistance. The typical site for lipid storage is the subcutaneous fat. However, when lipids are accumulated to excess in these fat depots, they are likely to be redistributed to other sites for deposit including abdominal fat depot and insulin-sensitive tissues such as liver and muscle [74]. When the acquisition of lipids within in liver exceeds the normal lipid turnover, hepatic steatosis arises. In the state of insulin resistance, principally in the context of abdominal obesity and MetS, the possible sources for the pathophysiology of hepatic steatosis may include: (1) increased influx of NEFA to liver; (2) increased de novo lipogenesis in liver; (3) reduced rate of β-oxidation; and (4) reduced TG export from liver in the form of VLDL. The increased influx of NEFA (60%) is considered as the largest contributor to steatosis in individuals with NAFLD [75]. This is predominantly due to the dietary intake of fat and increased lipolysis within abdominal fat. Approximately 25% of the TG accumulated in the liver of NAFLD individuals is derived from the de novo lipogenesis. This is mainly due to the increased activity of SREBP1c and carbohydrate response element-binding protein (ChREBP), both of which regulate the expression of genes involved in the lipogenic pathway. TGs are re-packaged within VLDL and exported from liver. Each VLDL particle contains only one molecule of apolipoprotein B (apoB), the

synthesis of which is a rate-limiting step in VLDL production. Under normal condition, insulin targets apoB for intracellular degradation, whereas in the state of insulin resistance, the compensated hyperinsulinemia may alter apoB synthesis or promote its degradation and thereby decreasing TG export in VLDL [76, 77].

The pathophysiological basis for the transition from steatosis to NASH is multifactorial and not fully understood. A "two-hit" theory was firstly postulated by Day to explain the NASH pathogenesis [78]. The disequilibrium between fat acquisition and removal within hepatocytes causing simple steatosis comprises the "first hit", and the susceptibility of a fatty liver to a separate injury ("second hit") results in inflammation, fibrosis, and apoptosis [78]. A variety of factors may be considered the "second hit" and contribute to the pathogenesis of NASH, such as oxidative stress, inflammatory cytokine and adipokine alteration, mitochondrial dysfunction, fatty acid lipotoxicity, innate immunity, and many others [78-84].

New suspects in the pathogenesis of NAFLD/NASH: Endoplasmic reticulum (ER) stress

Recently, accumulating data have indicated that the endoplasmic reticulum (ER) stress plays a crucial role in both the development of steatosis and the progression to NASH [85, 86]. ER is a central hub for the synthesis and post-translational modification of secretory and membrane proteins, lipid

biosynthesis, oxidative metabolism, and intracellular calcium homeostasis. Newly synthesized proteins in the ER lumen require the assistance of chaperone proteins to undergo post-translational modifications such as N-glycosylation and disulfide bond formation. The 78-kD glucose-regulated/binding immunoglobulin protein (GRP78) is one of the major ER chaperones particularly essential to the regulation of ER function due to its role in protein folding and assembly, targeting aberrant proteins for degradation, and controlling activation of ER stress sensors. When there are metabolic disturbances that compromise ER function, such as excessive protein synthesis, accumulation of unfolded or misfolded proteins, calcium depletion, or perturbation of redox status, the whole organelle enters into a state called "ER stress".

As a recovery and adaptation mechanism, the ER responds to ER stress by activating a series of signaling pathways, collectively named the unfolded protein response (UPR), to adjust to the protein-folding demand and promote cell survival and adaptation [87]. Three distinct stress sensors including protein kinase RNA-like endoplasmic reticulum kinase (PERK), inositol-requiring enzyme 1 (IRE1), and activating transcription factor 6 (ATF6) are well characterized to monitor the imbalance between protein load and folding capacity within ER (Fig 1.1) [88-90]. Under the normal physiological condition, GRP78 binds to the luminal domains of the three transducers remaining them in

the inactive state. Upon stress conditions, GRP78 is displaced from PERK, IRE1, and ATF6 resulting in their activation.

Upon dissociation from GRP78, PERK oligomerizes, autophosphorylates, and phosphorylates eukaryotic initiation factor 2 alpha (eIF2α) [89]. Phosphorylated eIF2α leads to a global repression of mRNA translation and reduced flux of protein entering ER to alleviated ER stress [91]. An exception is the activating transcription factor 4 (ATF4). It requires eIF2α phosphorylation to enhance its mRNA translation to regulate the downstream UPR target genes such as C/EBP homologous protein (CHOP) [92]. Upon ER stress conditions, IRE1 dimerizes and autophosphorylates to be activated. Activated IRE1 results in splicing of X-box binding protein 1 (XBP1) mRNA [93, 94]. Spliced XBP1 selectively upregulates chaperone proteins such as GRP78 and GRP94 to cope with increased protein-folding demand. ATF6 is a membrane bound transcription factor. Dissociation of GRP78 from ATF6 leads to its translocation to Golgi where it is cleaved by site 1 and site 2 proteases, generating a soluble form of ATF6 [95]. Upon entry to the nucleus, this processed form of ATF6 activates UPR target genes involved in protein folding and degradation. Postponed or inadequate UPR responses to ER stress may produce pathological consequences, including abnormal lipid accumulation, insulin resistance, inflammation, and apoptosis, all of which play key roles in the pathogenesis of NAFLD.

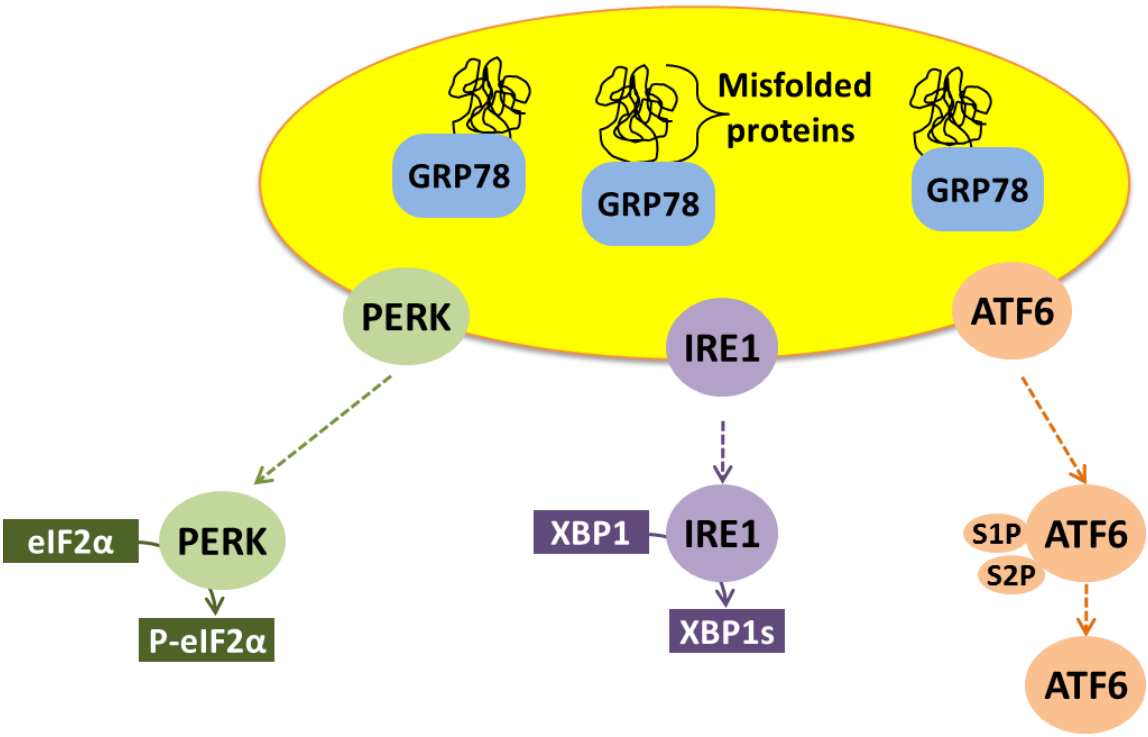

Figure 1.1 A diagram of the initiation of the UPR by unfolded or misfolded proteins. GRP78 releases from its binding state of PERK, IRE1, and ATF6 in response to the overwhelming accumulation of mal-folded proteins and triggers the UPR signaling. Dissociation of GRP78 from PERK results in the phosphorylation of eIF2α, which inhibits translation and leads to cell cycle arrest. The activated domain of IRE1 results in cleavage of XBP1, while activated ATF6 is transported to the Golgi, cleaved by site 1 and site 2 proteases to produce an active 50kDa form of ATF6. The cleaved XBP1 and the processed form of ATF6 selectively upregulate chaperone proteins to manage increased protein-folding demand.

The activation of ER stress was firstly described by Ozcan and colleagues in the livers of both diet-induced and genetic models of NAFLD in the setting of obesity [96]. In both models, phosphorylations of PERK and eIF2α as well as GRP78 expression were increased indicating activated UPR signaling [96]. Since then, these observations have been confirmed in other NAFLD/NASH animal models in the presence and absence of obesity [97-99]. Later, several UPR

components were reported to be induced in the livers of human subjects with NAFLD or NASH [100]. However, the precise contribution of ER stress to the development of NAFLD is not fully understood.

Hepatic steatosis, which is caused by the disequilibrium of lipid accumulation and removal as stated earlier, is the first step for the development of NAFLD. It is well accepted that a variety of components of the UPR signaling interfere with hepatic lipid metabolism by promoting lipogenesis and inhibiting VLDL production and secretion [101-108]. Hepatic lipogenesis is also dependent on the insulin-stimulated activation of SREBP1c despite the prevailing insulin resistance. Thus, ER stress can also indirectly promote hepatic TG accumulation by exacerbating insulin resistance. Several mechanisms are seemingly responsible for the effect of ER stress on hepatic insulin resistance. For example, Ozcan and colleagues have published data showing that ER stress promotes hepatic insulin resistance through IRE1α-mediated hyperactivation of c-Jun N-terminal kinase (JNK) and the serine phosphorylation of insulin receptor substrate-1 [96]. Additional support is derived from the PERK-mediated phosphorylation of FOXO [109]. Though further mounting evidence also indicates the impact of ER stress on insulin resistance, the exact contribution of ER stress to insulin resistance in NAFLD is still unclear. Other mechanisms by which ER stress potentiate NAFLD may include the production of reactive oxygen species (ROS), the activation of JNK, nuclear factor kappa-light-chain-

enhancer of activated B cells (NF-κB), and CHOP, which are actively involved in the inflammatory and apoptotic processes [110].

Ozcan and colleagues reported that chemical chaperones such as 4-Phenyl butyric acid (4-PBA) and tauroursodeoxycholic acid (TUDCA) alleviated ER stress both in vitro and in vivo. Administration of such chaperones to *ob*/*ob* mice alleviated ER stress, resulting in improved insulin sensitivity and glycemia as well as a resolution of steatosis [111]. Foufelle and colleagues reported that supplementation of chaperone protein GRP78, another approach to alleviate ER stress, also restored insulin sensitivity in *ob*/*ob* mice. Interestingly, the overexpression of GRP78 also inhibited SREBP1c activation, thereby reducing lipogenesis and improving the status of steatosis [112].

New suspects in the pathogenesis of NAFLD/NASH: Free cholesterol (FC)

The excess hepatic accumulation of lipids, particularly TG, as the key defect in NAFLD has been given the most intense investigation. However, two lipidomic studies have shown that apart from TGs, free cholesterol (FC) is also intensively accumulated in human NAFLD/NASH subjects [113, 114]. Thus, more efforts have been made to confirm this finding in different NAFLD/NASH models and to investigate the role of FC in the pathogenesis of NAFLD/NASH.

Cholesterol is a fundamental constituent of mammalian cell membranes and also serves as the fuel for the biogenesis of bile acids, vitamin D, and steroid

hormones. There are two mechanisms for the body to acquire a sufficient pool of cholesterol to maintain its normal function [115]. One is the intestinal absorption of dietary cholesterol by Niemann-Pick C1-like 1 (NPC1L1) transporter. Cholesterol is transported in the circulation predominantly in the form of cholesteryl ester (CE) carried by lipoproteins. Upon absorption, dietary cholesterol is transported from the intestine through the circulation within chylomicron (CM) and delivered to liver by CE-rich CM remnant (CMR) via endocytosis mediated by LDL receptor (LDLR) or LDLR related protein 1 (LRP-1) (Fig 1.2) [116]. However, in the context of NAFLD, the excess intake of dietary cholesterol may act synergistically with fat to facilitate the progression of NAFLD to NASH. For example, adding cholesterol to a high-fat (HF) diet in C57BL/6J mice leads to significantly more profound hepatosteatosis, inflammation, and fibrosis resembling human NASH [117]. Similarly, in LDLR deficient mice, adding cholesterol to a HF, high-sucrose diet exacerbates the development of insulin resistance and steatosis resulting in NASH [118].

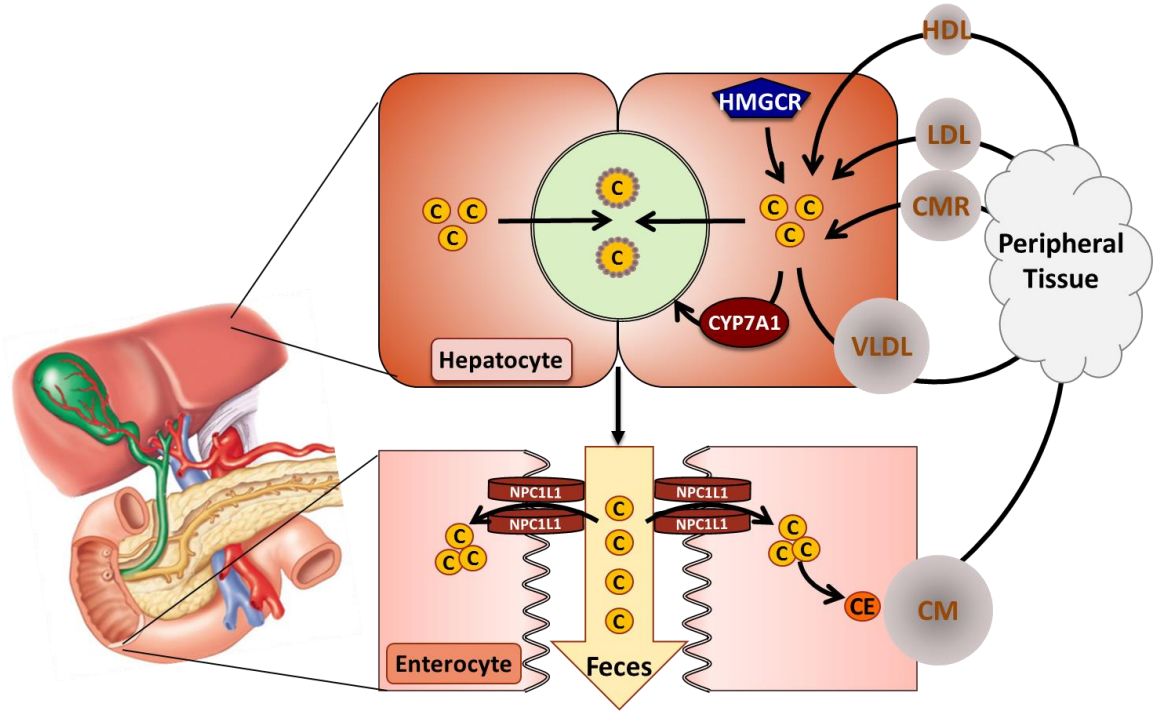

Figure 1.2 Overview of cholesterol metabolism. The body acquires cholesterol by two mechanisms including the intestinal absorption of dietary cholesterol and the de novo cholesterol biosynthesis. The liver is a central organ in maintaining cholesterol homeostasis by balancing de novo cholesterol synthesis and hepatic uptake of plasma lipoproteins from the circulation against bile acid synthesis and the excretion of hepatic cholesterol and bile acid excretion into bile. C, cholesterol; CE, cholesteryl ester; NPC1L1, Niemann-Pick C1-like 1 transporter; CM, chylomicron; CMR, chylomicron remnant; HMGCR, 3-hydroxy-3-methylglutary CoA reductase; VLDL, very low-density lipoprotein; LDL, low-density lipoprotein; HDL, high-density lipoprotein, CYP7A1, cholesterol 7alpha-hydroxylase.

The other way for the body to obtain cholesterol is through de novo cholesterol synthesis (Fig 1.2). It begins from acetyl-CoA and acetoacetyl-CoA, which are converted to 3-hydroxy-3-methylglutary CoA (HMG-CoA) by HMG-CoA synthase (HMGCS). The HMG-CoA reductase (HMGCR) subsequently catalyzes the irreversible and rate-limiting reaction by converting HMG-CoA to

mevalonate and is thus the target of the widely utilized cholesterol-lowing drugs collectively termed as the statins. Mevalonate is then converted to isopentenyl pyrophosphate (IPP), squalene, lanosterol, and eventually cholesterol.

The rate of cholesterol biosynthesis is relatively higher in liver, intestine, and adrenal glands. It is under tight transcriptional control via SREBP2 [39, 119]. SREBP cleavage-activating protein (SCAP), as a sterol sensor and escort protein, forms a protein complex with SREBP2. In response to deprivation of sterols, SCAP escorts SREBP2 from ER to Golgi where SREBP2 is processed into an active transcription factor that upregulates the expression of genes involved in cholesterol synthesis, e.g., HMGCR, and uptake, e.g., LDLR. Conversely, excess sterols accumulating in the ER membrane result in a conformational change of SCAP, which allows it to bind to the insulin-induced gene proteins (Insig1 or 2), the ER resident membrane proteins that prevent the SCAP/SREBP complex from migrating to the Golgi. Thus, HMGCR is rapidly degraded, resulting in the termination of cholesterol synthesis.

The liver is a central organ in maintaining cholesterol homeostasis by balancing de novo cholesterol synthesis and hepatic uptake of plasma lipoproteins from the circulation against bile acid synthesis and the excretion of hepatic cholesterol and bile acid into bile (Fig 1.2). Newly synthesized cholesterol in liver, as well as dietary cholesterol delivered to liver that exceeds the hepatic tolerance, is re-secreted to the circulation via VLDL. Secreted VLDL is converted to

intermediated IDL and further LDL through the hydrolysis action of endothelial cell-associated lipoprotein lipase (LPL). Cholesterol in the circulation and acquired from peripheral cells particularly macrophages can be returned to liver through HDL for biliary and fecal excretion, the whole process of which is widely known as reverse cholesterol transport (RCT) [120]. Ultimately, cholesterol is secreted into bile as FC or as bile salts following conversion to bile acids mediated by cholesterol 7alpha-hydroxylase, a rate-limiting enzyme encoded by *CYP7A1* [121-123].

The disruption of hepatic cholesterol homeostasis by excess FC accumulation has been recently appreciated as a possible player in the pathogenesis of NAFLD/NASH. For example, in a mouse model of Alström syndrome (*Alms1* mutant or *foz/foz* mice), an elevation in hepatic FC due to an increase in hepatic uptake and a decrease in biliary elimination is thought to play a contributing role in the development of NASH [124]. A recent human study also highlighted the emerging role of FC in the pathogenesis of NAFLD/NASH by determining the expression of SREBP2 and HMGCR in liver [114]. Both SREBP2 and HMGCR were overexpressed in subjects with NAFLD compared to those with normal liver histology. Furthermore, the expression of SREBP2 was much higher in subjects with NASH compared to those with simple steatosis, suggesting that the progressive increase in hepatic FC is positively associated with the induction of SREBP2 [114].

Based on the emerging role of excess FC in the pathogenesis of NAFLD/NASH, reducing the intracellular FC levels provides a new therapeutic target for the treatment of the disease. In the third chapter of this dissertation, a novel pharmacological strategy for the treatment of NAFLD/NASH was proposed and tested in vivo to promote the sterol flux into bile and eventually into feces for elimination

Clinical management of MetS and NAFLD

Given the progressively increasing prevalence and incidence of MetS and NAFLD, such conditions have gained worldwide attention and become major public health problems that are approaching epidemic proportions globally. Intense investigations are still needed to clarify the pathogenesis of MetS and NAFLD so as to establish effective treatments for both of them and ultimately reduce the risk and incidence of CVD.

The primary goal of clinical management in patients with MetS and NAFLD is to reduce the risk factors for CVD. The first-line intervention is directed toward mitigating the modifiable, underlying risk factors through lifestyle change [15]. For example, the weight reduction reinforced with regular exercise and diet modification decreases the effect of insulin resistance, lowers plasma cholesterol and TG, raises HDL-C, and reduces plasma glucose and pressure. If lifestyle change doesn't reach the expected outcome, pharmacological therapies are usually incorporated to the regimen.

Insulin resistance, as an underlying cause for MetS and NAFLD, carries increased risk of development of diabetes and CVD. Therefore, it as a target has caught the imagination of the pharmaceutical industry. Both Metformin and insulin sensitizer thiazolidinedione (STZ) have been approved for treatment of type II diabetes. They reduce insulin resistance and apparently modify several metabolic risk factors [125-129]. However, the heterogeneity of the studies conducted to evaluate their efficiency in insulin-resistant NAFLD patients prevents us from reaching firm conclusions about their effectiveness at reversing the disease and developing standard treatment guidelines [130]. Additionally, the clinical trials using these insulin sensitizers to prove reduction of CVD are lacking [15].

The current therapeutic strategies to reduce the risk factors of CVD are aimed primarily at lowering plasma LDL-C concentration by using lipid-lowering agents. Beyond lifestyle interventions and insulin sensitizers, the lipid-lowering drug therapies are also widely employed in the treatment of MetS and NAFLD.

Statins, which act as HMGCR inhibitors, are effective lipid-lowering agents. They reduce cholesterol synthesis, decrease the intracellular cholesterol pool, and stimulate the compensatory upregulation of LDLR to lower LDL-C. The beneficial effects of statins in lowering LDL-C appear to be particularly important for reducing risk of CVD in patients with MetS. Statins have also been used in small clinical trials to evaluate the efficacy in NAFLD/NASH [131, 132].

For example, in a small Japanese study including 31 patients with biopsy-proven NASH with dyslipidemia, the NASH-related metabolic parameters including fibrosis improved with the atorvastatin therapy in some patients. However, up to 25%of patients had progression of fibrosis over the 2-year period [131]. The efficacy of statins for the treatment of NAFLD/NASH is still under debating. Many physicians are concerned about the prescription of statins to patients with unexplained persistent elevation of liver enzymes or active liver disease. Hence, randomized clinical trials of suitable sample size and duration are needed.

Ezetimibe (EZ), another lipid-lowering drug, inhibits cholesterol absorption by selectively binding to the cholesterol transporter NPC1L1 at both hepatocytes and enterocytes [133, 134]. It is mainly used as a secondary therapy to statins to further reduce LDL-C. EZ has recently been used in the treatment of NAFLD/NASH and shown promise in both experimental animal models and small clinical trials [135-141]. It reduces insulin resistance and steatosis in both rats and mice [136-138]. In a non-obese population, a 6-month treatment of EZ reduced plasma alanine aminotransferase (ALT) and cholesterol by 40% and 10%, respectively [141]. In another 6-month open label, pilot study, EZ significantly improved liver histology and other markers of liver disease including serum ALT, aspartate aminotransferase (AST), and γ-glutamyl transpeptidase [139]. In the largest clinical study to date (n=45) in a Japanese population, EZ reduced ALT at 12 months and resulted in modest, but

significant reductions in steatosis, ballooning, and other indices of NAFLD by 24 months [135]. The mechanism by which EZ is thought to provide benefit in NAFLD is not fully understood but may be due to the reduced flux of cholesterol from the intestine to liver, thereby reducing the inflow of cholesterol to hepatocytes [142]. Currently, EZ monotherapy is not indicated in the treatment of NAFLD and large controlled clinical trials are needed to confirm its effectiveness in patients with NAFLD/NASH.

Although reducing plasma LDL-C levels by using lipid-lowering drugs significantly decreases total mortality from CVD, the protection is not complete [143]. In a large proportion of patients, even though LDL-C is intensively reduced with statin therapy, low HDL-C still promotes the progression of disease [143-146]. An emerging body of work suggests that the flux of cholesterol through lipoproteins is more relevant to CVD than their absolute levels in plasma. Consequently, there has been intensely increased interest in strategies aimed at enhancing cholesterol efflux from peripheral tissues and promoting its transport to the liver for excretion.

Reverse cholesterol transport (RCT): Current and future directions

The most widely accepted strategy to enhance sterol flux from peripheral tissues to liver for ultimate excretion into feces is through the acceleration of a process termed reverse cholesterol transport (RCT). HDL is the predominant cholesterol acceptor and carrier in RCT. Both liver (70%) and intestine (30%) synthesize the

principal protein component of HDL, apoAI, and release it as a lipid-free pre-β HDL particle to acquire FC exported by ABCA1 from peripheral cells such as macrophages [147]. The FC in nascent HDL, as it travels through circulation, is subsequently converted to cholesteryl ester by lecithin-cholesterol acyltransferase (LCAT), generating a mature form of HDL. The mature HDL then transports cholesterol back to the liver for excretion into the bile either as FC or bile salts. The uptake of cholesteryl ester from HDL is mediated by a membrane protein on hepatocytes, scavenger receptor class B member 1 (SR-BI). SR-BI is actively involved in the selective cholesterol uptake and trans-hepatic cholesterol elimination. In humans, due to the activity of plasma cholesteryl ester transfer protein (CETP), HDL can transfer cholesterol to VLDL and LDL via the remodeling action of CETP and eventually deliver cholesterol back to liver through LDLR-mediated endocytosis. However, in mice, a species that lacks CETP activity, the predominant lipoprotein in RCT is HDL.

A substantial amount of work has been devoted to the conceptual approaches to augment RCT by improving cellular cholesterol efflux from peripheral cells, enhancing the functionality of circulating HDL, and increasing hepatic uptake of returned cholesterol. Relatively little effort has been geared at developing therapeutic approaches to target the final step of RCT.

ABCG5 ABCG8 (G5G8) in accelerating RCT

The terminal hepatic and intestinal components of RCT are often overlooked due to their relatively less contribution to the anti-atherosclerotic effect of RCT. However, as the discovery of several transporters involved in the final step of RCT, there is nevertheless substantial interest in understanding the mechanisms that regulate the excretion of cholesterol into bile. Recent studies suggest that cholesterol taken up by hepatocytes is secreted into bile via the apical membrane sterol transporters ABCG5 and ABCG8 (G5G8) [2-4].

ABCG5 (G5) and ABCG8 (G8) are two independent ABC half transporters. They are located on chromosome 2P21 adjacent to each other in a head-to-head orientation separated by a short intergenic region [148]. This shared intergenic promoter contains response elements for a variety of transcriptional factors including liver X receptors (LXR) α and β, hepatocyte nuclear receptor 4α (HNF4α), GATA transcription factors, orphan nuclear receptor liver receptor homolog-1 (LRH-1), thyroid hormone receptor, and FOXO1[149-153]. It also ensures the simultaneous expression of both G5 and G8, which is required for the heterodimeric protein complex formation and trafficking to the cell surface [154, 155].

The G5G8 heterodimer is formed in the ER in an N-linked glycan dependent manner facilitated by the lectin chaperones calnexin and calreticulin [156, 157]. Upon formation, it travels through Golgi apparatus and is predominantly expressed at the apical surface of hepatocytes in the liver and enterocytes in the

small intestine. Overexpression of calreticulin increases the abundance of the G5G8 complex at the cell surface, indicating that protein folding and G5G8 complex formation is a limiting factor that determines G5G8 abundance and activity [156].

G5G8 is the primary mediator of hepatobiliary elimination, accounting for 70% to 90% of biliary cholesterol secretion [152]. This process requires bile salt micelles to effectively mediate cholesterol efflux[158]. In addition, G5G8 also opposes phytosterol absorption in the small intestine [148, 152].

Phytosterols are plant-derived compounds that naturally exist in diet. They share an identical ring structure with cholesterol, but differ in the side chain. Both cholesterol and phytosterols can be absorbed by NPC1L1 in the small intestine. Unlike cholesterol, phytosterols are not suitable substrates for the acetyl-CoA acetyltransferease 2 (ACAT2) and hence are not esterified in enterocytes. G5G8 recognizes the free form of phytosterols and transports them back into the intestine lumen for excretion. This coordinated mechanism of G5G8 and ACAT2 allows the body to proficiently distinguish cholesterol from phytosterols, prevent excess cholesterol being absorbed, and ensure low levels of plasma phytosterols [159, 160]. Though dietary supplementation of phytosterols has been reported to lower LDL-C levels, reduce plaque formation and atherosclerosis in both experimental and clinical studies, their overwhelming accumulation in tissues is deleterious[161-163].

Defects in either *G5* or *G8* produce Sitosterolemia (OMIM, #210250), a rare autosomal recessive disorder characterized by roughly a 50-fold increase in plasma concentrations of phytosterols. Patients with Sitosterolemia usually present increased intestinal absorption of dietary sterols and a defect in biliary sterol secretion, which result in the accumulation of both cholesterol and phytosterols in plasma and tissues [164]. The excess accumulation of phytosterols contributes to the development of tendon and tuberous xanthomas, hypercholesterolemia, atherosclerosis, and premature coronary artery disease.

A mouse model of Sitosterolemia has been generated and well-studied over the past decade, in which mice are homozygous for G5G8 mutations. G5G8 knockout (KO) mice present strikingly reduced levels of biliary cholesterol. While the fractional absorption of phytosterols (e.g., sitosterol, campesterol) is significantly increased, that of cholesterol maintains relatively unaltered. Both hepatic and plasma sterols are dramatically increased due to the disrupted biliary secretion and increased intestinal absorptions.

As reviewed earlier in this dissertation, obesity and insulin resistance may play a central role in the pathogenesis of MetS and NAFLD. ER stress and FC have also been recently appreciated as new suspects in the pathogenesis of NAFLD/NASH. There is emerging evidence that G5G8 ties the link of sterol flux to all these risk factors [165-167]. For example, the absence of G5G8 in mice challenged with a phytosterol-free, HF diet results in reduced biliary and fecal

cholesterol elimination, accelerated development of obesity and insulin resistance, increased accumulation of hepatic lipids in the form of both TG and FC, activated ER stress and UPR signaling, and worsening of NAFLD [165].

Conversely, increasing biliary cholesterol secretion by adenoviral expression of G5G8 improves hepatic insulin signaling and restores glycemic control and TG metabolism in *db/db* mice, a heavily used mouse model of MetS and NAFLD [167]. These observations indicate that the protective role of G5G8-mediated cholesterol flux through the biliary tract promises it as a conceptual target to accelerate RCT. Similarly, in LDLR deficient mice, expression of a G5G8 transgene reduces atherosclerosis, suggesting that therapeutic approaches that accelerate G5G8 activity may augment RCT and be beneficial in the prevention and treatment of CVD [168, 169]. Although G5G8 has been known to increase cholesterol excretion for over a decade, there has been little interest and progress in drug development for this target due to that several concerns have not been addressed.

First of all, to develop such an approach, the knowledge of molecular mechanism responsible for the regulation of G5G8 function is indispensable. Though the main steps involved in G5G8 transcriptional regulation have been elucidated, little is known about the mechanisms responsible for the post-transcriptional control of G5G8. Both *ob/ob* and *db/db* mice present multiple features of MetS and NAFLD, such as obesity, insulin resistance, hyperglycemia and

hypertriglyceridemia. However, they are paradoxically resistant to the formation of cholesterol gallstones when challenged with a lithogenic diet [170]. This is in part due to the downregulation of hepatic G5G8 protein and a reduction in biliary cholesterol [166, 171-176]. The underlying mechanisms responsible for the reduced G5G8 protein expression in these mice may provide a clue to the development of effective therapy for the metabolic disease. In Chapter 2, a series of mouse models were used to address the potential mechanisms responsible for the post-transcriptional regulation of G5G8 in leptin-axis deficient mice.

Secondly, previous studies suggest an interdependent relationship between liver and intestine for cholesterol elimination from the body. The beneficial effects of increased biliary cholesterol secretion are opposed by intestinal reabsorption, and similarly, the beneficial effects of blocking cholesterol absorption are opposed by reduced biliary secretion [167-169]. This suggests that a combination therapy that increases biliary cholesterol secretion and simultaneously reduces intestinal absorption is likely to act additively in the elimination of cholesterol from the body. Combination therapy is usually more effective, especially when complementary mechanisms of action are involved. Thus, in Chapter 3, we proposed a combined pharmacological approach to accelerate cholesterol elimination and tested its efficiency in mouse models.

Lastly, increasing biliary cholesterol secretion is expected to raise the cholesterol saturation index of bile and the risk for cholesterol gallstones. Thus, a

pharmaceutical candidate that increases biliary cholesterol secretion but has beneficial effect of dissolving cholesterol gallstone would be a viable option. In Chapter 3, we found that ursodeoxycholic acid (UDCA), an active pharmaceutical ingredient of ursodiol (Urso) is such an option.

Hepatic cholesterol catabolism: Bile acid synthesis

G5G8-mediated biliary cholesterol secretion is a direct pathway to excrete excess hepatic cholesterol. An alternative pathway for the body to excrete excess cholesterol is through cholesterol catabolism by converting cholesterol to bile acids. This is exclusively completed in liver. Both of them facilitate the final step of RCT.

Bile acid synthesis not only constitutes a route to consume cholesterol but also produces biological detergents important for producing micelles to solubilize dietary cholesterol, fats, and necessary nutrients. The conversion of cholesterol to bile acids includes both the neutral and acidic pathways initiated via the action of CYP7A1 and sterol 27-hydroxylase (CYP27A1), respectively [121-123]. As for the neutral or sometimes called the classic pathway, CYP7A1 is the rate-limiting enzyme that controls the hydroxylation of cholesterol to 7*a*-hydroxycholesterol [177, 178]. Another critical enzyme that catalyzes the subsequent reaction is sterol 12-alpha-hydroxylase (CYP8B1). For acidic pathway, the bile acid intermediates produced by sterol 27-hydroxylase (CYP27A1) are then participating in the reaction catalyzed by 25-hydroxycholesterol 7-alpha-hydroxylase (CYP7B1).

Bile acids are conjugated either with glycine or taurine to yield the glycol- or tauro-conjugates, respectively. The bile salt export protein (BSEP; ATP-binding cassette B11, ABCB11) subsequently transports the glycine or taurine conjugates of bile acids into bile. Once bile salts are secreted into intestinal lumen, the majority of them (~95%) are reabsorbed via the apical sodium-dependent bile transporter (ASBT) into ileal enterocytes. The ileal bile acid-binding protein (IBABP) then transports them across the enterocyte cytosol to the basolateral side, where bile salts are fluxed into the circulation via the heterodimeric organic solute transporter OSTα/OSTβ and eventually returned to hepatocytes by means of the sodium sodium (Na^+)-taurocholate cotransporting polypeptide (NTCP) and the organic anion transporters (OATP). The overall whole cycle is termed the enterohepatic recirculation. This recycling mechanism plays an essential role in maintaining the circulation pool of bile acids, normal bile flow, thereby maintaining the bile acid and cholesterol homeostasis.

Bile acid homeostasis must be tightly regulated due to the intrinsic toxic feature of bile acids. The most widely-studied transcriptional regulator of bile acid homeostasis is the farnesoid X receptor (FXR) which is highly expressed in liver and intestine [179]. It potently suppresses CYP7A1 through two interrelated mechanisms. One is that FXR induces the expression of small heterodimer partner (SHP), a transcriptional co-repressor that interacts with two other nuclear

receptors: LRH-1 and HNF4α and indirectly binds to the CYP7A1 promotor and suppresses its transcription [180-182].

The other mechanism is through the regulation of fibroblast growth factor (FGF) 15/19. FGF19 and FGF15 share 53% amino acid identity with each other. FGF19 in humans has similar tissue expression patterns, physiological functions, and pharmacological effects as FGF15 in mice [183-185]. There is definitive evidence that FGF15 and FGF19 are orthologous proteins. Hence, we refer to the hormone collectively as FGF15/19 unless referring to a specific ortholog. Unlike other FGFs that act in an autocrine or paracrine fashion, FGF15/19 has reduced heparin affinity that permits it to act as an endocrine hormone. FGF15/19 is predominately expressed in the ileum and controlled by FXR. When bile acids are (re)absorbed from the intestinal lumen, they act on the FXR/RXR heterodimer to induce FGF15/19 expression. The secreted FGF15/19 travels in circulation but fails to activate FGF receptors (FGFRs) on its own in liver due to the reduced affinity and interaction between FGFs and their receptors. It requires the assistant of β-Klotho, a transmembrane protein, which enables the binding of FGF15/19 to FGFR4 and functions as a co-receptor to initiate the FGF15/19-FGFR4 signaling and repress CYP7A1 in liver. It has been reported that in SHP KO mice, the FGF15/19-mediated suppression of CYP7A1 is lost [186]. This demonstrates that FGF15/19-FGFR4-β-Klotho signaling pathway and the SHP repression pathway converges in mediating CYP7A1 transcription.

In Chapter 3, we observed that UDCA stimulated the ileal expression of FGF15, suppressed CYP7A1 expression, and increased hepatic G5G8 protein expression. This underlines FGF15/19 as a post-transcriptional mechanism for G5G8 regulation. In Chapter 4, seeking evidence in support of this hypothesis, we tested the ileal FGF15 in LIRKO mice, which expressed higher levels of G5G8 protein, as well as the hepatic G5G8 protein expression in Asbt KO mice, which had suppressed ileal FGF15 expression.

Another endocrine action of FGF15/19 in bile acid regulation is to promote gallbladder filling at least in part by causing a cyclic adenosine monophosphate (cAMP)-dependent relaxation of gallbladder smooth muscle [187]. FGF15-KO, FGFR4-KO, and β-Klotho-KO mice all have small or even virtually empty gallbladders, while administration of recombinant FGF19 into FGF15-KO mice results in a rapid gallbladder filling [187-189]. Interestingly, it has been newly discovered that cAMP signaling machinery is responsible for the accelerated trafficking of G5G8 to the bile canalicular membrane in response to nutrient loading [190]. This further supports that FGF15/19 may be a regulator of G5G8 and it regulates G5G8 probably through the cAMP signaling. Unraveling the role of FGF15/19 in the regulation of G5G8 may provide an alternative strategy in drug development to target G5G8 activity and the final step of RCT.

Copyright © Yuhuan Wang 2015

CHAPTER 2: THE POST-TRANSCRIPTIOANL REGULATION OF ABCG5 ABCG8 STEROL TRANSPORTER IN LEPTIN-AXIS DEFICIENT MICE

INTRODUCTION

The *ABCG5 ABCG8* locus encodes a pair of ABC half transporters that form a G5G8 complex that promotes the secretion of cholesterol into bile and opposes the absorption of dietary sterols in the small intestine [191]. Mutations in either *ABCG5* or *ABCG8* cause Sitosterolemia, a recessive monogenic disorder characterized by elevated plasma cholesterol and plant sterols, tendon and tuberous xanthomas, and accelerated atherosclerosis [191]. G5G8 deficiency also results in reduced cholesterol elimination, exacerbated hepatic insulin resistance, and the development of NAFLD in a mouse model of diet-induced obesity [165]. Conversely, accelerated biliary cholesterol secretion through G5G8 overexpression improves glycemic control and hepatic insulin signaling in *db/db* mice [192]. In LDLR deficient mice, expression of a G5G8 transgene reduces atherosclerosis, suggesting that therapeutics that accelerate G5G8 activity may be beneficial in the prevention and treatment of CVD [168, 169].

G5G8 heterodimers are formed in the ER in an N-linked glycan dependent manner facilitated by the lectin chaperones calnexin and calreticulin [156, 157]. Overexpression of calreticulin increases the abundance of the G5G8 complex at the cell surface, indicating that protein folding and G5G8 complex formation is a

limiting factor that determines G5G8 abundance and activity [156]. G5G8 complex formation and trafficking to the cell surface requires simultaneous expression of both G5 and G8 [154, 155], which is accomplished by a common promoter containing response elements for a number of transcription factors including LXR α and β, HNF4α, GATA transcription factors, LRH-1, thyroid hormone receptor, and FOXO1 [149-153]. The upregulation of G5G8 by FOXO1 is clinically significant because it mechanistically ties an increased risk for cholesterol gallstones to a hepatic insulin resistance [193]. Additionally, quantitative trait locus mapping has identified *Abcg5Abcg8* as a lithogenic locus in mice, and polymorphisms in both *ABCG5* and *ABCG8* have been associated with increased risk of cholesterol gallstones in humans [194].

Mice lacking leptin (*ob*/*ob*) or its receptor (*db*/*db*) are obese and insulin resistant, but are paradoxically resistant to the formation of cholesterol gallstones when challenged with a lithogenic diet [170]. Multiple mechanisms appear to contribute to this phenotype, including a downregulation of hepatic G5G8 and a reduction in biliary cholesterol [166, 171-176]. Leptin replacement in *ob*/*ob* mice increases hepatic G5G8 and cholesterol concentrations in gallbladder bile, suggesting that leptin may directly regulate G5G8 abundance and activity [166, 175]. However, in the present study, leptin administration in *ob*/*ob* mice failed to acutely increase hepatic G5G8. In addition, hepatic branch vagotomy failed to alter G5G8 in obese mice, indicating that centrally acting leptin was not a direct

regulator of G5G8 abundance. Likewise, deletion of hepatic leptin receptors had no effect on G5G8.

Caloric restriction can partially rescue G5G8 and biliary cholesterol concentrations in *db*/*db* mice, suggesting that other mechanisms secondary to obesity may destabilize the G5G8 complex in mice that lack a functional leptin axis [166, 195]. Markers of ER stress are elevated in the liver of *ob*/*ob* mice and are associated with the development of hepatic insulin resistance and fatty liver disease [96, 111]. Alleviation of ER stress through the chemical chaperones 4-PBA and TUDCA restores insulin signaling and glycemic control [111]. We previously reported that TUDCA increases G5G8 in *db*/*db* mice; however, it has a virtually identical effect in lean C57BL mice in the absence of ER stress [166]. Furthermore, TUDCA stimulates bile flow and increases biliary cholesterol secretion in lean mice presenting no ER stress, suggesting its effects on G5G8 may be independent of chaperone function [196, 197]. Indeed, TUDCA has a number of effects beyond chaperone functions, including opposing mitochondrial depolarization, caspase activation, and apoptosis [198-200]. Therefore, whether the reduction of hepatic G5G8 in *ob*/*ob* and *db*/*db* mice is a consequence of ER dysfunction remains unclear.

GRP78 is an ER chaperone and component of UPR. In the face of ER stress, induction of GRP78 plays an essential role in promoting protein folding and assembly, targeting aberrant protein for degradation, and increasing the folding

capacity of ER. Hepatic ER stress also contributes to increased lipogenesis and steatosis by promoting the processing of SREBPs [112]. SREBPs are among a family of ER membrane proteins that traffic to the Golgi in response to metabolic signals and are proteolytically processed to release their respective transcription factor domains [39]. Exogenous expression of GRP78 by adenoviral administration reduces lipogenesis and steatosis by preventing the unregulated trafficking and activation of SREBP1-c [112]. Since ER folding capacity is a limiting factor in G5G8 abundance, we tested the hypothesis that adenovirus encoding GRP78 (AdGRP78) would restore G5G8 in *db/db* mice. As predicted, G5G8 abundance and biliary cholesterol increased following expression of AdGRP78. These results reveal a role for ER stress as a mechanism for reduced G5G8 in mice lacking a functional leptin axis.

MATERIALS AND METHODS

Chemicals, reagents and antibodies

General chemicals were purchased from Sigma, immunoblotting reagents from Pierce, real-time PCR reagents from Applied Biosystems, mouse recombinant leptin from Biomyx Technology (San Diego, CA), and mouse leptin ELISA from EMD Millipore. Calnexin and GRP78 antibodies were purchased from Nventa (San Diego, CA). The α-tubulin and β-actin antibodies were purchased from Cell Signaling and Sigma, respectively. Anti-SR-BI was purchased from Novus. Anti-ABCA1 antibody was a generous gift from Manson Freeman (Harvard Medical

School, Boston, MA). Anti-calreticulin antibody was purchased at Stressgen Bioreagents Corp. Total and phospho- PERK antibodies were purchased from Cell Signaling Technology. Experiments presented in Figure 2.1 were conducted with previously described antibodies directed against G5 and G8 [154, 155]. Stocks of the rabbit polyclonal antibody directed against G5 have become limited and suitable commercially available sources have not been identified. Therefore, we contracted ProSci Inc. (Poway, CA; NIH/OLAW assurance #A4550-01) to synthesize a peptide from the N-terminus of the rat ortholog of G5 (MGELPFLSPEGARGPHINRGSLSSLEC) for antibody development in chickens. Antibodies were affinity purified and tested for suitability in western blotting and immunofluorescence microscopy applications in mouse and rat livers. The chicken anti-G5 polyclonal antibody was used for experiments presented in Figures 2.3, 2.4, 2.6, 2.7, and 2.8.

Animal husbandry

Male mice lacking functional leptin (*ob*/*ob*, stock #000632), and the leptin receptor (*db*/*db*, stock #000697) on the C57BL/6J background and their lean littermate controls were purchased from The Jackson Laboratory (Bar Harbor, ME). Upon arrival mice were allowed to acclimatize for a period of 7 days prior to initiation of studies. Mice harboring two copies of the floxed leptin receptor allele ($ObR^{f/f}$) were provided by Dr. Jeffrey Friedman (The Rockefeller University) and maintained in our colony [201]. Animals were housed in individually ventilated cages in a temperature-controlled room with a 14:10 light:

dark cycle and provided with enrichment in the form of acrylic huts and nesting material. All mice were maintained on standard rodent chow (Harlan Teklad 2014S).

Leptin treatment

Mice lacking leptin (*ob*/*ob*, n=3) were injected (i.p.) with either saline or 10 mg/kg mouse recombinant leptin within 30 min of "lights-on" at 06:00. All mice were placed in clean cages with full access to water, but without food. Blood and tissues were collected 4, 8, and 16 h following leptin administration. For the 16 h time-point, a second injection of leptin was administered at 8 h. Blood leptin levels were determined at the time of tissue collection by ELISA.

Adenoviral mediated hepatic gene expression

AdGRP78 and a control virus (AdEmpty) were previously reported [112]. Adenovirus encoding Cre-recombinase (AdCre) was purchased from Microbix Biosystems, Inc. (Mississauga, Ontario, Canada). AdCre, AdGRP78, and AdEmpty were amplified in HEK293Q cells and purified on cesium chloride gradients as previously described [154]. Purified adenovirus was diluted in sterile saline and mice (8-12 weeks) were injected through the tail vein with $4x10^{12}$ particles/kg body weight. Analysis of AdCre injected $ObR^{f/f}$ and wild-type (ObR^{WT}) mice were conducted two weeks following viral delivery. Analysis of control and GRP78 expressing mice was conducted five days following infection.

Immunoblot and Quantitative Real-time PCR

Total membrane preparations from liver samples were prepared and proteins analyzed by SDS-PAGE (50 µg/lane) and immunoblotting as previously described [166]. The signals were quantified by densitometry using ImageJ software. Total RNAs were extracted from liver tissue using RNA STAT-60 (Tel-Test, Inc) and subjected to cDNA synthesis with iScript cDNA Synthesis Kit (BIO-RAD, Hercules, CA). To determine relative abundance of transcripts, RT-PCR was conducted using SYBRGreen as detector on Applied Biosystem 7900HT fast-Real Time PCR System (Carlsbad, CA) [165]. Glyceraldehyde 3-phosphate dehydrogenase (GAPDH) was used as an internal control for the normalization of data in all RT-PCR experiments.

Plasma and biliary lipid analysis

Plasma TG concentrations were determined enzymatically using the L-type TG M kit. Biliary cholesterol concentrations were determined using the cholesterol E kit (Wako Chemicals, Richmond, VA).

Statistical Analysis

All statistical analyses were conducted using GraphPad Prism. Data are expressed as mean ± SEM. Data were analyzed by two-tailed t-test, one-way ANOVA, or two-way ANOVA as indicated in figure legends. Post-hoc comparisons were conducted by using Dunnett's tests for one-way ANOVA and Bonferroni post-tests for two-way ANOVA, respectively. Differences were considered significant at $P < 0.05$.

RESULTS

To determine if leptin could acutely increase hepatic G5G8 abundance, we chose a 10 mg/kg dose that we previously reported to restore hepatic G5G8 in *ob/ob* mice following seven days of treatment [166]. To ensure that this dose was biologically active over the course of our study, we monitored food intake for three consecutive days prior to, and following, a single dose of leptin (Fig 2.1A). Leptin administration immediately suppressed food intake to levels generally observed in wild-type (WT) mice over the first 24 h, indicating that leptin was centrally active over the course of our experiment. Interestingly, food intake remained significantly suppressed for at least seven days following this single dose.

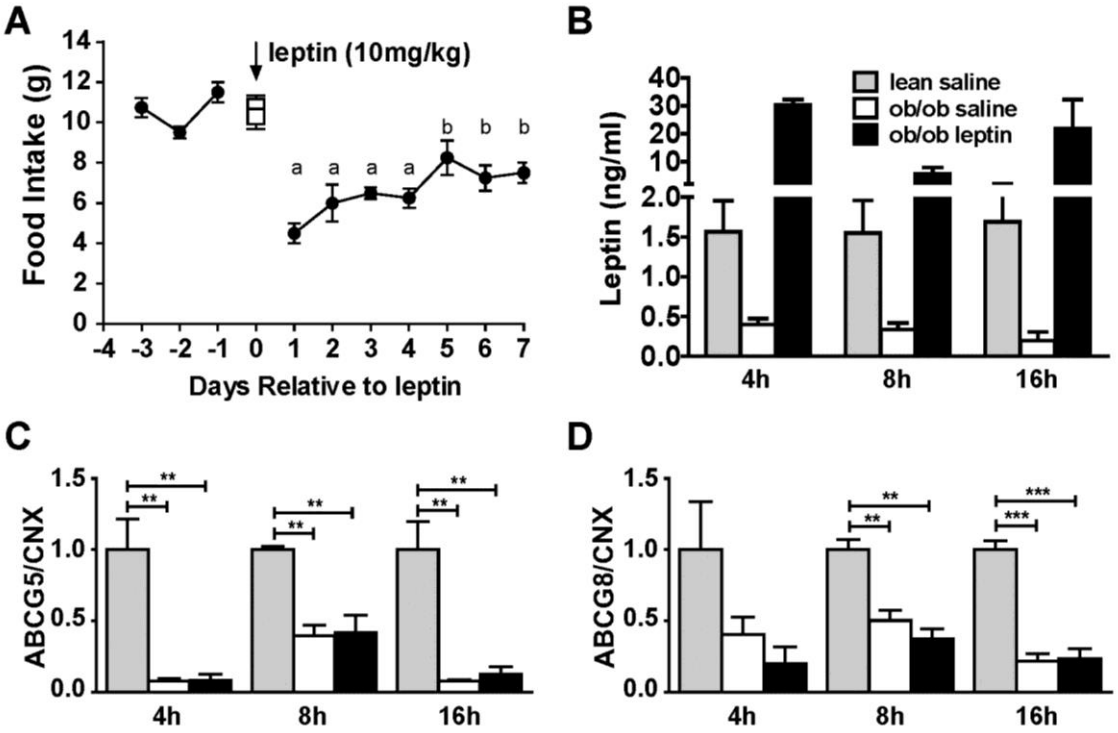

Figure 2.1. Leptin acutely suppresses food intake, but fails to restore hepatic G5G8 in *ob/ob* mice. (A) Food intake was monitored for three consecutive days in *ob*/*ob* mice (n=4). A single dose of leptin (10 mg/kg, ip) was administered (Day 0) and food intake monitored for seven additional days. Intake following leptin treatment was compared to the three-day pre-treatment mean by one-way ANOVA. A Dunnett's test was used to determine differences from the three-day pre-treatment mean (a, $p<0.01$; b, $p<0.05$). (B-D) In a second cohort of lean and ob/ob mice (n=3), tissues were harvested at 4, 8, and 16 h following the initial injection of either saline or leptin. (B) Serum leptin levels at the time of tissue collection were determined by ELISA. (C-D) Relative protein abundance was determined by densitometry using ImageJ software after normalization to calnexin (CNX). Data are mean ± SEM and were analyzed by one-way ANOVA. Post-hoc comparisons were conducted using Dunnett's tests ** $p<0.01$, ***$p<0.001$.

Ob/ob mice were injected with saline or leptin and tissues collected 4, 8, and 16 h after administration. For the 16 h time-point, a second injection of leptin was administered at 8 h. Blood leptin levels were determined by ELISA at the termination of the experiment (Fig 2.1B). Lean control mice had leptin levels of 1.5 ng/ml, while levels in saline treated *ob/ob* mice were at the lower limit of detection in our assay. Serum leptin in *ob/ob* mice injected with leptin was 30 ng/ml at 4 h and declined to 8 ng/ml by 8 h, but increased to 20 ng/ml at 16 h following the second injection. While these levels of leptin were substantially higher than lean controls, they are typical of obese mice maintained on HF diets [202]. Hepatic levels of G5 and G8 were analyzed by immunoblotting (Fig 2.2). Densitometric analysis of immunoblots of hepatic G5 and G8 confirmed that G5 and G8 protein levels were low in *ob/ob* mice compared to lean littermates (Fig 2.1C, D). Administration of leptin failed to increase G5 or G8 at 4, 8, or 16 h

following the initial injection, indicating that centrally acting leptin had no immediate impact on hepatic G5G8 protein.

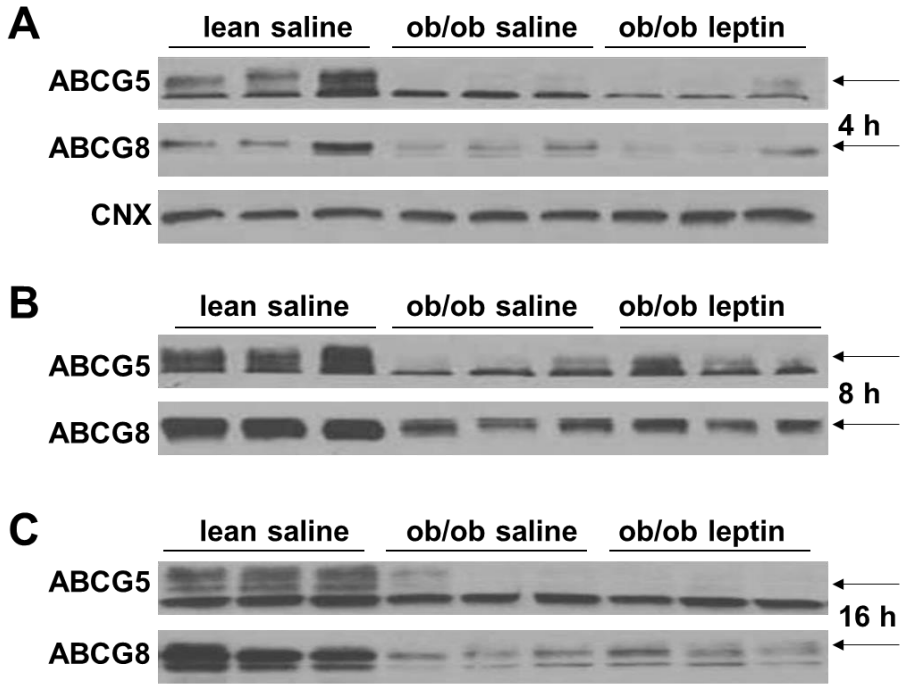

Figure 2.2 G5/G8 protein expression in liver tissues of *ob/ob* mice and their lean controls. Liver tissues of lean and ob/ob mice (n=3) were harvested at 4, 8, and 16 h following the initial injection of either saline or leptin. Hepatic levels of G5 and G8 were analyzed by immunoblotting. Membrane proteins were also blotted for calnexin (CNX) as controls for equal protein loading.

As an alternative approach to hormone replacement, hepatic G5G8 was examined in obese mice that had undergone hepatic vagotomy to determine if vagal mediated effects of chronic, centrally-acting leptin could regulate G5G8 abundance. Hepatic vagotomy was performed in anesthetized 8-week-old male mice on the C57BL/6 background as previously described [203]. Mice were allowed to recover, maintained on standard chow diet for one week after vagotomy, and then switched to HF diet (Bio-Serv, #F3282) feeding for 10 weeks.

At termination, liver tissues were harvested and hepatic levels of G5 and G8 analyzed by immunoblotting (Fig 2.3). Neither G5 nor G8 protein levels were affected by hepatic branch vagotomy, indicating that centrally acting leptin failed to regulate hepatic G5G8 via vagal innervation in obese mice.

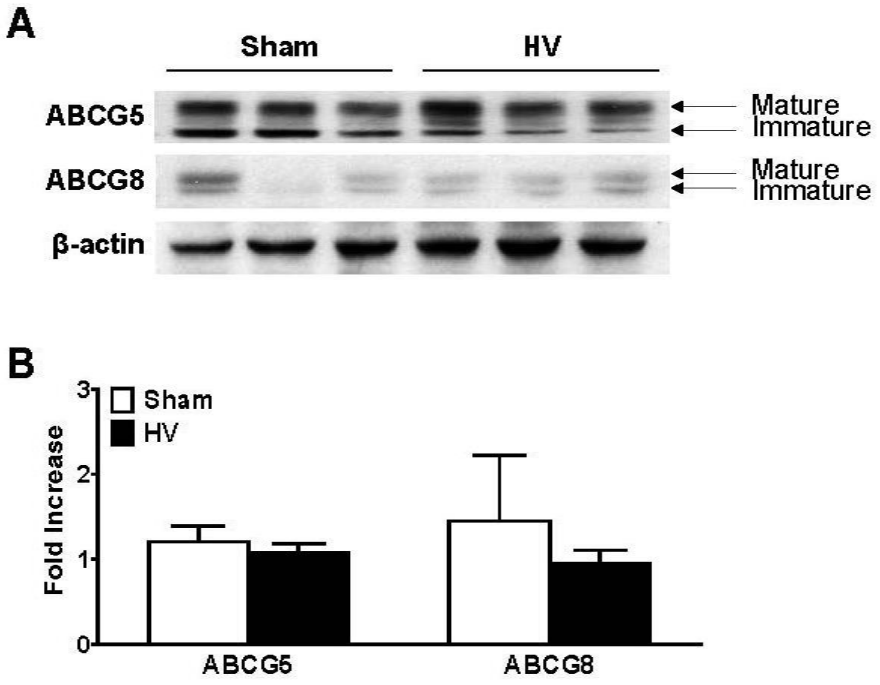

Figure 2.3 Hepatic branch vagotomy fails to alter the abundance of G5G8 in the setting of obesity. Liver tissues of obese mice that had undergone hepatic vagotomy (HV) and their sham-operated controls (n = 3) were harvested after being maintained on high fat feeding for 10 weeks. (A) Hepatic levels of G5 and G8 were analyzed by immunoblotting. (B) Relative protein abundance was determined by densitometry using ImageJ software after normalization to β-actin. Data are mean ± SEM. Differences were determined by two-tailed t-test.

Although expression of the long, signaling form of the leptin receptor is low in peripheral tissues, a number of studies indicate functions for peripheral leptin receptor isoforms [204, 205]. Hepatic leptin receptors from mice harboring floxed leptin receptor alleles ($ObR^{f/f}$) were selectively depleted with AdCre. WT and

$ObR^{f/f}$ mice were injected with AdCre and analyzed 2 weeks following treatment (Fig 2.4). Commercially available antibodies for leptin receptor proved unsatisfactory for hepatic protein level determination. An RT-PCR assay detecting all ObR isoforms demonstrated a 70% reduction in hepatic mRNA levels (Fig 2.4A). Food intake was not affected over this period and there were no differences in body weight (data not shown). Neither G5 nor G8 mRNA or protein levels were affected by depletion of hepatic leptin receptors (Fig 2.4A, B). Similarly, no changes were observed in biliary cholesterol concentrations (Fig 2.4C). These results failed to support direct effects of centrally or peripherally acting leptin on G5G8 abundance.

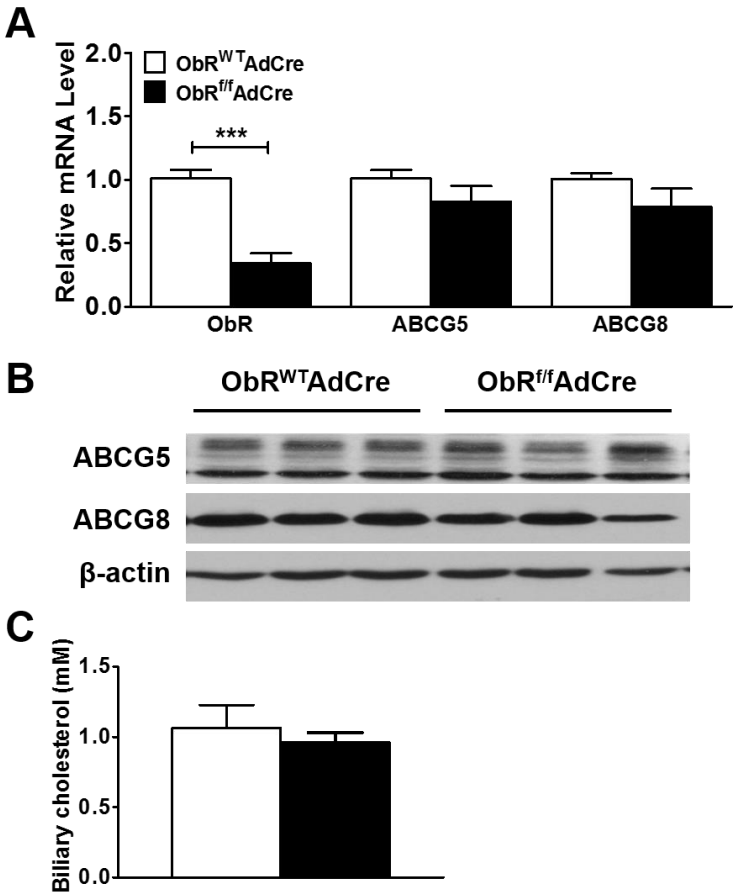

Figure 2.4 Depletion of hepatic leptin receptors does not reduce G5G8. An adenoviral vector encoding Cre recombinase (AdCre) was administered to WT (n = 3) and mice harboring two floxed alleles for leptin receptor ($ObR^{f/f}$, n = 3). (A) Hepatic levels of leptin receptor (ObR), G5 and G8 mRNA were quantified by RT-PCR. (B) The abundance of hepatic G5 and G8 protein was determined by immunoblotting. (C) Biliary cholesterol concentrations were determined by colorimetric-enzymatic assay. Data are mean ± SEM. Differences were determined by two-tailed t-test ***$p<0.001$.

Expression of the ER chaperone protein GRP78 has been shown to alleviate markers of ER stress and reverse key features of the fatty liver phenotype in *ob/ob* mice [112]. The formation and trafficking of the G5G8 heterodimer is critically dependent upon the ER calnexin/calreticulin chaperone system. Therefore, we tested the hypothesis that elevated expression of GRP78 could restore G5G8 in *db/db* mice. A small cohort of lean mice (n = 3) was also administered AdEmpty and AdGRP78 as an additional control. Tissues were harvested 5 days following viral administration. AdGRP78 increased hepatic GRP78 compared to mice infected with the control virus (Fig 2.5A). Immunoblot analysis demonstrated a reduction in phospho-PERK following GRP78 expression, indicating a reduction in UPR signaling (Fig 2.5A, B). As previously published in *ob/ob* mice, expression of AdGRP78 reduced expression of SREBP1-c, as well as its target genes acetylCoA carboxylase 1 (ACC1) and fatty acid synthase (FAS), in the lipogenic pathway (Fig 2.5C). Similarly, plasma TGs and liver to body weight ratios were elevated in obese, *db/db* mice and reduced by elevated GRP78 expression to levels observed in lean controls (Fig 2.5D, E). These data confirmed the primary

observations previously made in *ob/ob* mice and extended them to the *db/db* model.

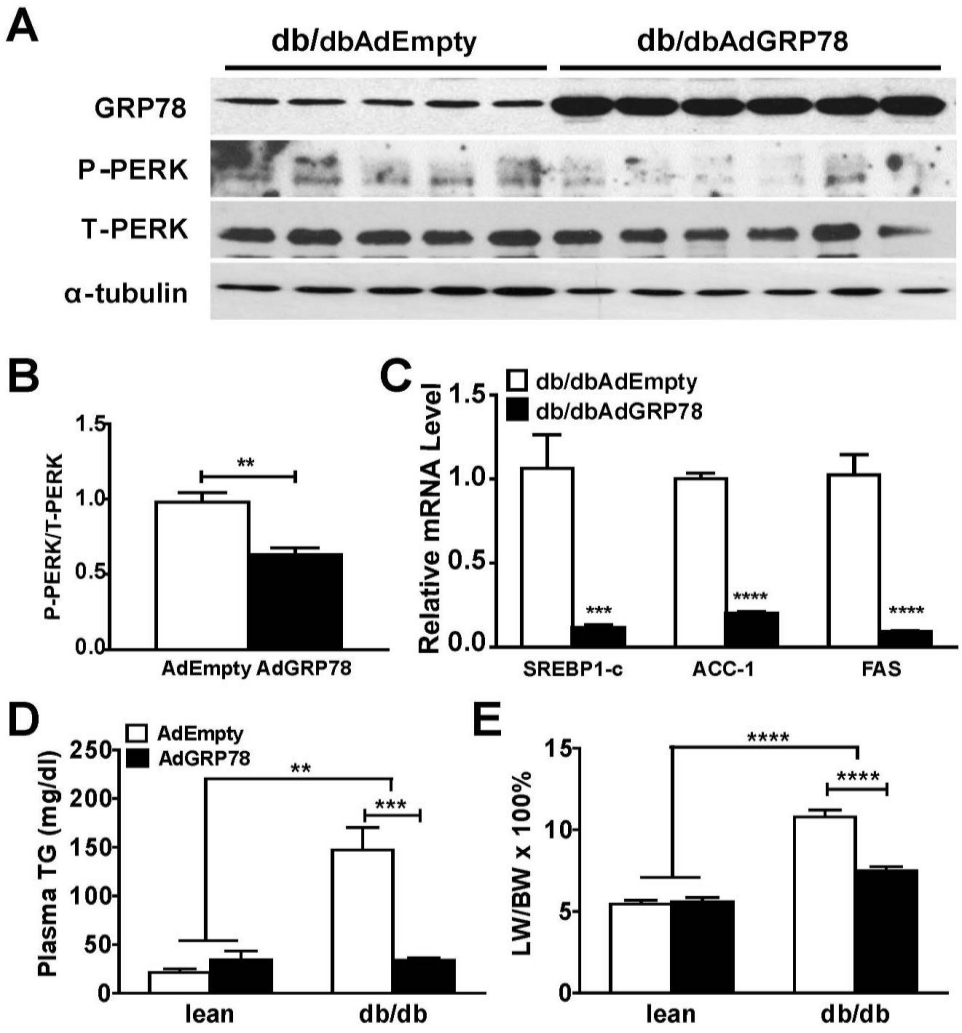

Figure 2.5 AdGRP78 alleviates ER stress, reduces lipogenic gene expression, and normalizes plasma TGs and liver weight in *db/db* mice. Control (AdEmpty) and GRP78 (AdGRP78) adenoviral vectors were administered to lean (n = 3) and db/db (n = 5 WT and 6 KO) mice. Tissues were harvested for analysis 5 days following viral expression. (A) GRP78, total and phosphorylated (P-) PERK in db/db mice were assessed in hepatic lysates by SDS-PAGE and immunoblotting. α-tubulin was used as a loading control. (B) The ratio of phosphorylated to total PERK was determined by desitometry using ImageJ. (C) The mRNA for lipogenic genes SREBP1-c, acetylCoA carboxylase 1 (ACC1), and fatty acid synthase (FAS) was determined by RT-PCR. (D) Plasma TGs and (E) liver weight to body weight ratio (LW/BW) were determined in both lean and db/db mice. Data are mean ± SEM and were analyzed by two-tailed t-test (B-C)

and two-way ANOVA followed by Bonferroni post-tests (D-E) ** $p<0.01$, ***$p<0.001$, ****$p<0.0001$.

As previously reported in both *ob/ob* and *db/db* mice, hepatic G5 protein expression was reduced in *db/db* mice compared with their lean controls (Fig 2.6). No difference was observed in the expression of GRP78, calnexin, or calreticulin.

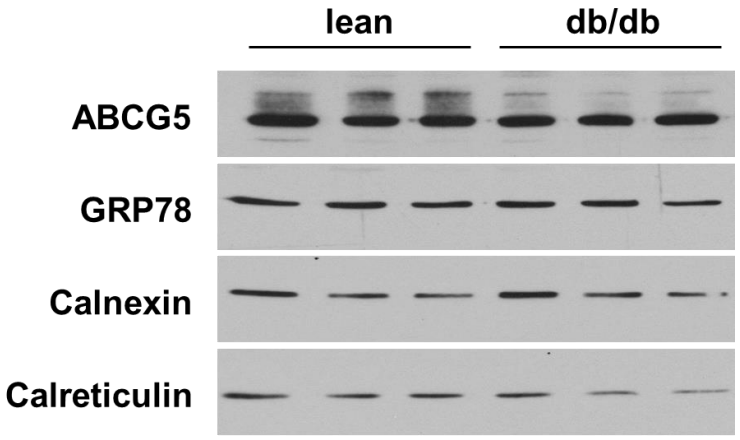

Figure 2.6 Hepatic expression of G5, GRP78, calnexin, and calreticulin in db/db mice and their lean controls was determined by immunoblot analysis.

In db/db mice, AdGRP78 increased G5 and G8 by 2.2 and 2.4 fold, respectively. The increase in G5 and G8 protein occurred in the absence of an increase in mRNA encoding either protein, consistent with a mechanism of increased efficiency of G5G8 complex formation within the ER (Fig 2.7A, B). An increase in protein expression of the ER chaperone calnexin was observed in the absence of an increase at its mRNA level (Fig 2.7A, B). Total cholesterol content in gallbladder bile was elevated most likely due to increased G5G8 (Fig 2.7C). We also observed significant, albeit modest, increases in both mRNA and protein expression of SR-BI, which is another contributor to biliary cholesterol secretion

(Fig 2.7A, B) [197, 206, 207]. However, there was no direct relationship between SR-BI and G5G8 abundance as shown in SR-BI deficient mice (Fig 2.8). Protein expression of ABCA1 also increased in *db/db* mice following AdGRP78 treatment (Fig 2.7A).

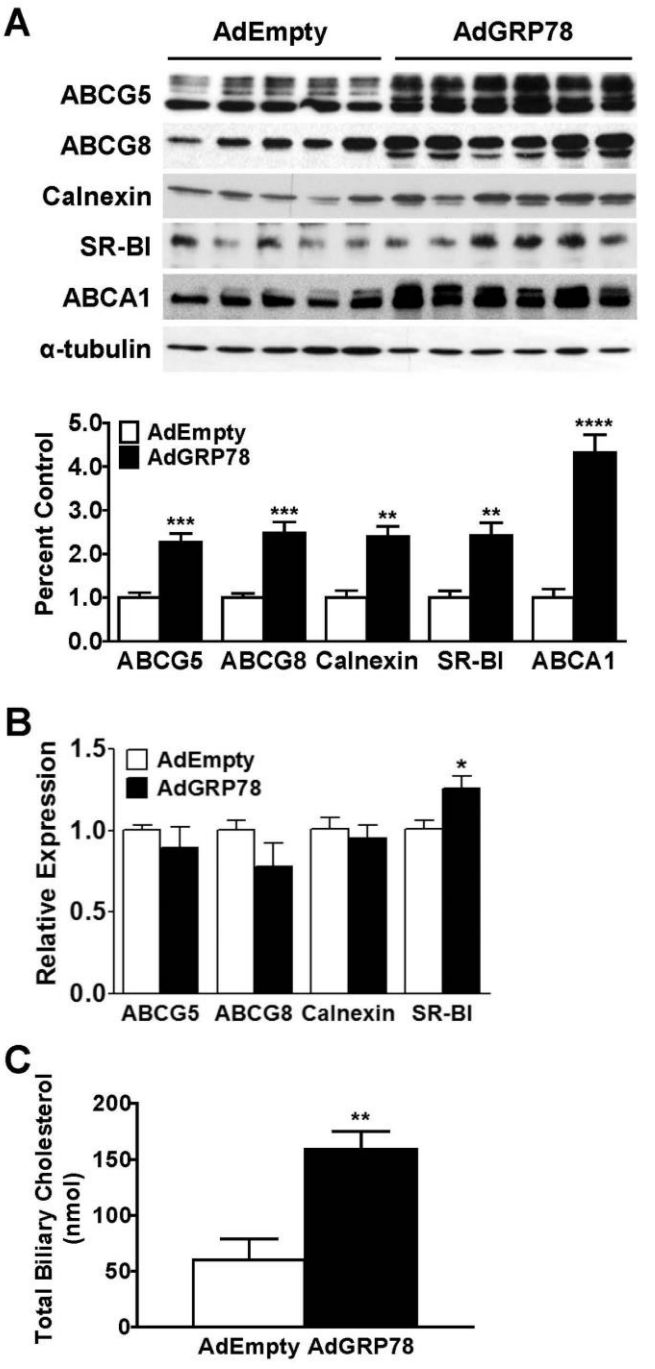

Figure 2.7 AdGRP78 increases G5G8 at the protein level and elevates biliary cholesterol in *db/db* mice. (A) Immunoblot analysis of hepatic G5, G8, calnexin, SR-BI, and ABCA1. Data were analyzed by densitometry and normalized to α-tubulin. (B) Levels of G5, G8, calnexin, and SR-BI mRNA were determined by RT-PCR. (C) Total biliary cholesterol was determined by colorimetric-enzymatic assays. Data are mean ± SEM (n=5 WT and 6 KO). Differences were determined by two-tailed t-test ** p<0.01, ***p<0.001, ****p<0.0001.

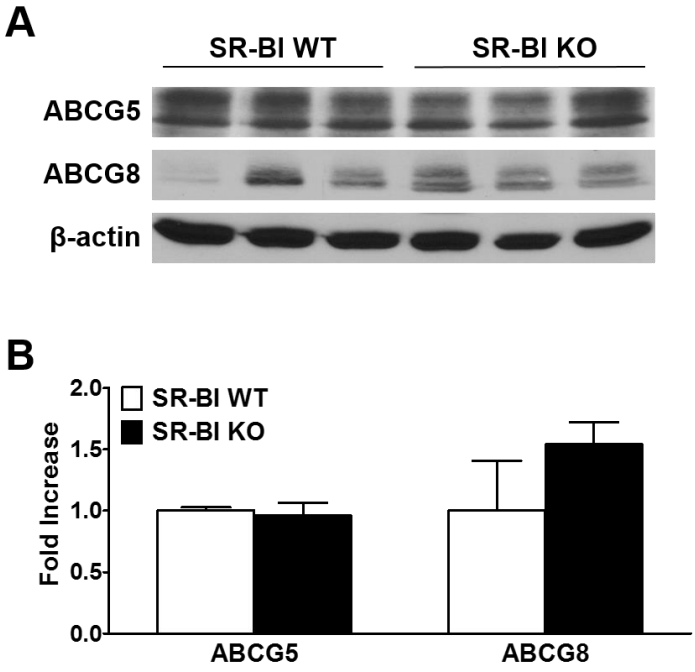

Figure 2.8 SR-BI deficiency does not directly affect hepatic G5G8. Liver tissues of SR-BI KO mice and their WT littermates were harvested. (A) Hepatic levels of G5 and G8 were analyzed by immunoblotting. (B) Relative protein abundance was determined by densitometry after normalization to β-actin.

DISCUSSION

The key finding of the present study is that expression of the ER chaperone, GRP78, restores hepatic G5G8 in *db/db* mice, whereas there is no apparent direct central or peripheral effect of leptin signaling on the complex. In the context of previously published studies that established a role for biliary cholesterol

secretion in opposing ER stress, the present study suggests a reciprocal relationship between ER function and G5G8-mediated biliary cholesterol secretion.

Leptin signaling

Leptin replacement reduces food intake and induces weight loss in *ob/ob* mice. Therefore, it is difficult to establish which effects are truly dependent upon central or peripheral leptin signaling or are secondary to changes in energy balance. We previously reported the restoration of G5G8 in *ob/ob* mice following long-term leptin replacement [166]. While an increase in immunoreactive G5G8 was observed in pair-fed controls, leptin replacement resulted in a far greater increase, suggesting a direct role for leptin signaling as a regulator of hepatic G5G8 abundance. In the present study, leptin administration failed to acutely increase G5G8 after 4, 8, or 16 h when plasma levels of leptin were more than sufficient to mediate the central effects of this hormone. The absence of an effect over this period fails to support a role for centrally acting leptin on hepatic G5G8 abundance. While it is possible that centrally acting leptin may take a greater period of time to restore hepatic G5G8, the abundance of G5 and G8 mRNAs increase after a 24 h fast in a peroxisome proliferator-activated receptor alpha (PPARα)-dependent fashion [195]. Consequently, observations at later time-points would be confounded by induction of the PPARα-mediated fasting response.

Long-term stimulation of the hepatic branch of the vagus nerve reduces body weight and fat mass in rats [208]. Although effects of leptin in liver have been shown to be mediated by vagal stimulation or by hepatic leptin receptors, neither pathway appears to regulate hepatic G5G8 abundance [209, 210]. In our studies, mice that had undergone hepatic branch vagotomy failed to show any difference in hepatic levels of G5G8 compared with their sham-operated controls. Similarly, depletion of hepatic leptin receptors also failed to reduce G5G8. While these results support a hepatic leptin receptor-independent mechanism for reduced G5G8 in *db/db* and *ob/ob* mice, this experiment was limited by incomplete ObR depletion at the mRNA level and that hepatic leptin receptor depletion could not be confirmed at the protein level.

Restoration of G5G8 by AdGRP78 in *db/db* mice

The increase in G5G8 following AdGRP78 treatment was consistent with a mechanism that includes the improvement of ER folding capacity and greater efficiency of G5G8 complex formation within the ER. When expressed individually in cells, G5 and G8 have short half-lives and are rapidly degraded [155]. Co-expression allows for the formation of G5G8 heterodimers through a process that is dependent on the presence of their N-linked glycans and interactions with calnexin [157]. In cultured cells, co-expression of either calnexin or calreticulin with G5 and G8 increases the appearance of G5G8 at the cell surface [156]. It is important to note that GRP78 does not bind either G5 or G8

[157]. Therefore, it is unlikely to directly facilitate G5G8 folding. An increase in calnexin was also observed and is more likely to account for G5G8 rescue in *db/db* mice (Fig 5A). However, whether the increase in calnexin is required for the effect of GRP78 on G5G8 abundance is unknown. Apart from increased G5G8 complex formation in the ER, other mechanisms that may account for increased G5G8 levels include an increase in the rates of translation for each monomer or increased stability of the mature, post-Golgi complex. While these alternate explanations have not been formally explored, the parallel increase in the immature and mature forms of G5 and G8 suggest that post-Golgi complex stability was not altered as this would result in selective accumulation of the mature form of each protein.

ER function and G5G8

ER **s**tress is thought to play a causative role in the development of liver dysfunction in mice lacking leptin or its receptor and may directly contribute to the reduction in G5G8 in db/db mice. However, markers of ER stress are also induced in mice following high fat feeding and G5G8 levels are unaffected or even increased depending on the lipid composition of the diet [211-213]. While these observations were suggestive of a direct effect of leptin signaling on G5G8 abundance, direct effects of leptin could not be demonstrated. The reduction in G5G8 associated with ER stress in *ob/ob* and *db/db* mice may simply be a matter of degree. The extent of obesity, steatosis, insulin resistance, and ER dysfunction is

generally greater in these mice compared those with an intact leptin axis and challenged with various high fat diets. Alternatively, the lack of reduction in G5G8 protein in other models may reflect a compensatory increase in G5G8 transcription that overcomes reduced efficiency of complex formation within the ER. In addition, we previously reported that other glycoproteins, including the closely related family member ABCG2, were not affected in mice harboring defects in leptin or its receptor [166]. Rescue of the complex by AdGRP78 implicates ER dysfunction as a mechanism contributing to reduced G5G8, but what accounts for the selective depletion of G5G8 in *db/db* and *ob/ob* mice remains unknown. Perhaps G5G8 assembly is particularly sensitive to ER dysfunction. Alternatively, there may be some synergistic effect of the absence of leptin signaling and fatty liver phenotype on G5G8 abundance.

We previously reported that the loss of G5G8 increased markers of ER stress in HF-fed mice, establishing that biliary cholesterol secretion is essential to maintain hepatocyte function [165]. Excess unesterified cellular cholesterol is known to induce ER stress in a number of cell types, including hepatocytes [124, 214, 215]. Conversely, ER stress reduces ABCA1 and SR-BI and impairs cholesterol efflux in cultured hepatocytes [216]. Similar to G5G8, AdGRP78 increased ABCA1 and SR-BI in *db/db* mice, suggesting that ER dysfunction perturbs multiple facets of hepatic sterol metabolism in *db/db* mice. Collectively, the data support a reciprocal relationship between ER function and cholesterol

metabolism in which disturbances in cholesterol homeostasis contribute to ER stress and ER stress contributes to disruptions in cellular cholesterol metabolism.

Copyright © Yuhuan Wang 2015

CHAPTER 3. THE COMBINATION OF EZETIMIBE AND URSODIOL PROMOTES FECAL STEROL EXCRETION AND REVEALS A G5G8-INDEPENDENT PATHWAY FOR CHOLESTEROL ELIMINATION

INTRODUCTION

Elevated cholesterol is an important risk factor for CVD and strategies to promote cholesterol elimination have long been employed to reduce the risk of atherosclerosis. An emerging body of literature suggests that cholesterol also plays an active role in the development of NAFLD and its progression to NASH. Adding cholesterol to a HF diet in C57BL/6J mice leads to significantly more profound hepatosteatosis, inflammation, and fibrosis resembling human NASH [117]. Similarly, in LDLR deficient mice, adding cholesterol to a HF, high-sucrose diet exacerbates the development of insulin resistance and steatosis resulting in NASH [118]. In a mouse model of Alström syndrome (*Alms1* mutant or *foz/foz* mice), an elevation in hepatic FC due to an increase in hepatic uptake and a decrease in biliary elimination is thought to play a contributing role in the development of liver disease [124]. Strategies that promote hepatic cholesterol elimination are likely to have therapeutic benefit in NAFLD.

The G5G8 heterodimer is the primary mediator of hepatobiliary elimination, accounting for 70% to 90% of biliary cholesterol secretion [152]. In addition, it also opposes phytosterol absorption in the proximal small intestine [148, 152].

We previously reported that G5G8 plays an essential role in the development of diet-induced obesity phenotypes independent of its role in opposing phytosterol accumulation. The absence of G5G8 and reduced biliary cholesterol secretion resulted in hepatic cholesterol accumulation, acceleration of obesity and insulin resistance, and worsening of NAFLD in mice challenged with a plant sterol-free (PSF) HF diet [165]. Conversely, increasing biliary cholesterol secretion by adenoviral expression of G5G8 restored glycemic control, improved hepatic insulin signaling, and lowered plasma TGs in genetically obese, *db/db* mice [167].

Increased biliary and fecal sterol elimination following adenoviral G5G8 would presumably lower plasma cholesterol levels in *db/db* mice. However, a significant portion of the secreted cholesterol was reabsorbed, resulting in a paradoxical increase in plasma cholesterol despite increased biliary output. This effect of adenoviral G5G8 can be overcome by co-administration of EZ, a potent inhibitor of cholesterol absorption that blocks NPC1L1 activity in the intestine [167, 217]. Similar observations were made in atherosclerosis studies in which a G5G8 transgene expressed in both liver and intestine lowered LDL-C and reduced lesion area, whereas a liver specific transgene was ineffective in the absence of EZ [168, 169]. These observations indicate an interdependent relationship between biliary secretion and intestinal absorption for effective fecal cholesterol elimination. Consequently, therapeutic approaches to promote cholesterol elimination by targeting the hepatobiliary pathway are likely to be limited by

intestinal reabsorption of secreted cholesterol. Thus, a combination therapy that increases biliary cholesterol secretion and simultaneously reduces intestinal absorption is likely to act additively in the elimination of cholesterol from the body.

While EZ is effective in reducing cholesterol absorption, no currently available therapeutics directly target the G5G8 sterol transporter to increase biliary cholesterol secretion. However, we previously published that TUDCA increases G5G8 and biliary cholesterol in both lean and obese, *db/db* mice [166]. TUDCA is a first pass metabolite of ursodiol (Urso). Studies in mice have shown that TUDCA and its unconjugated precursor, Urso, have a number of beneficial effects on liver function including alleviation of ER stress, improved insulin sensitivity and reduced lipogenesis [111, 166, 218]. However, the effect of Urso on increasing G5G8 and promoting biliary secretion of cholesterol has not been characterized.

In the present study, we confirmed that Urso had similar effects on G5G8 as TUDCA. Urso increased hepatic G5G8 and dose-dependently accelerated both biliary and fecal sterol excretion. We then tested whether an Urso-EZ combination treatment would act additively to promote cholesterol elimination. We treated mice with a constant dose of Urso or Urso in combination with two doses of EZ. EZ produced an additive effect for fecal sterol excretion in the presence of Urso. Although biliary and fecal neutral sterols (FNS) were

invariably lower in G5G8 KO mice, we observed an increase in FNS following Urso alone or Urso-EZ combination treatments. The magnitude of this increase was not affected by genotype suggesting that there may be a G5G8-independent pathway for cholesterol elimination stimulated by Urso.

MATERIALS AND METHODS

Chemicals, reagents and antibodies

General chemicals were purchased from Sigma, immunoblotting reagents from Thermo/Pierce, real-time PCR reagents from Applied Biosystems. Tauroursodeoxycholic acid, sodium salt (580549-5GM) was purchased from Calbiochem. Ursodiol capsules, USP (NDC 42806-503-01) were purchased from Epic Pharma, LLC and Zetia (ezetimibe) tablets (NDC 66582-414-54) from Merck & Co., Inc. Urethane, bromodeoxyuridine (BrdU), and the silylation reagent *N*, *O*-Bis (trimethylsilyl) trifluoroacetamide (BSTFA) were purchased from Sigma-Aldrich. The chicken anti-G5 polyclonal antibody and the monoclonal antibody directed against G8 were previously reported [154, 165]. The β-actin antibody was purchased from Sigma. Anti-ABCA1, [26, 26, 26, 27, 27, 27-$^{2}H_{6}$] cholesterol and [5, 6, 22, 23-$^{2}H_{4}$] sitostanol were generous gifts from Ryan Temel (University of Kentucky) [219]. The anti-CD3 monoclonal antibody (clone 145-2C11) was purified over protein G beads (Amersham Pharmacia Biotech, Piscataway, NJ). Anti-BrdU was purchased from MPL International, Woburn, MA.

EZ- and/or Urso-supplemented diets

Powdered rodent chow diet (T.2018M.15) was purchased from Harlan Laboratories. Custom formulated pellet (D10040301) and powdered (D10040301M) PSF diets were purchased from Research Diets, Inc. Macronutrient composition and sterol content were previously described [165]. There was no added cholesterol in the diet. Both Urso and EZ were ground into a fine powder, and then thoroughly mixed with control diet (T.2018M.15 or D10040301M) to obtain the desired concentrations. Powdered diets were provided to mice in glass feeding jars and replaced daily.

Animal husbandry

C57BL/6J (Stock #000664) mice were purchased from The Jackson Laboratory (Bar Harbor, ME). Mice homozygous for the *Abcg5* and *Abcg8* mutant alleles (KO) and their WT littermates were obtained from heterozygous, trio matings as previously described [165]. Mice were housed in individually ventilated cages in a temperature-controlled room with a 14:10 light: dark cycle and provided with enrichment in the form of acrylic huts, wood chew sticks, and nesting material. Mice were adapted to powdered diet for a period of 7 days prior to initiation of studies. The diet was then changed to those containing various concentrations of Urso and EZ. All animal procedures conform to PHS policies for humane care and use of laboratory animals and were approved by the institutional animal care and use committee at the University of Kentucky. All surgery was performed under anesthesia, and all efforts were made to minimize suffering.

Animal experiments

Male C57BL/6J mice (n=6/group) were fed chow (control), chow supplemented with 0.4% TUDCA (w/w), or Urso at concentrations of 0.1%, 0.3%, or 1% (w/w) for 7 days. Mice were housed (2 per cage) in individually ventilated cages. Mice were placed in clean cages to collect feces for 3 days prior to termination. On the final day of the study, mice were transferred to clean cages and fasted for 4 hours. The bile duct was ligated, and the gallbladder cannulated for basal bile collection (30 min) under urethane (1 g/kg body weight) anesthesia. Bile flow was determined gravimetrically assuming a density of 1 g/ml. Mice were then exsanguinated, and tissues dissected, frozen in liquid nitrogen, and stored at -80°C until analysis. Details were shown in the experimental outline for Urso dose-dependent study (Fig 3.1).

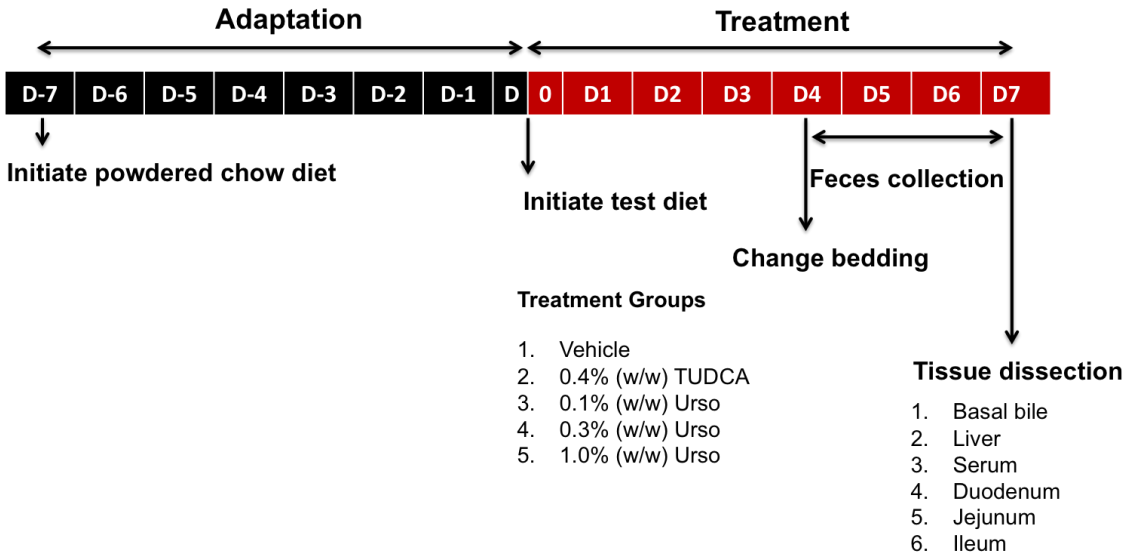

Figure 3.1 Experimental outline for the Urso dose-dependent study.

Another cohort of male C57BL/6J mice (n=7) were fed chow (control), chow supplemented with 0.3% Urso or 0.3% Urso combined with 0.001% or 0.005% EZ for 14 days and were housed individually. Feces, basal bile, and other tissues were collected as described above (Fig 3.2).

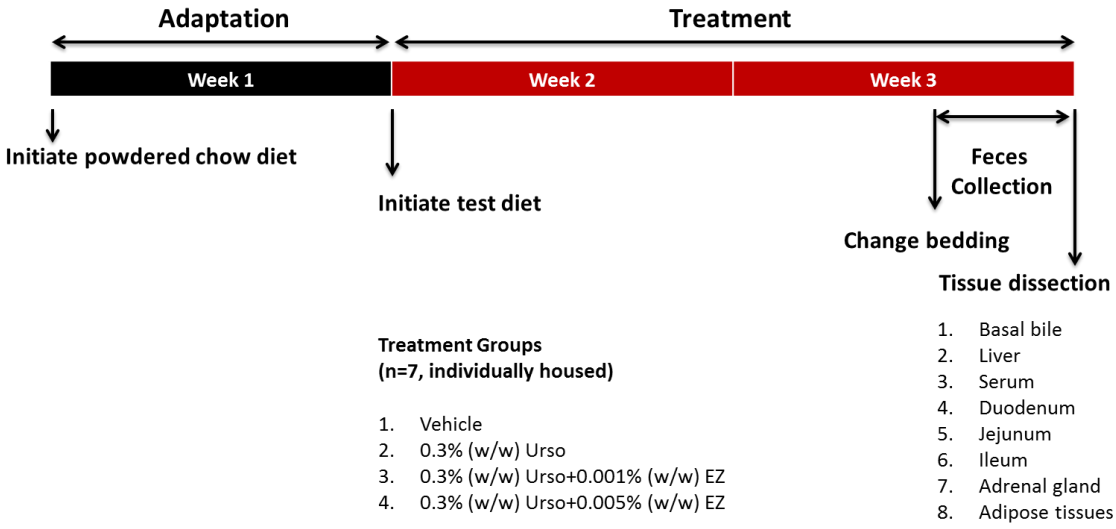

Figure 3.2 Experimental outline for the Urso-EZ combination study.

G5G8 KO mice (n=4 both male and female) and their WT littermates (n=6 male and 7 female) were weaned between 18 and 21 days onto a pellet PSF diet to prevent the development of Sitosterolemia [165]. When maintained on this diet, serum levels of phytosterols are less than 10% of those observed in G5G8 KO mice maintained on chow diet and do not differ between genotypes (Fig 3.3). Prior to initiation of the study, mice were adapted to a powdered PSF (vehicle) diet for 7 days. Then, mice were fed a vehicle diet for 10 days (Phase I) followed by 0.3% Urso for 7 days (Phase II). All mice were then treated with 0.3% Urso

combined with 0.005% EZ for 14 days (Phase III). Feces were collected the final 3 days of each phase. Blood samples were collected by cheek bleed at the final day of each phase. At termination following phase III, basal bile and tissues were harvested as described above (Figure 3.4).

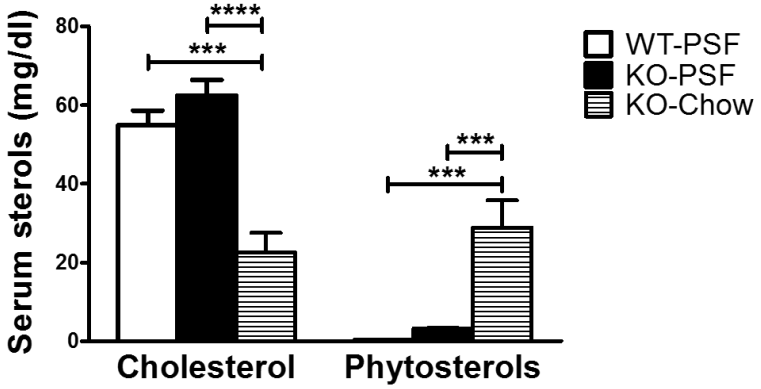

Figure 3.3 Serum levels of cholesterol and dietary phytosterols in mice maintained on a PSF diet. The concentrations of cholesterol and dietary phytosterols in G5G8 KO mice (n=3) and their WT littermates (n=3) were simultaneously determined by GC-MS. Serum samples from KO mice maintained on standard rodent chow were used as positive controls. Data are mean ± SEM. Differences were determined by one-way ANOVA followed by Bonferroni post-hoc tests. ***p<0.001, ****p<0.0001.

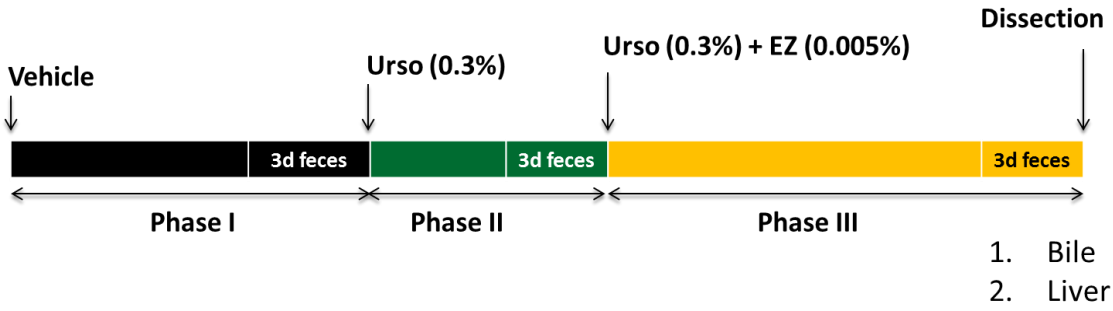

Figure 3.4 Experimental outline for the G5G8-dependent study

Another cohort of male and female G5G8 KO and WT mice (n=3 for each gender and genotype) treated with 0.3% Urso or a PSF vehicle diet for 7 day were used

to measure both fractional cholesterol absorption and intestinal epithelial cell sloughing as described with modifications [220, 221]. Mice were individually housed and adapted to a powdered PSF (vehicle) diet 7 days prior to the experiment in wire bottom cages. Each mouse was gavaged with 50 µl of deuterated sterol/stanol-oil mixture. Feces were collected for 3 days after oral gavage. To determine the relative rates of intestinal epithelial cell proliferation and turnover, each mouse was injected i.p. with 1 mg BrdU 2 hours before tissue dissection. Blood samples were collected, and three segments of the small intestine were harvested and fixed in 10% neutral buffered formalin for immunohistochemistry.

Immunoblot and Quantitative Real-time PCR

The preparations of proteins, SDS-PAGE, and immunoblotting were conducted as previously described [165, 167]. Total RNAs were extracted from each liver using the RNA STAT-60 (Tel-Test, Inc.) and subjected to cDNA synthesis with iScript cDNA Synthesis Kit (BIO-RAD, Hercules, CA). To determine relative abundance, RT-PCR was conducted using SYBRGreen detector on Applied Biosystem 7900HT fast-Real Time PCR System (Carlsbad, CA) [165].

Hepatic, serum, and biliary lipid analysis

Hepatic lipids were extracted by using folch reagents as previously described [167]. Total and non-esterified hepatic and serum cholesterol, as well as cholesterol and phospholipids in gallbladder bile, were determined using

commercial colorimetric-enzymatic assays (Wako Chemicals, Richmond, VA). The quantitation of total bile acids in bile was performed enzymatically by measuring 3α-hydroxy bile acids as previously described [222]. Serum was fractionated by fast protein liquid chromatography (FPLC), and fractions were analyzed for total cholesterol content as previously described [165]. The concentrations of lathosterol and phytosterols in serum were measured by LC/MS/MS and GC-MS, respectively using modifications of previously published methods [2, 223-225].

Fecal Neutral Sterols (FNS)

FNS were analyzed as previously described with minor modifications [167]. Briefly, total feces from the 72-h period were collected, dried at 37 °C, weighed, and ground to powder. An aliquot of 0.30 g of feces was placed into a glass tube with 2.5 ml of ethanol and 0.5 ml of 10 N NaOH. Lipids were saponified at 72 °C in a water-bath for 2 h and extracted (water: ethanol: petroleum ether, 1:1:1, v/v/v). 0.12 mg of 5α-cholestane (1 μg/μl) was used as the internal standard. Following extraction, the organic phase was dried under nitrogen gas and solubilized in hexane. The amount of neutral sterols (cholesterol, coprostanol, and cholestanol) was quantified by GC-MS.

Lathosterol Analysis

Serum lathosterol concentrations were measured by LC/MS/MS. Lipids and sterols were extracted from 10 μl mouse serum by the modified Bligh/Dyer method [224]. D7-Lathosterol (10 μl of 100 ng/mL in methanol; Avanti Polar

Lipids, Alabaster, Al) was added to serum as internal standard and extracted sterols were converted to picolinyl esters by derivatization [225], and reconstituted into 300 µl acetonitrile. Lathosterol calibrators (30, 60, 100, 150, 250 and 500 ng/ml) and quality control samples (50, 125, and 200 ng/ml) were prepared in the absence of serum. Processed samples were analyzed immediately for lathosterol content by injection (45 µl) onto a Shimadzu Prominence LC system coupled to an API 2000 MS/MS through an electrospray ionization source (+mode/5500V/500˚C/GS1 at 50/GS2 at 40). The picolinyl esters (PE) of D7-lathosterol and of lathosterol, were resolved from the cholesterol-PE (R_t of 31.2, 32.0, and 34.5 min, respectively) using a Luna C_{18} (2)-HST analytical column (2.5 µ; 100x2 mm) with a guard column (C18; 4x2-mm). The isocratic mobile phase (0.25 mL/min) was 96:4 acetonitrile: 10 mM ammonium formate. Molecular ion transitions (499.4/376.5 (D7-PE) and 492.5/369.5 (lathosterol-PE) m/z) were monitored using voltages optimized from the individual analyte infusions in mobile phase. Linear regression analysis (R^2=0.9985 with 1/x weighting) relating the mass ratios to the area ratios of lathosterol to D7-lathosterol was performed with Analyst® software (Ver. 1.4.2). Repeated processing of pooled control serum indicated adequate reproducibility (avg=90.6 ng/mL ± 2.2, RSD=2.4%, n=4) of the overall method. Standard and quality control samples processed alongside experimental samples, demonstrated accuracy of 92.7-109% of nominal values.

Phytosterol analysis

Total cholesterol and phytosterol concentrations in serum were measured by GC-MS as described with minor modifications [223]. Briefly, 20 µl of serum was saponified in 4% sodium hydroxyide/ethanol at 65°C for 2 h after addition of 5α-cholestane as a quantitative internal standard. Lipids were extracted using 2 ml of petroleum ether and the organic fraction from each extract was removed and dried under nitrogen. The residual lipids were reconstituted in *N*, *O*-Bis (trimethylsilyl) trifluoroacetamide (BSTFA, Sigma-Aldrich) and derivatized at 75°C for 15 min. The samples were fractionated by GC using an HP-5MS 5% Phenyl Methyl Siloxane column and quantified by electron ionization-MS operating in single-ion-monitoring mode. Each sterol was quantified using ions with the following m/z: cholesterol 458; campesterol 472; sitosterol 486.

Determination of fractional cholesterol absorption

Fractional absorption of cholesterol was measured as described with modifications [220]. Briefly, a mixture containing 8 mg of [26, 26, 26, 27, 27, 27-$^{2}H_{6}$] cholesterol and 8 mg of [5, 6, 22, 23-$^{2}H_{4}$] sitostanol was prepared and dissolved in 4 mL of vegetable oil. A single dose of the deuterated sterol/stanol-oil mixture (50 µl) was gavaged to each mouse. Feces were collected for 3 days after oral gavage, pooled, dried, and homogenized. An 80mg aliquot of stool from each mouse was saponfied in 4% sodium hydroxyide/ethanol at 65°C for 2 h after addition of 80 µg of 5α-cholestane as an internal standard. Two milliliters of nano-pure water were added, and sterols and stanols were extracted with 2 ml

of hexane. Five hundred microliters of organic fraction were dried under nitrogen, and the residual sterols and stanols were dissolved in 400 µl of BSTFA and reacted at 75°C for 15 min. A 10 µl aliquot of oil mixture was extracted following the same procedure as fecal samples. Sterols and stanols were separated by GC on an HP-5MS column. Selective ion monitoring was performed at m/z 464 for D6-cholesterol, m/z 493 for D4-sitostanol. The fractional absorption of cholesterol was calculated using the following equation.

$$\frac{\left(\frac{[2H6]\text{cholesterol}}{[2H4]\text{sitostanol}}\ \text{dose ratio} - \frac{[2H6]\text{cholesterol}}{[2H4]\text{sitostanol}}\ \text{feces ratio}\right)}{\frac{[2H6]\text{cholesterol}}{[2H4]\text{sitostanol}}\ \text{dose ratio}}$$

$$\times\ \text{dose ratioanoll. Selective ion mon}$$

Determination of intestinal epithelial cell sloughing

The jejunal epithelial cell sloughing was indirectly determined by doing a pulse chase experiment using Bromodeoxyuridine (BrdU) as described with modifications [221]. Briefly, each mouse was injected i.p. with 1mg BrdU 2 hours before killing. Antibodies directed against CD3 were used as positive control to stimulate proliferation and cell turnover. A group of 3 WT mice were injected with anti-CD3 18 hours before BrdU injection. Detection of nuclei that had incorporated BrdU was performed by immuno-histochemistry. The anti-BrdU antibody was diluted 1:400 in Powerblock (Dako, Carpinteria, CA). The rat IgG ABC kit (Vector Laboratories, Burlingame, CA) and DAB substrate chromagen

(DAKO) were used to develop BrdU staining. Images were acquired using an Olympus DP71 camera (Tokyo, Japan) and measurements were made using ImageJ (NIH, Bethesda, MD). Sections were analyzed by scoring 20 crypts per mouse, 3 mice per group. Each crypt unit was scored for BrdU positive cells. Villus height and crypt depth were measured as well. The slides were also stained with hemotoxylin and eosin (H&E) to visualize the enterocyte histology. The scale bar represents 50 microns for BrdU staining and 100 microns for H&E.

Statistical Analysis

All statistical analyses were conducted using GraphPad Prism. Data are expressed as mean ± SEM. Data shown in Fig 3.5-7 were analyzed by two-tailed t-test or one-way ANOVA followed by Dunnett's post-hoc comparisons. Data shown in Fig 3.8-14 were analyzed by one-way ANOVA followed by Bonferroni post-hoc tests. Data shown in Fig 3.15-17 were analyzed by a two-way ANOVA or a repeated measure two-way ANOVA using genotype and treatment as factors. Post-hoc comparisons were made using Bonferroni tests. Differences were considered significant at $P < 0.05$. Where genotype and treatment by sex interactions were not significant, data were analyzed independent of sex.

RESULTS

Urso increases G5G8 and both biliary and FNS in a dose-dependent manner

To determine if Urso could increase G5G8 and biliary cholesterol secretion and elimination, mice were fed chow (control) or chow supplemented with 0.1%,

0.3%, or 1% (w/w) Urso. TUDCA (0.4%, equal molar ratio to 0.3% Urso) was used as a positive control as it was previously shown to increase G5G8 and biliary cholesterol secretion. The abundance of hepatic G5 and G8 was evaluated by immunoblot analysis (Fig 3.5A). Urso increased hepatic G5G8 to a similar level at all tested doses. Its effects were equal to, or slightly greater than TUDCA, particularly for G8. Biliary cholesterol and FNS were used as indirect measures of G5G8 activity. Hepatobiliary cholesterol secretion rates under basal conditions were calculated from the product of bile flow and cholesterol concentration. Urso dose-dependently increased both biliary cholesterol secretion rates and FNS (Fig 3.5B-C). Similarly, Urso increased biliary secretions of both phospholipids and bile acids in a dose-dependent manner (Fig 3.6).

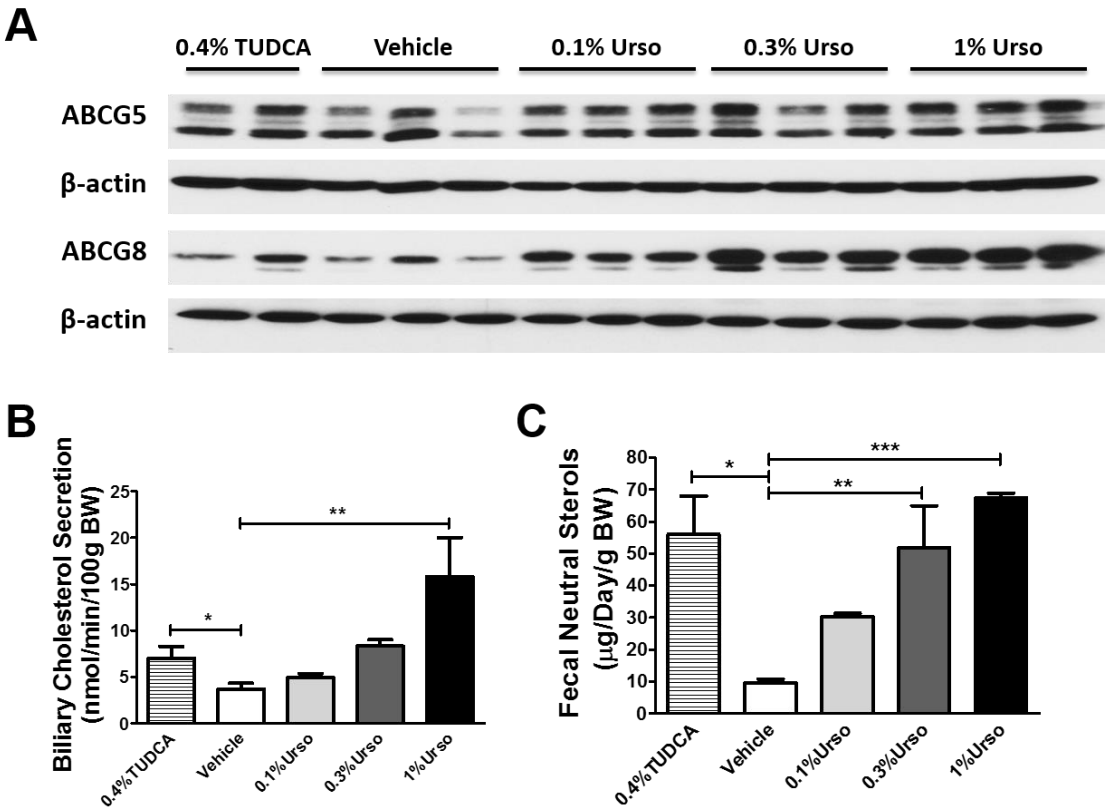

Figure 3.5 Urso increases G5G8 and both biliary and FNS in a dose-dependent manner. Male C57BL/6 mice were fed with control, 0.4% TUDCA, or three doses of Urso for 7 days. (A) Hepatic levels of ABCG5 and ABCG8 protein expression were determined by immunoblotting. Membrane preparations were blotted for β-actin as controls. (B) Hepatobiliary cholesterol secretion rates under basal conditions. Gallbladder was cannulated and basal bile was collected for 30 min. n=6 for each group. (C) FNS was determined by GC-MS. n=3 for each group. Data are presented as mean ± SEM. Differences between TUDCA and control were determined by two-tailed t-test. Differences between control and three doses of Urso were determined by one-way ANOVA followed by Dunnett's tests. *p<0.05, **p<0.01, ***p<0.001.

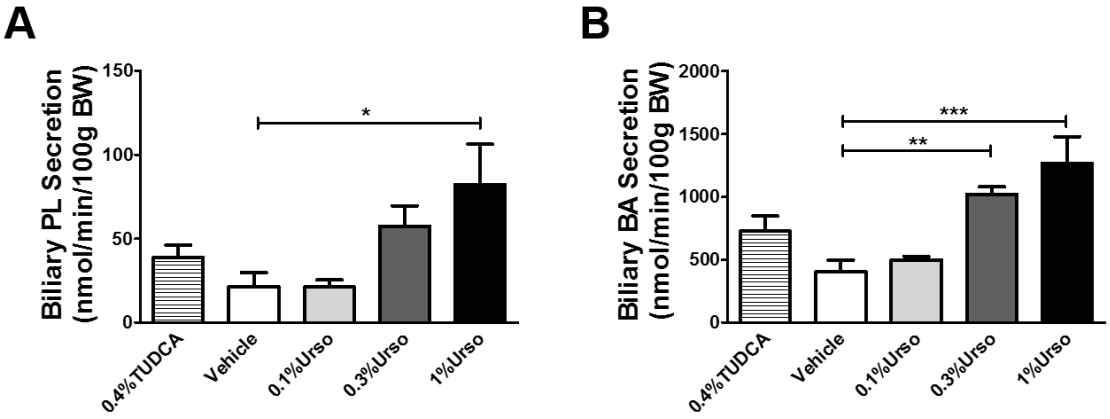

Figure 3.6 Urso increases biliary secretion rates of phospholipids and bile acids. Male C57BL/6 mice were fed with control, 0.4%TUDCA, or three doses of Urso for 7 days. Hepatobiliary secretion rates of phospholipids (A) and bile acids (BAs) (B) under basal conditions. n=6 for each group. Data are presented as mean ± SEM. Differences between TUDCA and control were determined by two-tailed t-test. Differences between control and three doses of Urso were determined by one-way ANOVA followed by Dunnett's tests. *p<0.05, **p<0.01, ***p<0.001.

Urso suppresses bile acid synthesis, but had no effect on cholesterol levels in liver or serum.

Urso had no effect on either serum or hepatic total cholesterol at any of the doses examined (Fig 3.7A, B). To determine if the increased FNS was due to increased cholesterol synthesis, we measured the mRNA expression level of HMGCR and

HMGCS and observed no virtual differences (Fig 3.7C). To investigate the effects of Urso on bile acid biosynthesis, the mRNA expression level of CYP7A1, CYP8B1, CYP7B1, and CYP27A1 was quantified by RT-PCR (Fig 3.7D). TUDCA significantly decreased both CYP7A1 and CYP8B1, but not CYP7B1 and CYP27A1 (not shown). Similarly, both CYP7A1 and CYP8B1 decreased in a dose-dependent manner following Urso treatment. As with TUDCA, Urso had no effect on CYP7B1 and CYP27A1 expression levels (not shown).

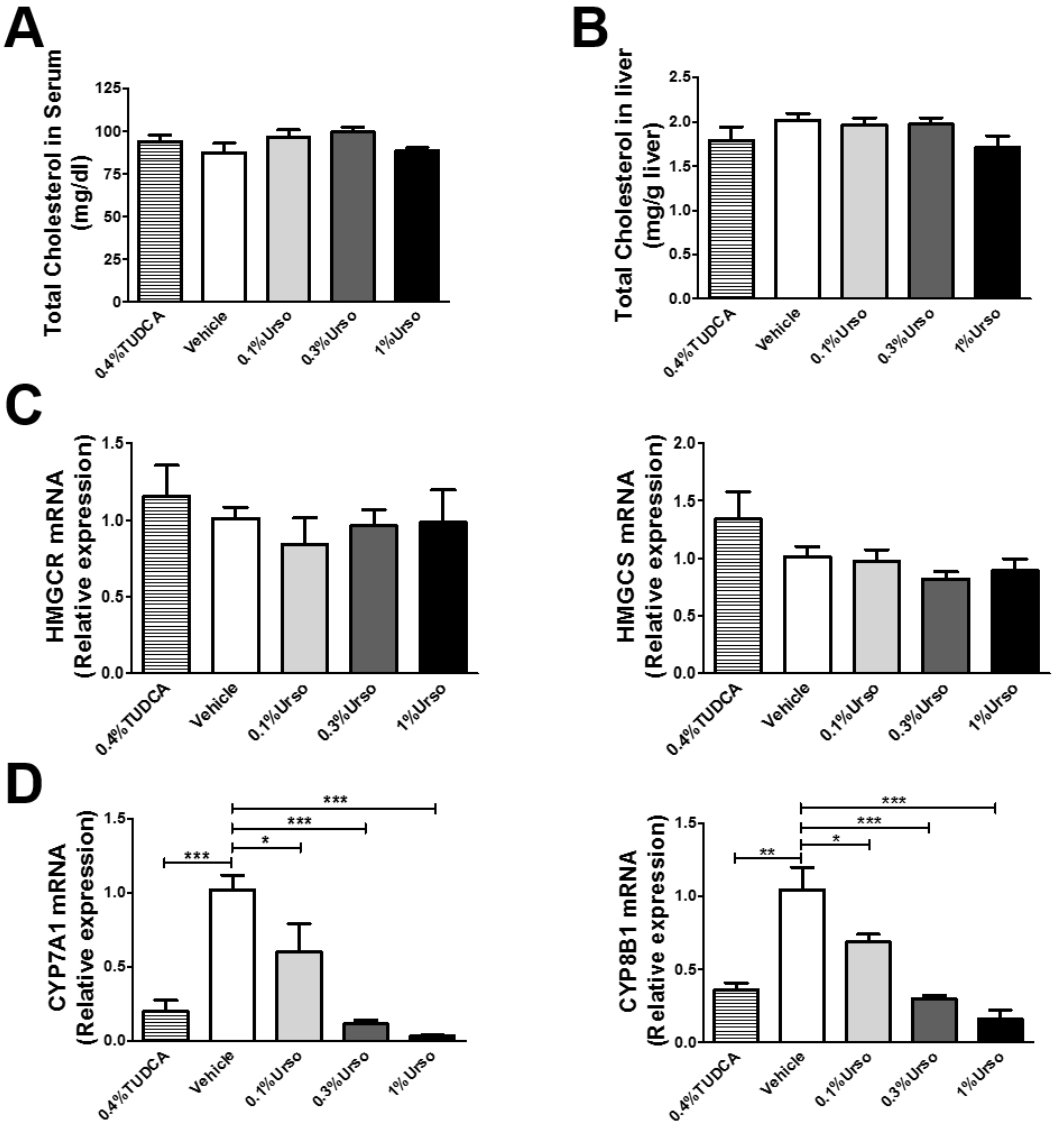

Figure 3.7 Urso suppresses bile acid synthesis, but had no effect on cholesterol levels in liver or serum. (A) Total cholesterol concentrations in serum. n=6 for each group. (B) Hepatic total cholesterol per gram of wet tissue weight. n=6 for each group. The mRNA expression for de novo cholesterol synthetic genes HMGCR and HMGCS (C) and bile acid synthetic genes CYP7A1 and CYP8B1 (D) was determined by RT-PCR. n=4-5 for each group. Data are mean ± SEM. Differences between TUDCA and control were determined by two-tailed t-test. Differences between control and three doses of Urso were determined by one-way ANOVA followed by Dunnett's tests. *p<0.05, **p<0.01, ***p<0.001.

EZ produces an additive effect for fecal sterol elimination.

To determine if EZ plays an additive role for accelerating cholesterol elimination, we treated mice with 0.3% Urso combined with two doses of EZ for 14 days. As with 7-day treatment, 0.3% Urso increased G5G8 protein levels in liver. This effect was maintained in the presence of both low- and high-doses of EZ (Fig 3.8A). The presence of EZ had no effect on biliary secretion rates of cholesterol as well as phospholipids and bile acids following 2-weeks of treatment (Fig 3.8B, 3.9). However, EZ dose-dependently increased FNS in the presence of 0.3% Urso (Fig 3.8C).

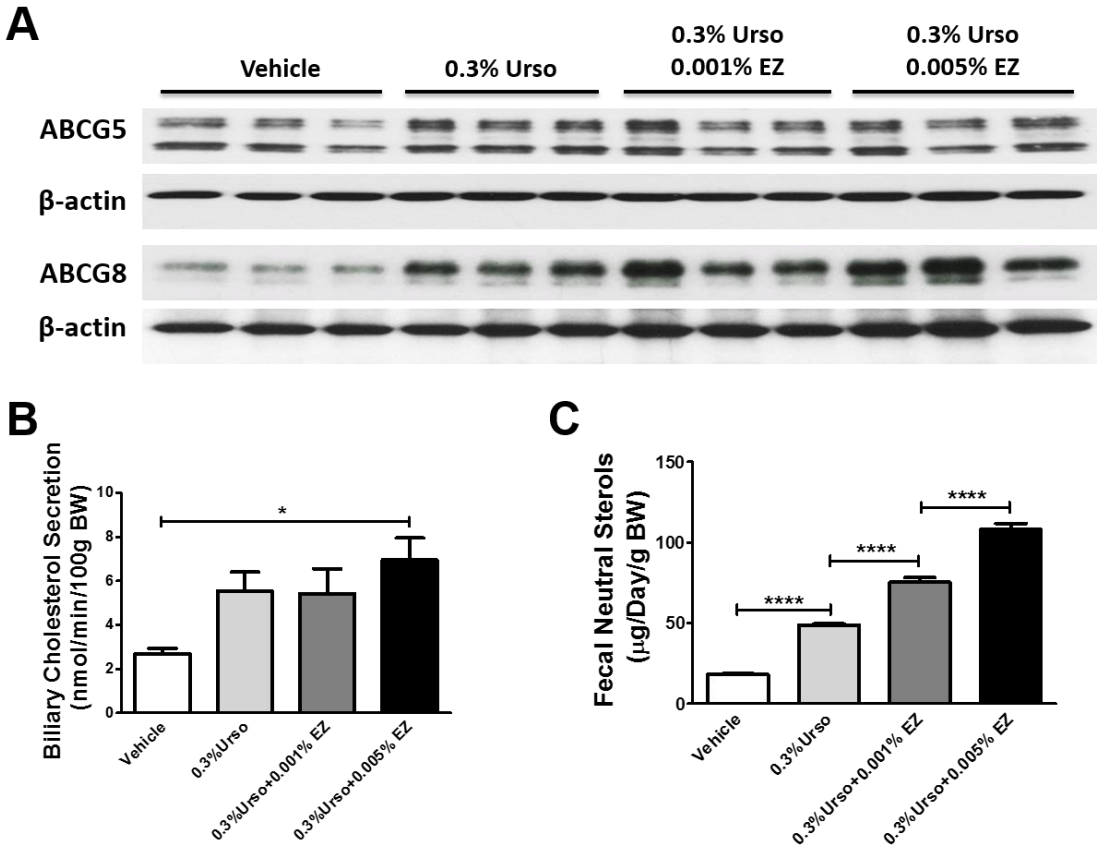

Figure 3.8 EZ produces an additive effect for fecal sterol elimination. Male C57BL/6 mice were fed with control, 0.3% Urso, or 0.3% Urso combined with a low or high dose of EZ for 14 days. (A) Hepatic levels of ABCG5 and ABCG8 protein expression were determined by immunoblotting. (B) Hepatobiliary cholesterol secretion rates under basal conditions. n=5-7 for each group. (C) FNS was determined by GC-MS. n=7 for each group. Data are presented as mean ± SEM. Differences were determined by one-way ANOVA followed by Bonferroni post-hoc tests. *p<0.05, ****p<0.0001.

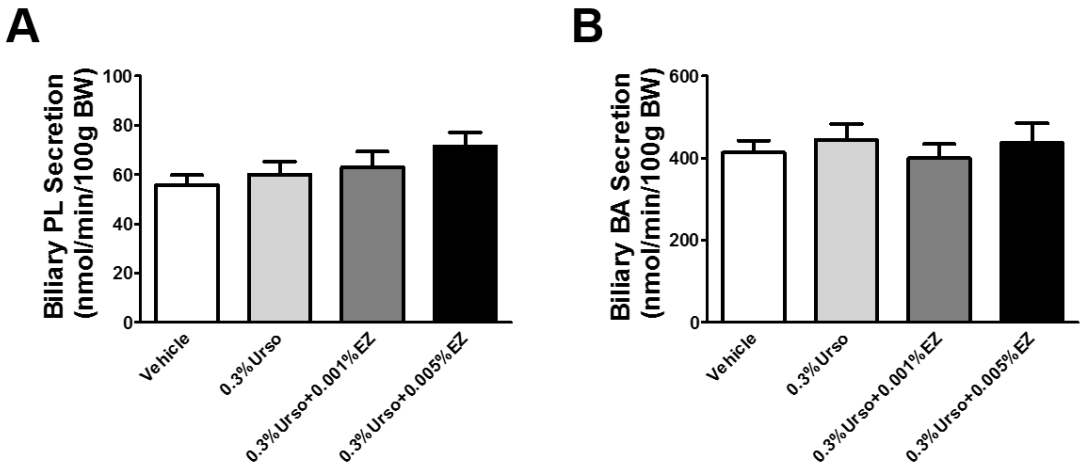

Figure 3.9 EZ has no additive effect on biliary secretion rates of phospholipids and bile acids. Male C57BL/6 mice were fed with control, 0.3% Urso, or 0.3% Urso combined with two doses of EZ for 14 days. Hepatobiliary secretion rates of phospholipids (A) and bile acids (BAs) (B) under basal conditions. n=5-7 for each group. Data are presented as mean ± SEM. Differences were determined by one-way ANOVA followed by Bonferroni post-hoc tests.

EZ reduces FC in serum, but has no additive effect on the biosynthesis of bile acids and cholesterol in liver.

EZ at a concentration of 0.005% slightly reduced serum total cholesterol. This was predominantly due to the significant reduction of FC (Fig 3.10A). No differences were observed in hepatic free (not shown) or total cholesterol (Fig 3.10B). Although there was a tendency towards suppression of cholesterol synthetic genes at the mRNA level, none achieved statistical significance (Fig 3.10C). We confirmed the prominent repression of CYP7A1 and CYP8B1 at the mRNA level in mice treated with Urso. EZ had no additional effect on their mRNA levels (Fig 3.10D). This effect of Urso is likely due to the stimulation of ileal FGF15 which feeds back to repress hepatic bile acid synthesis (Fig 3.11). To

determine if extrahepatic sources might contribute to the increased FNS in response to Urso-EZ, we examined the mRNA expression level of HMGCR and HMGCS in adrenal glands, epididymal adipose tissues, and jejuna as well as the circulating lathosterol, an indicator of whole body cholesterol synthesis (Fig 3.12, 13) [226]. Urso did not alter the expression level of HMGCR and HMGCS in tested tissues. However, the Urso-EZ combination increased HMGCS mRNA expression in both adrenal glands and jejuna (Fig 3.12). Circulating levels of lathosterol tended to increase, but did not reach statistical significance (Fig 3.13).

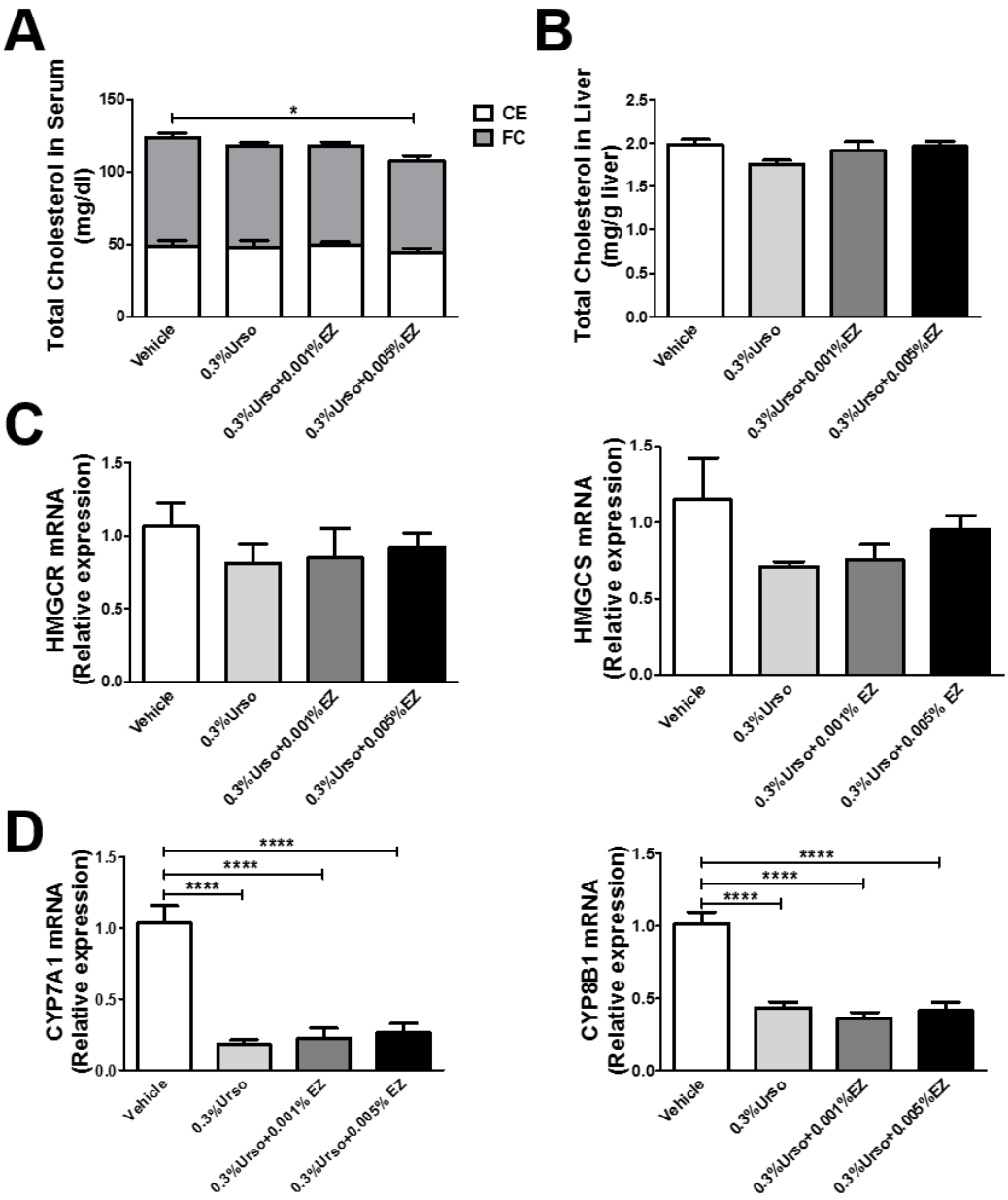

Figure 3.10 EZ reduces FC in serum, but has no additive effect on the biosynthesis of bile acids and cholesterol in liver. (A) Total cholesterol and non-esterified cholesterol (FC) were determined by Wako enzymatic-colorimetric kits. Cholesterol esters (CE) were calculated from the difference in total and FC. n=7 for each group. (B) Hepatic total cholesterol per gram of wet tissue weight. n=7 for each group. The mRNA expression for de novo cholesterol synthetic genes HMGCR and HMGCS (C) and bile acid synthetic genes CYP7A1 and CYP8B1 (D) was determined by RT-PCR. n=6 for each group. Data are mean ± SEM. Differences were determined by one-way ANOVA followed by Bonferroni post-hoc tests. *p<0.05, ****p<0.0001.

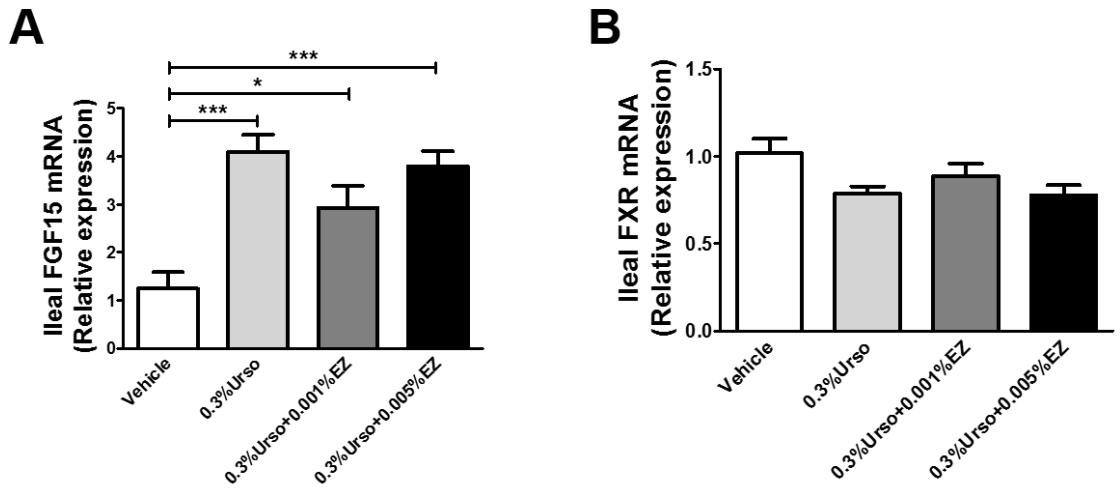

Figure 3.11 Urso decreases bile acid synthesis by stimulating ileal FGF15 expression. The mRNA expression for ileal FGF15 (A) and FXR (B) was determined by RT-PCR. n=6 for each group. Data are mean ± SEM. Differences were determined by one-way ANOVA followed by Bonferroni post-hoc tests. *p<0.05, ***p<0.001.

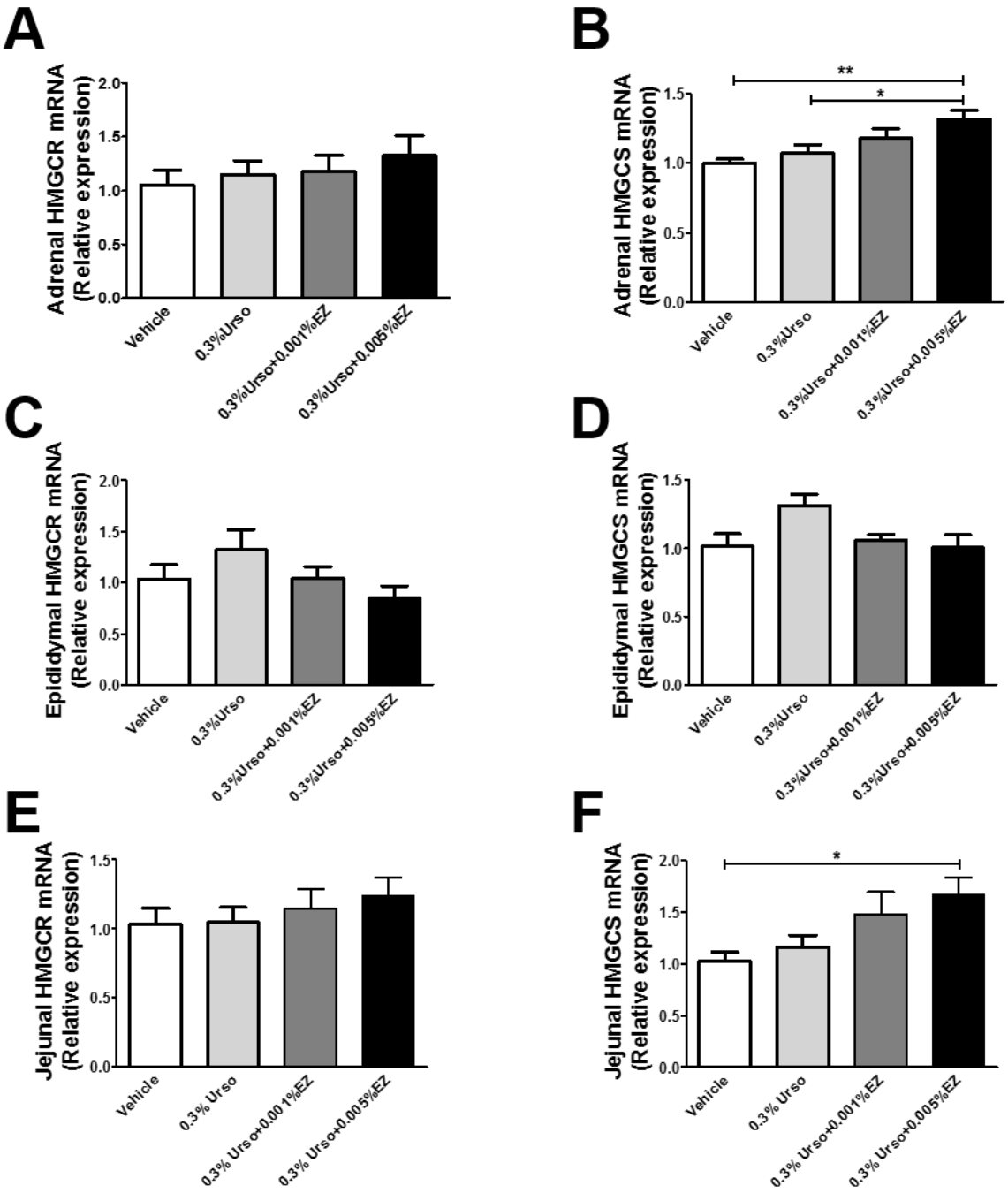

Figure 3.12 EZ increases HMGCS expression in adrenal glands and jejuna. The mRNA expression for de novo cholesterol synthetic genes HMGCR and HMGCS in adrenal glands (A-B), epididymal adipose tissues (C-D), and jejuna (E-F) was determined by RT-PCR. n=6 for each group. Data are mean ± SEM. Differences were determined by one-way ANOVA followed by Bonferroni post-hoc tests. *$p<0.05$, **$p<0.01$.

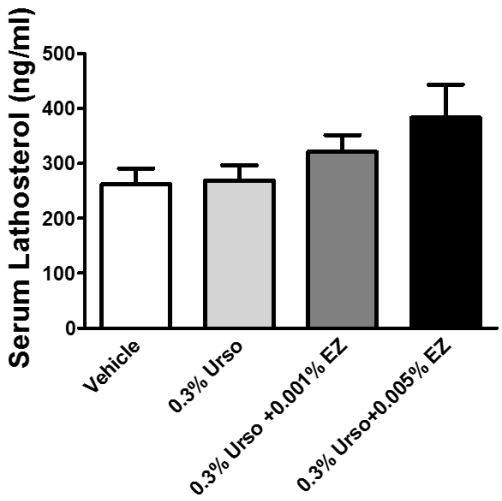

Figure 3.13 EZ has no additive effect on circulating lathosterol levels. Serum lathosterol concentrations were determined by LC/MS/MS. Data are mean ± SEM. Differences were determined by one-way ANOVA followed by Bonferroni post-hoc tests.

EZ reduces intestinal G5G8 and ABCA1.

With recent studies characterizing trans-intestinal cholesterol excretion (TICE) as an alternative route for cholesterol elimination, the role of the intestine has regained attention [227]. G5G8 is also abundantly expressed at the intestine to oppose cholesterol and phytosterol absorption. Therefore, we measured the jejunum expression of G5G8 at both mRNA and protein levels as well as intestinal ABCA1, which contributes to intestinal HDL biogenesis [228]. Urso alone tended to decrease jejunum G5G8 at the mRNA level, but didn't reach statistical significance (Fig 3.14A, B). However, immunoblot analysis indicated a marked reduction in G5G8 protein levels (Fig 3.14E). The combination of 0.005% EZ further reduced G5G8 both at mRNA and protein levels. We did not observe any change in NPC1L1 at the mRNA level (Fig 3.14C). The combination of Urso

and EZ also significantly decreased intestinal ABCA1 at both the mRNA and protein levels (Fig 3.14D, E). FPLC fractionation of serum indicated a reduction in HDL cholesterol and a modest shift toward smaller HDL particles (Fig 3.14F). Thus, the reduction in serum cholesterol concentrations is likely attributed to reduced ABCA1 and intestinally-derived HDL.

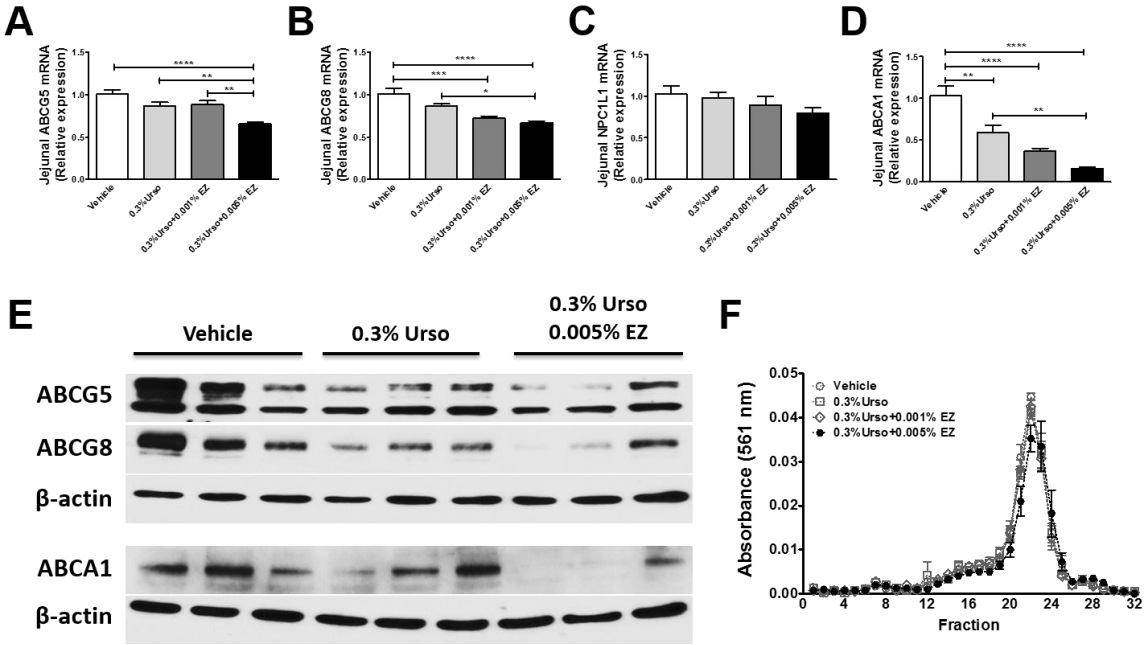

Figure 3.14 EZ reduces intestinal G5G8 and ABCA1. (A-D) The mRNA expression for jejunum ABCG5, ABCG8, NPC1L1, and ABCA1 was determined by RT-PCR. n=6 for each group. (E) Immunoblot analysis of jejunum ABCG5, ABCG8, and ABCA1. (F) Serum (60 µl) from 4 mice in each group was fractionated by FPLC and analyzed for the distribution of cholesterol among lipoproteins. Horizontal bars indicated elution fractions for lipoproteins. Data are mean ± SEM. Differences were determined by one-way ANOVA followed by Bonferroni post-hoc tests. *p<0.05, **p<0.01 ***p<0.001, ****p<0.0001.

Urso-EZ induced increase in FNS does not require G5G8.

To determine the extent to which the effect of Urso and Urso-EZ treatments were G5G8 dependent, WT and KO mice were maintained on a control diet, followed by Urso (0.3%), and then Urso-EZ (0.3%-0.005%). Each mouse served as its own control. 3-day fecal samples and blood were collected at the end of each treatment period. G5G8 KO mice presented slightly lower bile flow rates, but invariably lower rates of biliary cholesterol secretion (Fig 3.15A-B). In the absence of drugs, FNS were reduced by 52% in G5G8 KO mice compared to WT littermates (Fig 3.15C). Urso increased FNS in both WT and G5G8 KO mice by 900% and 700%, respectively (Fig 3.15D). EZ produced a further 2-fold increase in both genotypes (Fig 3.15D). Thus, while FNS were invariably lower in G5G8 KO mice, the drug-induced increase remained largely constant. Differences were not observed in serum cholesterol (not shown).

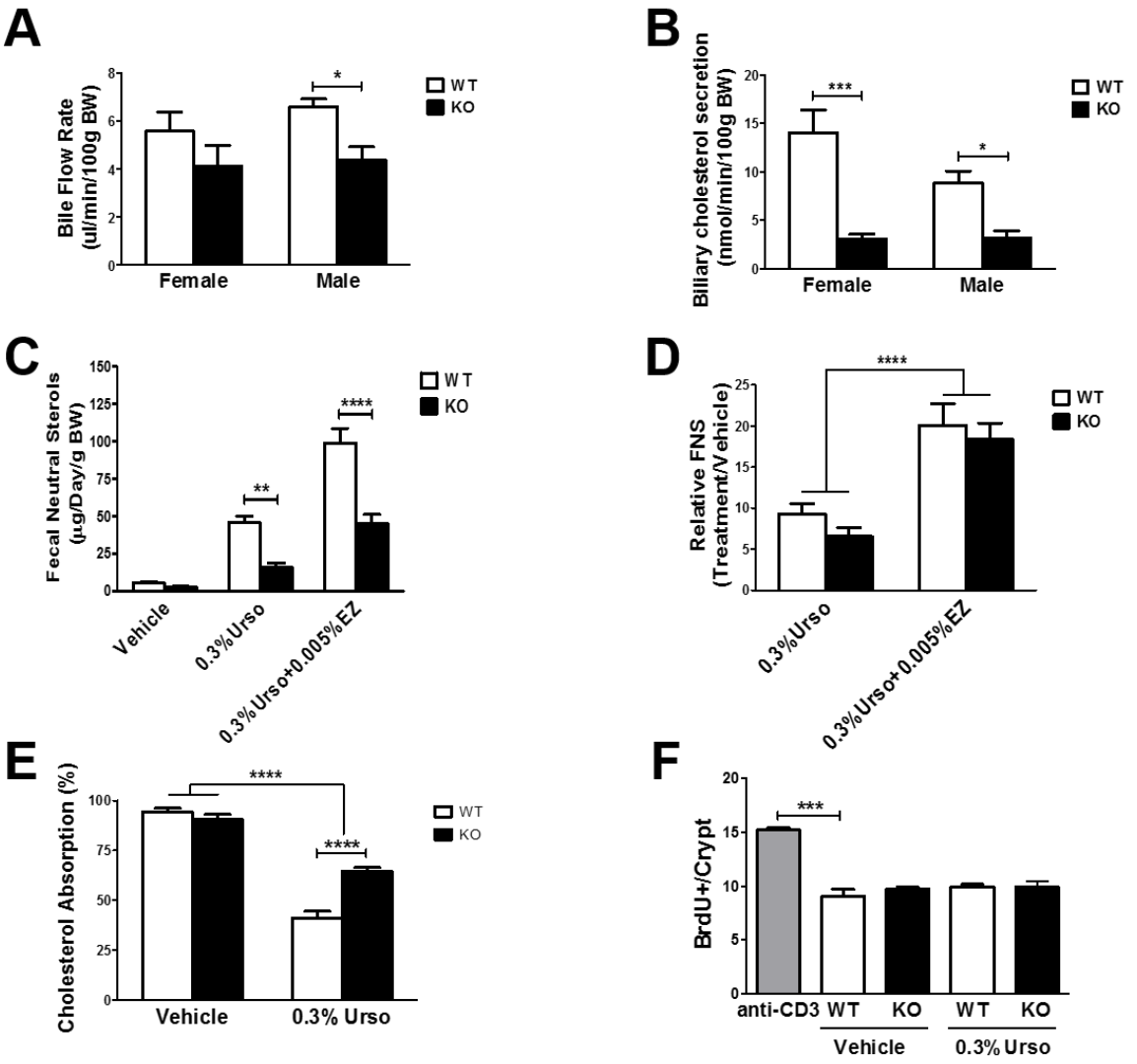

Figure 3.15 Urso-EZ induced increase in FNS does not require G5G8. G5G8 KO mice (n=4 both sexes) and their WT littermates (n=6 male and 7 female) were sequentially fed with control, 0.3% Urso, and 0.3% Urso plus 0.005% EZ for 14 days. (A-B) Bile flow and biliary cholesterol secretion rates by sex. (C-D) FNS and the relative difference in fecal sterol loss normalized to controls. Another cohort of male and female KO and WT mice (n=3 of each gender and genotype) were fed a PSF diet or 0.3% Urso for 7 days. (E) The fractional cholesterol absorption was measured by stable dual isotope method and represented irrespective of sex. (F) The relative rates of intestinal epithelial cell proliferation and turnover were determined by BrdU staining. Sections were scored, 20 villi/crypts per mouse, 3 mice per group, and the number of cells proliferating in jejunal crypts was determined. Data are expressed as mean ± SEM. Differences were determined by two-way ANOVA followed by Bonferroni post-tests (A, B, and E), a repeated measure two-way ANOVA using diet and genotype as factors followed by

Bonferroni post-hoc tests (C-D), and one-way ANOVA followed by Dunnett's post-hoc comparisons (F). *p<0.05, **p<0.01, ***p<0.001, ****p<0.0001.

Possible factors contributing to fecal neutral sterol excretion include intestinal cholesterol absorption and epithelial cell sloughing. There was no cholesterol added to the PSF diet. Under this condition, fractional cholesterol absorption approached 90% in both WT and KO mice (Fig 3.15E). Urso reduced absorption in both genotypes. This may reflect the role of G5G8 in cholesterol absorption or the dilution of the cholesterol isotope associated with increased biliary cholesterol output. Effects were virtually identical in male and female mice (Fig 3.16).

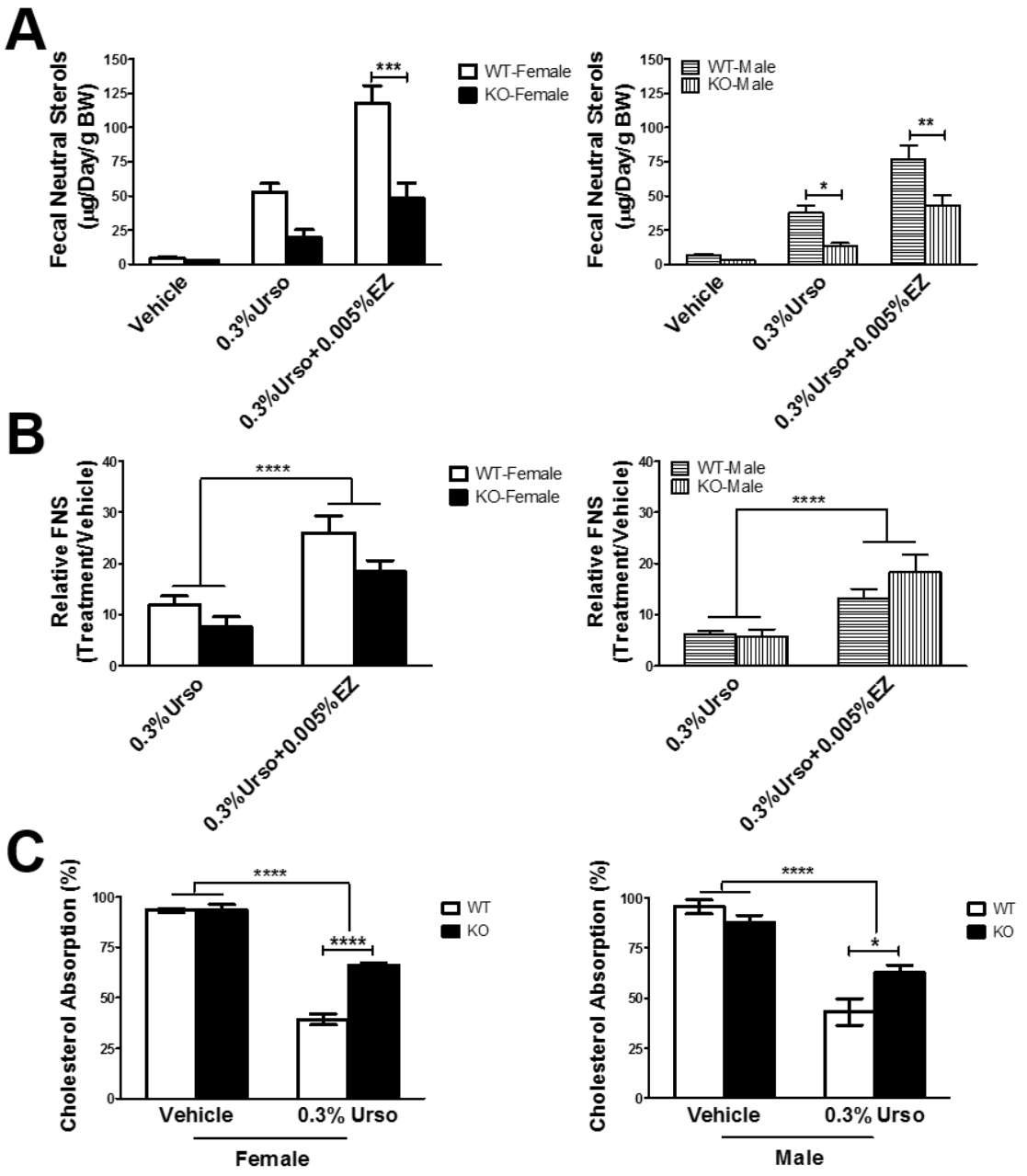

Figure 3.16 No sexual dimorphisms are observed in FNS, the relative difference in sterol loss, and cholesterol absorption. G5G8 KO mice (n=4 for both sexes) and their WT littermates (n=6 for male and 7 for female) were sequentially fed with control, 0.3% Urso, and 0.3% Urso plus 0.005% EZ for 14 days. (A-B) FNS and the relative difference in fecal sterol loss were represented by sex. Another cohort of male and female KO and WT mice (n=3 for each gender and genotype) were fed a PSF diet or 0.3% Urso for 7 days. (C) The fractional cholesterol absorption was measured by stable dual isotope method and represented by sex. Data are expressed as mean ± SEM. Differences were

determined by a repeated measure two-way ANOVA using diet and genotype as factors followed by Bonferroni post-hoc tests (A-B) and two-way ANOVA followed by Bonferroni post-tests (C). *p<0.05, **p<0.01, ***p<0.001, ****p<0.0001.

The effects of Urso on intestinal epithelial cell proliferation and turnover are not known. To understand Urso's effect in this process, we performed a BrdU incorporation study [221]. Anti-CD3 monoclonal antibody was used as a positive control by stimulating T cell-induced epithelial cell proliferation (18 hr) and increased crypt depth/villus blunting. In contrast, G5G8 deficiency failed to alter epithelial cell responses to Urso (Fig 3.12F, 14). These findings indicate that drug-induced cholesterol elimination is independent of G5G8.

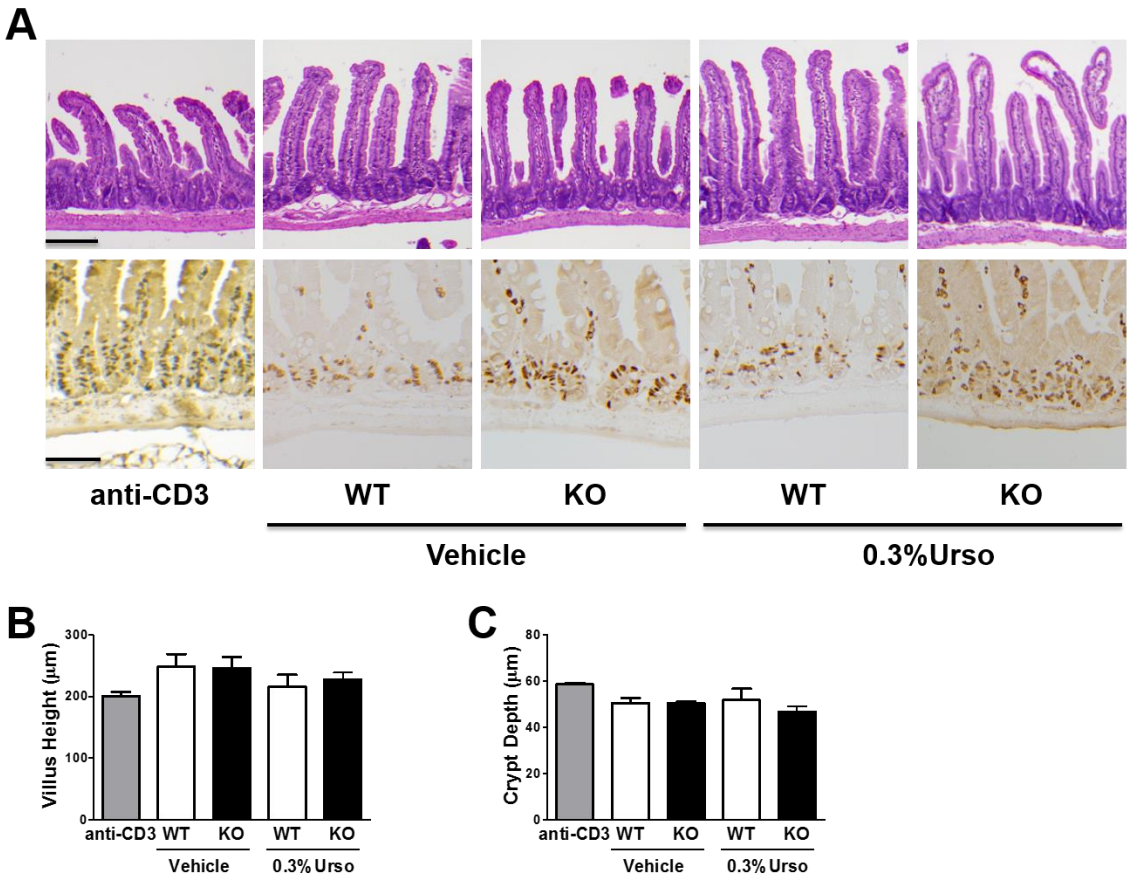

Figure 3.17 Intestinal epithelial cell proliferation and turnover in vehicle and 0.3% Urso treated WT and G5G8 KO mice. Male KO (n=3) and their WT littermates (n=3) were fed a PSF diet or 0.3% Urso for 7 days. Mice were injected with BrdU 2 hrs before killing. Antibodies directed against CD3 were injected to male WT mice 18 hours prior to BrdU injection. (A) Formalin-fixed jejunal sections stained with hematoxylin and eosin (H&E) and immunohistochemistry allowed visualization of proliferating cells incorporated with BrdU in representatives of each group. Scale bar, 100 microns for H&E; 50 microns for BrdU staining. (B-C) Sections were scored, 20 villi/crypts per mouse, 3 mice per group. Villus height and crypt depth were determined. Data are mean ± SEM. Differences were determined by one-way ANOVA followed by Dunnett's post-hoc comparisons.

DISCUSSION

The major findings of the present study are that Urso increases G5G8 abundance and activity in liver and that Urso-EZ acts in an additive fashion to promote fecal sterol excretion in mice. While G5G8 is the primary route for biliary cholesterol secretion, our studies reveal a G5G8-independent pathway for cholesterol elimination stimulated by Urso and Urso-EZ combination treatments. Whether this is attributed to other biliary or non-biliary pathways, such as TICE, remains to be determined.

Biliary cholesterol secretion represents an essential step of the RCT process which involves the transport of cholesterol from peripheral cells to the liver for secretion into bile and subsequent elimination in feces [120]. Accelerating RCT has long been a therapeutic goal in the treatment of atherosclerosis [144, 229]. However, the role of biliary cholesterol secretion in the development and severity of NAFLD is a relatively recent discovery. We have published the only

reports detailing G5G8 and biliary cholesterol secretion in the context of NAFLD [165, 167]. Consequently, studies to date have not examined accelerated biliary secretion as a therapeutic strategy in either preclinical models or humans in the treatment of NAFLD. Although G5G8 has been known to increase cholesterol excretion for over a decade, there has been little interest in drug development for this target. This is mainly because increasing biliary cholesterol secretion is expected to raise the cholesterol saturation index of bile and the risk for cholesterol gallstones. However, Urso is a hydrophilic bile acid with choleretic, cytoprotective, and antiapoptotic properties [230, 231]. It was originally used for cholesterol gallstone dissolution mainly because it reduces hydrophobicity of the bile acid pool and increases bile flow, two factors that oppose gallstone formation. Therefore, increasing G5G8 with Urso to increase biliary cholesterol secretion in the absence of increased risk of gallstone formation may be a viable therapeutic strategy to accelerate RCT.

A number of preclinical studies and clinical trials have evaluated either Urso or EZ in the treatment of NAFLD or NASH. Results with Urso were mixed. Low-dose Urso (13-15 mg/kg/day) reduced some markers of inflammation including serum alanine transaminase (ALT), but failed to significantly improve NASH in two separate studies [232, 233]. High-dose Urso (28-32 mg/kg/day) failed to reduce ALT at either 3 or 6 months in one trial (n=12); in a separate trial, high-dose Urso lowered ALT levels by an average of 40% at 3, 6, 9 and 12 months and

normalized ALT values in 25% of patients compared to no reductions or normalizations in the placebo group [234, 235]. Although the numbers of studies and patients were limited, EZ monotherapy showed promise in the treatment of NAFLD. In a 6-month pre-/post treatment open-label trial in 10 patients, EZ reduced serum ALT, γ-glutamyl transpeptidase, plasma TGs and hepatic fat, but measures of insulin resistance were unchanged [236]. In the largest study to date (n=45) in a Japanese population, EZ reduced ALT at 12 months and resulted in modest, but significant reductions in steatosis, ballooning, and other indices of NAFLD by 24 months [135]. However, neither monotherapy is currently indicated in the treatment of NAFLD. The limited benefit may be due to the interdependent nature of biliary secretion and intestinal absorption with respect to cholesterol elimination. Therefore, a combination therapy that simultaneously increases biliary secretion and reduces cholesterol absorption may provide greater therapeutic benefit compared to Urso or EZ monotherapies.

It was expected that Urso-EZ combination treatment would further stimulate fecal sterol loss and create a negative sterol balance or "cholesterol drain". In the steady state, the extent of cholesterol loss is directly reflected by the rate of cholesterol synthesis. In the present study, no evidence supports an increase in whole body cholesterol synthesis except a modest increase in adrenal and jejunal HMGCS gene expression. In addition, feeding an Urso-containing diet led to a robust repression of hepatic CYP7A1 and CYP8B1. Thus, the observed increase in

FNS may reflect diversion of cholesterol away from bile acid synthesis into the G5G8 accessible pool, rather than the establishment of a cholesterol drain.

The mechanism(s) by which Urso simultaneously increases G5G8 and suppresses bile acid synthesis is not known. It may be due to the stimulation of ileal FGF15, which acts on FGFR4/β-Klotho receptor complexes in liver to repress bile acid synthesis [185]. FGF15 also induces the protein synthesis in liver, but the effect of FGF15 on G5G8 is not known [185, 237]. Alternatively, recent studies suggest that the α5β1- integrin is a sensor for TUDCA that promotes choleresis [238, 239]. However, the effect of integrin signaling on G5G8 is not known. Therefore, it remains unclear whether the suppression of bile acid synthesis and the stimulation of G5G8 in response to Urso utilize common or independent mechanisms. If the mechanisms are independent, there may be a therapeutic window whereby biliary cholesterol secretion could increase to a greater extent than bile acid suppression in order to promote RCT. If not, other therapeutic approaches aimed to increase G5G8 and biliary cholesterol secretion would need to be developed in combination with EZ to accelerate RCT. However, such an approach may increase the risk of gallstone formation.

Another intriguing observation in our present studies was that Urso and Urso-EZ similarly increased FNS in G5G8 KO mice as in their WT littermates. This could be partially attributed to the most studied non-biliary route, TICE, which may account for approximately 33% of total fecal sterol loss in mice and is now

considered as an essential alternative route to the hepatobiliary pathway [227]. We did not simultaneously measure biliary and intestinal cholesterol secretion in our studies, nor did we evaluate to what extent biliary vs. non-biliary pathways contribute to the total fecal sterol loss. However, Urso and Urso-EZ in G5G8 deficient mice may be useful tools in identifying novel biliary and non-biliary pathways for cholesterol elimination.

Copyright © Yuhuan Wang 2015

CHAPTER 4. ROLE OF FGF15/19 IN THE REGULATION OF ABCG5 ABCG8 STEROL TRANSPORTER

INTRODUCTION

FGF15/19 is a metabolic hormone expressed in the enterocytes in the ileal segment of the small intestine. It has been recently discovered to play a crucial role in the cross-talk between liver and intestine in control of bile acid and energy homeostasis [183, 184, 186, 237, 240, 241]. Mouse FGF15 shares approximately 50% amino acid identity with its human orthologue, FGF19. However, they have similar tissue expression patterns, physiological functions, and pharmacological effects in mice [183-185]. One well-characterized action of FGF15/19 is to suppress bile acid synthesis [186, 188, 242, 243]. When (re)absorbed from the intestinal lumen, bile acids act on the FXR/RXR heterodimer to induce FGF15 expression. Secreted FGF15 acts on the liver via its receptor complex FGFR4/β-Klotho to repress CYP7A1 expression and bile acid synthesis.

In Chapter 3, we showed that while Urso suppressed the major bile acid synthetic genes including CYP7A1 and CYP8B1, it increased expression of G5G8 predominantly at the protein level in liver [244]. Consistently, both biliary cholesterol secretion and fecal neutral sterol output increased [244]. However, the mechanism(s) by which Urso simultaneously suppresses bile acid synthesis and increases G5G8 is (are) not known. Though Urso was reported to be a weak

agonist or even a partial antagonist for FXR, our results demonstrated that ileal FGF15 mRNA expression was strikingly increased in response to Urso treatment [244-246]. The repression of bile acid synthesis may at least in part be due to the stimulation of ileal FGF15, which acts on FGFR4/β-Klotho receptor complexes in liver to activate the downstream signaling cascade. Whether FGF15 would concurrently have a direct effect on G5G8 is unknown. However, our results from Chapter 3 provide very positive evidence.

Additional evidence also supports the hypothesis that FGF15/19 directly regulates G5G8 protein abundance. Beyond suppressing bile acid synthesis, FGF15/19 is thought to promote gallbladder filling by increasing cAMP levels [187]. Intriguingly, the cAMP signaling machinery has recently been discovered to mediate the trafficking of G5G8 to the bile canalicular membrane in response to hypernutrition. Administration of a protein kinase A inhibitor decreases G5G8 protein expression, whereas injection of a cAMP analog transiently increases their levels [190].

In this chapter, two additional mouse models were tested to confirm the positive correlation between ileal FGF15 expression and hepatic G5G8 protein abundance. One is Asbt KO mouse model. Dawson and coworkers generated the Asbt KO mice to decipher the in vivo functions of Asbt in bile acid homeostasis [247, 248]. In this mouse model, the disruption of Asbt blocks the apical uptake of bile acids, thereby resulting in decreased expression of ileal FGF15 and reduced

entry of bile acids into enterohepatic cycling, both of which are thought to contribute to increased bile acid synthesis. However, the protein expression of hepatic G5G8 has never been tested. The other one is LIRKO mouse model, in which hepatic G5G8 protein levels and biliary cholesterol secretion are elevated. However, the ileal FGF15 expression has never been reported.

Then the hypothesis was directly tested by determining the G5G8 protein abundance and biliary cholesterol secretion in mice administered with recombinant human FGF19. As predicted, FGF19 elevated G5G8 protein levels specifically in liver not in intestine. It also increased biliary cholesterol secretion in the absence of increasing the cholesterol saturation index (CSI). This is likely due to the proportional increase in the biliary secretion rates of both phospholipids and bile acids.

MATERIALS AND METHODS

Chemicals, reagents and antibodies

General chemicals were purchased from Sigma, immunoblotting reagents from Thermo/Pierce, real-time PCR reagents from Applied Biosystems. The chicken anti-G5 polyclonal antibody and the monoclonal antibody directed against G8 were previously reported [244]. Total and phospho-eIF2α antibodies were purchased from Cell Signaling. The ABCA1 and SR-BI antibodies were generously provided by Mason Freeman (Harvard Medical School) and Deneys R. van der Westhuyzen (University of Kentucky), respectively. The β-actin

antibody was purchased from Sigma. Calnexin and GRP78 antibodies were purchased from Nventa (San Diego, CA). The antibody to Calriticulin was purchased from Stressgen.

Animal husbandry

Male C57BL/6J (Stock #000664) mice at an age of 8 weeks were purchased from the Jackson Laboratory (Bar Harbor, ME). Upon arrival mice were allowed to acclimatize for one week prior to initiation of studies. Mice were housed in individually ventilated cages in a temperature-controlled room with a 14:10 light: dark cycle and provided with enrichment in the form of acrylic huts and nesting material. Mice were maintained on standard rodent chow (Harlan Teklad 2014S). All animal procedures conform to PHS policies for humane care and use of laboratory animals and were approved by the institutional animal care and use committee at the University of Kentucky. All surgery was performed under anesthesia, and all efforts were made to minimize suffering.

Human recombinant FGF19 injection experiment

Human recombinant FGF19 (CYT-700) was purchased from ProSpec (Protein-Specialists). Vehicle or FGF19 (1 µg/g body weight) was injected into mice intraperitoneally twice every four hours in a total volume of 200 µl of PBS. All mice were placed in clean cages with full access to water, but without food. Four hours after a second injection of FGF19, mice were sacrificed. Basal bile, liver, and three segments of the small intestine were collected as described previously [244].

Immunoblot and quantitative Real-time PCR

The preparations of proteins, SDS-PAGE and immunoblotting were conducted as previously described [166, 249]. Total RNAs were extracted from each liver using RNA STAT-60 (Tel-Test, Inc) and subjected to cDNA synthesis with iScript cDNA Synthesis Kit (BIO-RAD, Hercules, CA). To determine relative abundance, RT-PCR was conducted using SYBRGreen as detector on Applied Biosystem 7900HT fast-Real Time PCR System (Carlsbad, CA).

Serum and biliary lipid analysis

Total cholesterol in serum, as well as cholesterol and phospholipids in gallbladder bile, were determined using commercial colorimetric-enzymatic assays (Wako Chemicals, Richmond, VA). The quantitation of total bile acids in bile was performed enzymatically by measuring 3α-hydroxy bile acids as previously described [222].

Statistical analysis

All statistical analyses were conducted using GraphPad Prism. Data are expressed as mean ± SEM. Data were analyzed by two-tailed t-test. Differences were considered significant at $P < 0.05$.

RESULTS

The liver tissues of Asbt KO mice and their WT controls were generously provided by Paul Dawson (Emory University). Hepatic protein levels of G5 and G8 were analyzed by immunoblotting (Fig 4.1). As expected, we observed

reduced hepatic G5G8 protein abundance in Asbt KO mice compared with their WT controls (Fig 4.1). This positively correlates with the low expression of FGF15 in ileal enterocytes in Asbt KO mice. However, we cannot exclude the possibility that the increased bile acid synthesis tightly regulated via the classical feedback mechanism may deprive the G5G8 accessible pool of cholesterol.

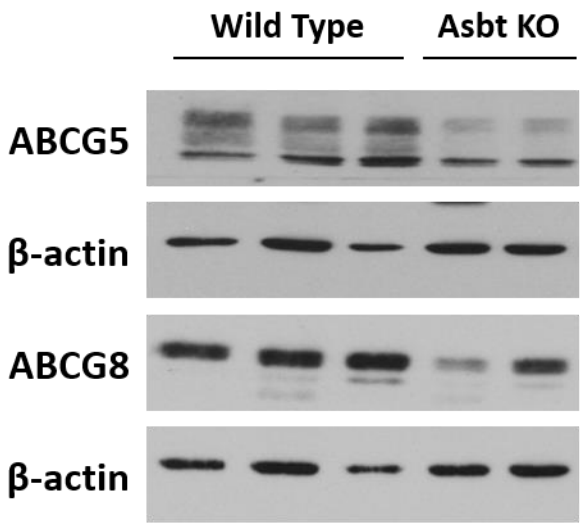

Figure 4.1 Asbt KO mice present lower G5G8 abundance in liver. Male WT and Asbt KO mice were maintained on a prepared basal diet [248]. Hepatic levels of G5 and G8 protein expression were determined by immunoblotting. Membrane preparations were blotted for β-actin as loading controls.

We then looked at the association between ieal FGF15 expression and hepatic G5G8 protein levels in LIRKO mice. We selectively deleted the hepatic insulin receptor from insulin receptor-floxed mice using adeno-associated virus (AAV) expressing a Cre recombinase (AAV-Cre) driven by the albumin promoter and generated the LIRKO mouse model. We confirmed the deletion of insulin receptor and the increase of hepatic G5G8 abundance by immunoblotting

analysis (Fig 4.2B). Consistently, we observed a significant increase in ileal FGF15 expression in LIRKO mice compared with their controls (Fig 4.2A).

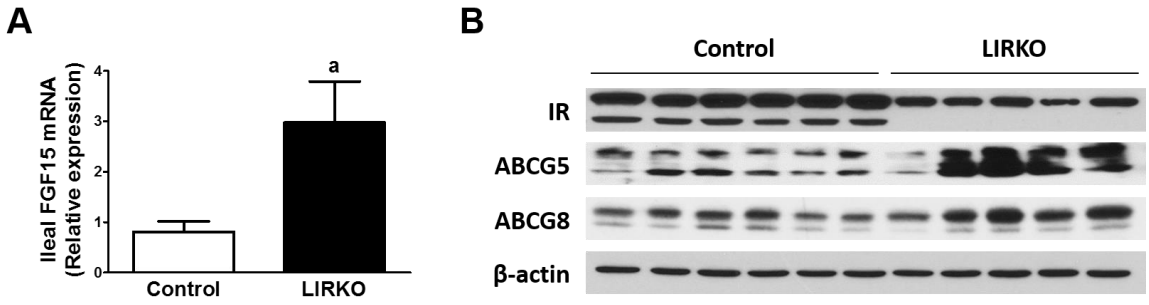

Figure 4.2 Elevated hepatic G5G8 abundance of LIRKO mice is associated with stimulated ileal FGF15 expression. Male insulin receptor (IR) floxed mice at 8-week old age were injected through the tail vein with $5x10^{11}$ particles of adeno-associated virus encoding Cre-recombinase (AAV-Cre) or empty AAV vectors. Two weeks following virus infection for hepatic insulin receptor deletion, mice were sacrificed. The liver and ileal segment of intestine were harvested for IR, G5G8 immunoblotting and ileal FGF15 mRNA expression, respectively.

Next, we directly tested if FGF15/19 could acutely increase hepatic G5G8 abundance. Due to the decreased stability of recombinant FGF15, we used the human orthologue, FGF19, for our studies. Body weight tended to decrease after FGF19 treatment, but didn't reach significant differences (Fig 4.3A). No change was noted for liver weight (Fig 4.3A). One major effect of FGF19 is to suppress bile acid synthesis in liver via a mechanism involving FGFR4 activation and SHP induction and stability [186, 250-252]. As previously reported, FGF19 significantly reduced the mRNA expression of CYP7A1 whereas it induced that of SHP (Fig 4.3B). Similar results were observed for CYP8B1 and CYP27A1. However, no decrease was detected in CYP7B1. To determine if FGF19 would

directly regulate G5G8, we measured G5G8 expression at both mRNA and protein levels in liver by RT-PCR and immunoblotting analysis, respectively (Fig 4.3B-C). FGF19 tended to increase the mRNA expression of both G5 and G8, but only reached statistical significance for G8 (Fig 4.3B). However, immunoblotting analysis confirmed a marked increase in both G5 and G8 protein expression (Fig 4.3C). This was observed only in liver not in intestine (Fig 4.3D).

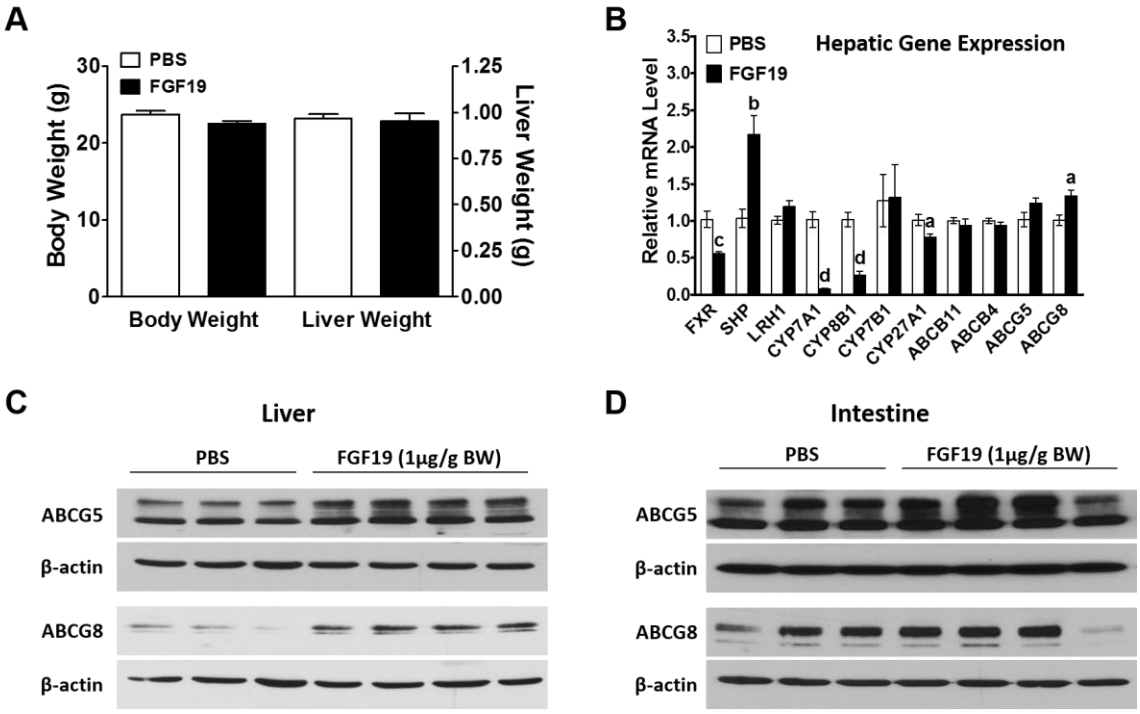

Figure 4.3 FGF19 increases hepatic G5G8 at protein levels. Male C57BL/6J mice at an age of 8 weeks were treated with PBS or FGF19 (1 μg/g) by i.p. injection twice every four hours. (A) Body weight and liver weight. (B) Relative mRNA levels of major transcription factors, enzymes, and transporters involved in bile acid metabolism in liver. (C) Hepatic and (D) jejunal levels of G5G8 protein expression were determined by immunoblotting. Membrane preparations were blotted for β-actin as controls. Data are presented as mean ± SEM. Differences between FGF19- and PBS-treated groups were determined by two-tailed t-test. a: $p<0.05$, b: $p<0.01$, c: $p<0.001$, and d: $p<0.0001$.

FGF19-treated mice displayed similar rates of hepatic bile flow but significantly elevated total bile lipid (Fig 4.4A). Hepatobiliary secretion rates of lipids including cholesterol, phospholipid, and bile salt under basal conditions were calculated from the product of bile flow and lipid concentration. Significant increases were not only observed in bile salt secretion rates in FGF19-treated mice, but also in phospholipid and cholesterol during the 30-min collection period (Fig 4.4B). However, no differences were detected in bile salt, phospholipid, or cholesterol compositions when we expressed the biliary lipid data proportionally (Fig 4.4C). We then measured the CSI of gallbladder bile (Fig 4.4D). Both groups exhibited CSI<1 in gallbladder bile indicating that the administration of FGF19 increases biliary cholesterol secretion without increasing the risk for gallstone formation.

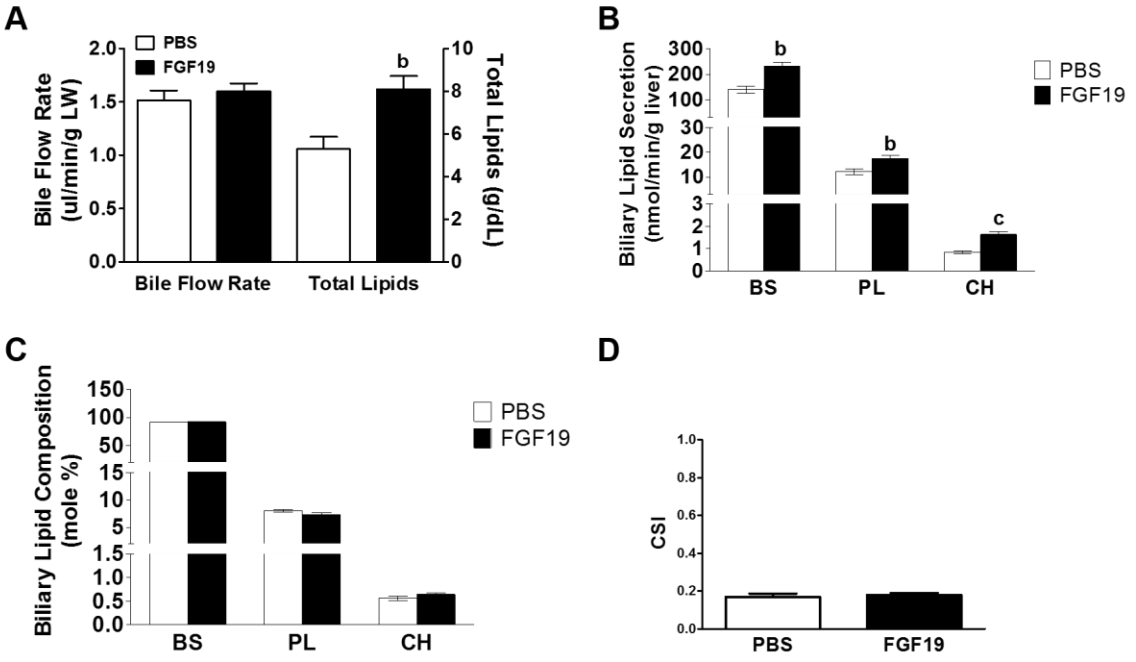

Figure 4.4 FGF19 increases the biliary secretion rates of cholesterol, phospholipids (PL), and bile salts (BS). (A) Hepatic bile flow and total lipids concentrations. (B) Biliary lipid secretion rates under basal conditions. Gallbladder was cannulated and basal bile was collected for 30 min. (C) Biliary lipid composition (mole %). (D) Cholesterol saturation index of gallbladder bile was calculated from the critical tables. Data are presented as mean ± SEM. n=6-7 for each group. Differences between FGF19- and PBS-treated groups were determined by two-tailed t-test. b: $p<0.01$ and c: $p<0.001$.

To determine if increased biliary cholesterol secretion stimulated by FGF19 changed the hepatic cholesterol metabolism, we measured the mRNA expression of major genes involved in cholesterol synthesis and efflux (Fig 4.5A). FGF19 moderately increased SREBP2 and HMGCS with a tendency to increase HMGCR at the mRNA level, indicating that the increased biliary cholesterol secretion provides a driving force to cholesterol synthesis (Fig 4.5A). Even though we observed a significant increase in both ABCA1 and SR-BI at mRNA level, we didn't detect any difference in their protein expression by immunoblotting analysis (Fig 4.5A-B). This is likely due to that an eight-hour interval is not long enough to allow us to see changes of ABCA1 and SR-BI at the protein level. FGF19 had no effect on serum total cholesterol or phospholipids (Fig 4.5C).

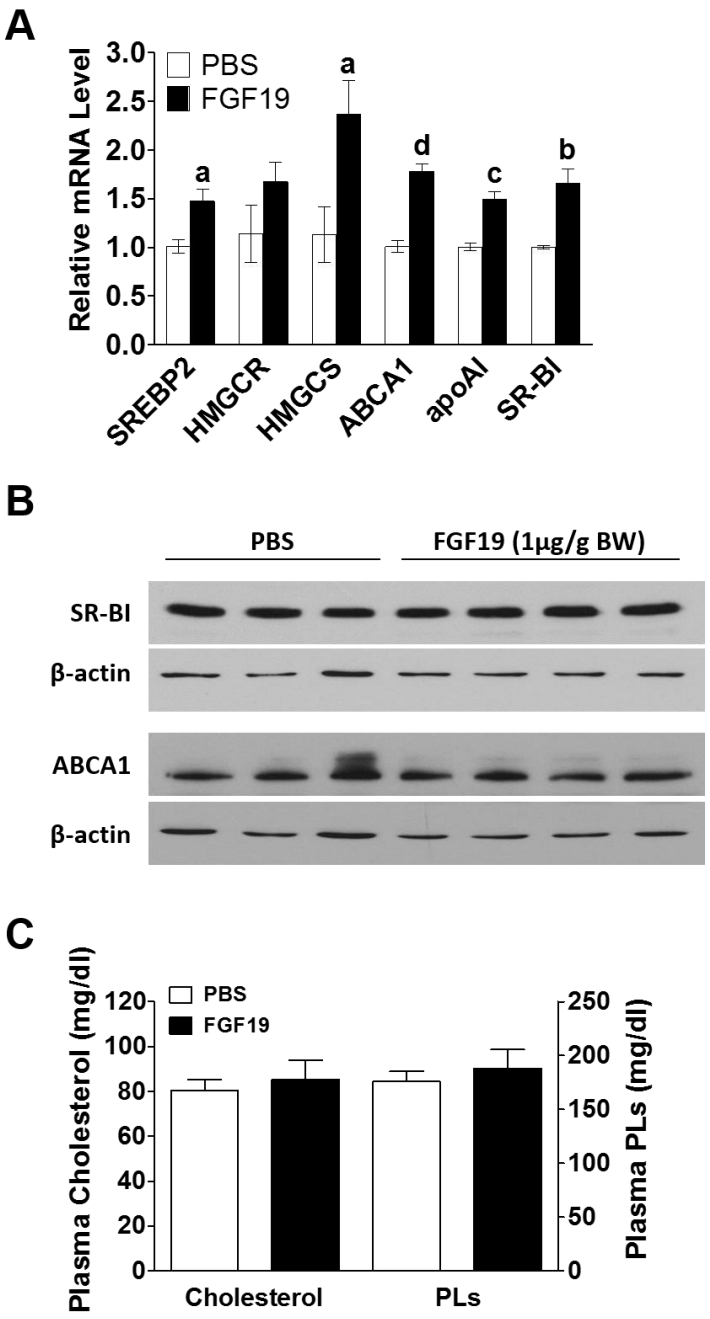

Figure 4.5 FGF19 increases the expression of major genes in cholesterol synthesis and efflux at the mRNA level. (A) The mRNA expression for major genes involved in de novo cholesterol synthesis and efflux was determined by RT-PCR. n=5-7. (B) Immunoblot analysis of hepatic SR-BI and ABCA1. (C) Total cholesterol and phospholipids (PLs) concentrations in serum. n=6 for each group. Data are presented as mean ± SEM. Differences between FGF19- and PBS-treated groups were determined by two-tailed t-test. a: $p<0.05$, b: $p<0.01$, c: $p<0.001$, and d: $p<0.0001$.

To determine if FGF19 altered the TG metabolism in liver, we measured the mRNA expression of the major genes involved in in lipogenesis and fatty acid oxidation (Fig 4.6). Results showed that a double-injection of FGF19 significantly suppressed the expression of SREBP1c, malic enzyme 1(ME1), and acetyl-CoA carboxylase 2 (ACC2). This confirmed the role of FGF19 in fatty acid synthesis and oxidation.

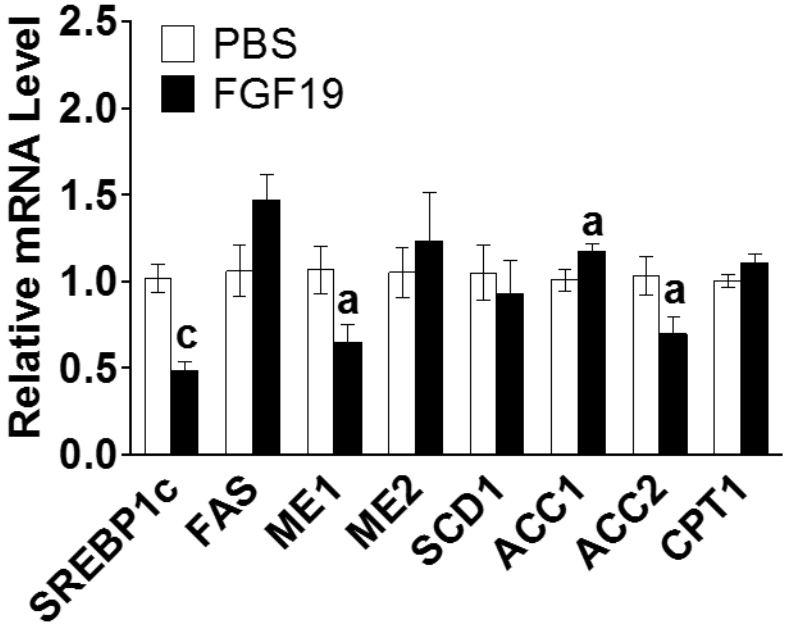

Figure 4.6 FGF19 reduces lipogenesis in liver. The mRNA expression for major genes involved in fatty acid synthesis and oxidation was determined by RT-PCR. n=5-7 for each group. Data are presented as mean ± SEM. Differences between FGF19- and PBS-treated groups were determined by two-tailed t-test. a: $p<0.05$ and c: $p<0.001$.

DISCUSSION

The major findings of the study are that FGF15/19 increases the expression of G5G8 predominantly at the protein level as well as biliary cholesterol secretion. This effect is only restricted to G5G8 in liver other than intestine. Interestingly, the proportional increase in both biliary phospholipids and bile acids explains the unaltered CSI. Moreover, FGF19 also suppresses the expression of major lipogenic genes and those involved in fatty acid oxidation.

A mouse model of liver-specific insulin resistance in the absence of obesity (LIRKO) has been previously published and the impact of selective insulin receptor deletion in liver on several features of sterol homeostasis was reported [48, 193]. Biddinger and coworkers proposed two distinct mechanisms that tie links between gallstones and MetS. While increasing hepatic G5G8 via a mechanism involving the disinhibition of FOXO1, hepatic insulin resistance decreases expression of major bile acid synthetic genes resulting in a lithogenic bile salt profile. Our results confirmed the stimulation of ileal FGF15 in LIRKO mice. As the roles of FGF15/19 in bile acid homeostasis have been widely appreciated, FGF15 may mechanistically contribute to the repressed expression of major bile acid synthetic genes and the elevated G5G8 abundance in LIRKO.

Remarkably similar as insulin, FGF15/19 also stimulates hepatic glycogen synthesis and represses gluconeogenesis [237, 253]. In addition, FGF15 signaling has also been previously shown to decrease hepatic FOXO1 activity through the

phosphorylation of PI3K [242]. The stimulated FGF15 expression in LIRKO mice may not only explain the overall suppressed bile acid synthetic genes and increased G5G8 but also function as a compensatory mechanism to counteract the loss of insulin signaling.

Controversial results have been previously reported for the roles of FGF15/19 in lipogenesis [237, 240, 241, 254]. Bhatnagar and coworker investigated the roles of FGF19 in modulating hepatic fatty acid synthesis via primary hepatocyte cultures with recombinant FGF19 and concluded that FGF19 suppressed insulin-stimulated fatty acid synthesis and SREBP1c expression [254]. Stewart's group generated the FGF19 transgenic mice and reported that these mice had increased energy expenditure and decreased liver TGs which could be partially due to the decreased ACC2 expression in liver [240]. They also observed similar phenotypes in *ob/ob* and HF diet-fed FVB mice injected with FGF19 [241]. However, when Kir and coworker overnight-fasted C57BL/6 mice and injected them subcutaneously with FGF19, they didn't observe any change in lipogenic gene expression 6 hours following FGF19 injection [237]. Our results align with the previous observations but against Kir's. The roles of FGF15/19 in lipogenesis need further investigation.

Cholic acid is a strong FXR agonist that stimulates FGF15 expression and activates its downstream signaling cascade. Watanabe and coworker reported that cholic acid reduced the expression of SREBP1c and other lipogenic genes,

lowered hepatic and serum TG levels. Moreover, it also attenuated LXR agonist-stimulated lipogenesis [255]. Whether the effects of cholic acid on lipogenesis and TG homeostasis are dependent on FGF15 signaling has never been addressed. However, this may provide indirect evidence that as opposed to insulin, which promotes lipogenesis, FGF15/19 may mitigate the induction of hepatic lipogenesis.

Overall, the overlapping but distinct actions of FGF15/19 and insulin may promise the use of FGF15/19 as a therapeutic strategy in the treatment of diabetes or in combination with LXR agonists to correct atherosclerotic cardiovascular disease. However, the potential use of FGF19 as a chronic treatment may have concerns. Long-term treatments of FGF19 have been implicated to associate with liver tumors or hepatocellular carcinoma [256, 257]. Strategies aiming at developing synthetic FGF19 variants that preserve the metabolic effects of FGF19 but silence its mitogenic effects need to be explored.

Copyright © Yuhuan Wang 2015

CHAPTER 5. SUMMARY AND FUTURE DIRECTIONS

Summary of major findings

The goal of this dissertation thesis is to understand the mechanisms responsible for the post-transcriptional regulation of sterol transporter G5G8 in vivo such that appropriate therapeutics could be employed to target cholesterol elimination pathways to oppose MetS and NAFLD and prevent the onset and progression of CVD.

In Chapter 2, acute replacement of letpin in *ob/ob* mice, liver-specific ablation of leptin receptor in lean mice, and hepatic vagotomy in diet-induced obese mice all failed to alter hepatic G5G8 protein levels. Therefore, the reduction of G5G8 in leptin axis deficient mice is not a direct consequence of leptin signaling. Alternatively, G5G8 may be decreased in *ob/ob* and *db/db* mice due to ER dysfunction, the site of G5G8 complex assembly. Our data showed that overexpression of the ER chaperone GRP78 alleviated ER stress and reduced expression of lipogenic genes and plasma TGs in *db/db* mice. As we hypothesized, both G5 and G8 protein levels increased as did total biliary cholesterol in the absence of changes in G5 or G8 mRNAs.

Leptin axis deficient mice (*ob/ob* and/or *db/db*) have been frequently used in the pathogenic studies of MetS and NAFLD. Available data from previous studies using these mice establish the role of G5G8-mediated biliary cholesterol secretion

in opposing many risks factors for MetS and NAFLD, such as insulin resistance, elevated plasma TG, and ER stress. Alleviation of ER stress by TUDCA and GRP78 overexpression both restore insulin sensitivity and hepatosteatosis. TUDCA has been reported to increase G5G8 protein abundance and biliary cholesterol secretion. In Chapter 2, we conclude that alleviation of ER stress by GRP78 also rescues G5G8 and elevates biliary cholesterol secretion. This not only suggests a reciprocal relationship between ER function and G5G8-mediated biliary cholesterol secretion, but also establishes a proof-of-principle that improving ER function rescues G5G8 and may account for a potential approach to target G5G8 activity in the treatment of metabolic disease.

Results in Chapter 3 demonstrated that a FDA approved drug for the treatment of primary biliary cirrhosis and dissolution of gallstones, Urso, pharmacologically increased hepatic G5G8 protein expression and both biliary and fecal sterols in a dose-dependent manner. Given the interdependent relationship between liver and intestine for cholesterol elimination from the body, we proposed that a combined therapy aimed at increasing biliary cholesterol secretion and simultaneously reducing intestinal absorption is likely to act additively in enhancing cholesterol elimination from the body. Indeed, our data demonstrated that EZ, an inhibitor of intestinal cholesterol absorption, produced an additive and dose-dependent increase in FNS elimination in the presence of Urso. The stimulatory effect in response to Urso or Urso-EZ treatments was not

G5G8 dependent. This may be partially attributed to the non-biliary route for cholesterol elimination. Little has been known about the mechanisms responsible for the non-biliary pathway. Urso and Urso-EZ in G5G8 KO mice may provide very useful tools in identifying novel biliary and non-biliary pathways for cholesterol elimination.

We originally expected that in the absence of cholesterol feeding, the combined pharmacological therapy would create a net negative sterol balance or "cholesterol drain" that significantly drives the rate of whole body cholesterol synthesis. However, we only detected a very modest increase in adrenal and jejunal HMGCS gene expression. This indicates that Urso, as a pharmacological approach to target G5G8, increases biliary and fecal sterol excretion. However, this comes at the expense of diverting cholesterol away from bile acid synthesis into the G5G8 accessible pool. Though such an effect of Urso dampens our enthusiasm for the Urso-EZ combination therapy, it sheds light on another regulator of G5G8, FGF15/19.

Beyond increasing hepatic G5G8 protein expression and biliary cholesterol secretion, Urso also stimulates the ileal FGF15 expression in mice. In Chapter 4, stimulated ileal FGF15 expression in LIRKO and reduced hepatic G5G8 protein levels in Atsb KO mice both indicated the previous unrecognized role of FGF15/19 in the regulation of G5G8 and its activity. Indeed, this was

subsequently confirmed by our results from the direct test of recombinant human FGF19 on G5G8.

Future directions

In this dissertation, we postulate, for the first time, a concept of "cholesterol drain" achieved by simultaneously increasing G5G8-mediated biliary cholesterol secretion and inhibiting intestinal absorption for the treatment of metabolic disease. Moreover, our work presented in this dissertation also demonstrate, for the first time, that recombinant human FGF19 increases hepatic G5G8 abundance and activity, and thereby uncovering a previously unappreciated link between FGF15/19 and sterol flux. However, many questions remain to be addressed in the future.

In Chapter 3, the mechanism(s) by which Urso simultaneously increases G5G8 and suppresses bile acid synthesis is not known. Previous studies and our results from Chapter 4 imply that FGF15/19 is likely to account for the Urso's dual effects and work more efficiently than Urso to oppose metabolic disease in combination with EZ. Supportive rationales and evidence are listed below.

Bile acid synthesis is tightly regulated via both a classical feedback mechanism and FGF15/19 signaling to ensure that sufficient amounts of cholesterol are catabolized to bile acids so as to facilitate biliary cholesterol secretion and provide adequate emulsification for lipid absorption in the intestine. Urso, as a bile acid itself, represses the bile acid synthesis via dual mechanisms. The Urso-

stimulated biliary and fecal sterol loss comes at the expense of diverting cholesterol away from bile acid synthesis into biliary secretion. This is reflected by the unaltered expression of major genes involved in the de novo cholesterol synthesis shown in Chapter 3. However, treatment of FGF15/19, though suppresses bile acid synthesis, may still adapt to the negative feedback mechanism to catabolize excess hepatic cholesterol and compensate the bile acid loss. Our results from Chapter 4 demonstrate that the administration of recombinant FGF19 itself is sufficient to stimulate the expression of major genes involved in cholesterol biosynthesis in liver. Additionally, FGF19 stimulates G5G8-mediated biliary cholesterol secretion without increasing cholesterol saturation index.

Moreover, insulin resistance is widely considered as the central source for the pathogenesis of MetS and NAFLD. FGF15/19 possesses very similar effects as insulin in stimulating hepatic glycogen synthesis and repressing gluconeogenesis, but likely an opposite effect in lipogenesis. The overlapping but distinct effects of FGF15/19 make it very promising in the treatment of metabolic disease.

Given that the prolonged exposure of FGF19 has been implicated in liver tumorigenesis or hepatocellular carcinogenesis, nontumorigenic FGF19 variants that preserve the metabolic effects of FGF19 should be used in combination with

EZ for relatively long-term treatments. One of such FGF19 variants that have been tested in both in mice and humans is M70 [258, 259].

In mouse liver, FGF15 acts through a cell surface receptor complex composed of FGFR4 and βKlotho and promotes gallbladder filling by increasing cAMP levels. The cAMP analog has been recently shown to enhance canalicular trafficking of G5G8. Thus, the FGF15/FGF19-FGFR4-cAMP signaling pathway is likely to account for the regulation of hepatic G5G8 abundance and activity. Future investigation of the hepatic G5G8 protein abundance and biliary cholesterol in FGF15-KO mice, FGFR4-KO and β-Klotho-KO mice will be necessary.

The work presented in this dissertation is mainly focused on targeting the classic G5G8-mediated biliary pathway to oppose metabolic disease. However, there is evidence that non-G5G8-mediated biliary route and non-biliary route may also contribute to the cholesterol elimination. The molecular components involved in these pathways are not known. Urso and Urso-EZ treatments in G5G8 KO mice suggest the G5G8-independent pathway for cholesterol elimination. Whether FGF15/19-stimulated biliary cholesterol secretion is dependent on G5G8 and whether FGF15/19 stimulates the non-biliary pathway for cholesterol elimination, e.g., TICE, would be interesting questions needed to be addressed by future studies.

Copyright © Yuhuan Wang 2015

APPENDICES

ABBREVIATIONS

AAV: adeno-associated virus
AAV-Cre: adeno-associated virus expressing a Cre recombinase
ACAT2: acetyl-CoA acetyltransferease 2
ACC: acetyl-CoA carboxylase
AdCre: adenovirus encoding Cre-recombinase
AdGRP78: adenovirus encoding GRP78
ALT: alanine aminotransferase
apoB: apolipoprotein B
ASBT: apical sodium-dependent bile transporter
AST: aspartate aminotransferase
ATF6: activating transcription factor 6
ATP III: Adult Treatment Panel III
BSEP: bile salt export protein BrdU: bromodeoxyuridine
BSTFA: *N*, *O*-Bis (trimethylsilyl) trifluoroacetamide
cAMP: cyclic adenosine monophosphate
CE: cholesteryl ester
CETP: cholesteryl ester transfer protein
CHOP: C/EBP homologous protein
CM: chylomicron
CMR: chylomicron remnant
ChREBP: carbohydrate response element-binding protein
CRP: C-reactive protein
CSI: cholesterol saturation index
CVD: Cardiovascular disease
CYP7A1: cholesterol 7alpha-hydroxylase.
CYP7B1: 25-hydroxycholesterol 7-alpha-hydroxylase
CYP8B1: sterol 12-alpha-hydroxylase
CYP27A1: sterol 27-hydroxylase
db/db: leptin receptor deficient mice
eIF2α: eukaryotic initiation factor 2 alpha
ER: Endoplasmic reticulum
EZ: Ezetimibe
FAS: fatty acid synthase
FC: free cholesterol
FGF: fibroblast growth factor
FGFR: fibroblast growth factor receptor
FOXO: forkhead box protein O
FPLC: fast protein liquid chromatography
FXR: farnesoid X receptor

G5G8: ABCG5 ABCG8
GRP78: the 78-kD glucose-regulated/binding immunoglobulin protein
HCC: hepatocellular carcinoma
HDL: high-density lipoprotein
HDL-C: high-density lipoprotein cholesterol
HF: high fat
HMG-CoA: 3-hydroxy-3-methylglutary CoA
HMGCR: HMG-CoA reductase
HMGCS: HMG-CoA synthase
HNF4α: hepatocyte nuclear receptor 4α
IBABP: ileal bile acid-binding protein
IDF: International Diabetes Federation
IL-6: interleukin-6
Insig: insulin-induced gene proteins
IPP: isopentenyl pyrophosphate
IRE1: inositol-requiring enzyme 1
IRS: insulin receptor substrate
JNK: c-Jun N-terminal kinase
KO: knockout
LCAT: lecithin-cholesterol acyltransferase
LDL: low-density lipoprotein
LDL-C: low-density lipoprotein cholesterol
LDLR: low-density lipoprotein receptor
LIRKO: liver-specific insulin receptor knockout
LPL: lipoprotein lipase
LRH-1: orphan nuclear receptor liver receptor homolog-1
LRP-1: low-density lipoprotein receptor related protein 1
LXR: liver X receptor
NAFLD: Nonalcoholic fatty liver disease
NASH: Nonalcoholic steatohepatitis
NEFA: nonesterified fatty acid
NF-κB: nuclear factor kappa-light-chain-enhancer of activated B cells
NTCP: sodium sodium (Na^+)-taurocholate cotransporting polypeptide
NPC1L1: Niemann-Pick C1-like 1
MAP: mitogen activated protein
MetS: Metabolic syndrome
PBA: Phenyl butyric acid
PAI-1: plasminogen activator inhibitor-1
PERK: protein kinase RNA-like endoplasmic reticulum kinase
PI3K: phosphatidylinositol 3-kinase
PPARα: peroxisome proliferator-activated receptor alpha
OATP: organic anion transporters
Ob/ob: leptin deficient mice

ObR: leptin receptor
PSF: plant sterol-free
RCT: Reverse cholesterol transport
ROS: reactive oxygen species
SCAP: SREBP cleavage-activating protein
SHP: small heterodimer partner
SR-BI: scavenger receptor class B member 1
SREBP: sterol regulatory element binding protein
STZ: thiazolidinedione
TICE: trans-intestinal cholesterol excretion
TNFα: tumor necrosis factor-alpha
TUDCA: tauroursodeoxycholic acid
UDCA: ursodeoxycholic acid
UPR: unfolded protein response
Urso: ursodiol
VLDL: very low density lipoprotein
WT: wild-type
XBP1: X-box binding protein 1

REFERENCES

1. Qiao, Q., et al., *Metabolic syndrome and cardiovascular disease.* Ann Clin Biochem, 2007. **44**(Pt 3): p. 232-63.
2. Yu, L., et al., *Disruption of Abcg5 and Abcg8 in mice reveals their crucial role in biliary cholesterol secretion.* Proc Natl Acad Sci U S A, 2002. **99**(25): p. 16237-42.
3. Yu, L., et al., *Expression of ABCG5 and ABCG8 is required for regulation of biliary cholesterol secretion.* J Biol Chem, 2005. **280**(10): p. 8742-7.
4. Wittenburg, H. and M.C. Carey, *Biliary cholesterol secretion by the twinned sterol half-transporters ABCG5 and ABCG8.* J Clin Invest, 2002. **110**(5): p. 605-9.
5. Reaven, G.M., *Banting lecture 1988. Role of insulin resistance in human disease.* Diabetes, 1988. **37**(12): p. 1595-607.
6. Desroches, S. and B. Lamarche, *The evolving definitions and increasing prevalence of the metabolic syndrome.* Appl Physiol Nutr Metab, 2007. **32**(1): p. 23-32.
7. Kolovou, G.D., et al., *The prevalence of metabolic syndrome in various populations.* Am J Med Sci, 2007. **333**(6): p. 362-71.
8. Kaur, J., *A Comprehensive Review on Metabolic Syndrome.* Cardiol Res Pract, 2014. **2014**: p. 943162.
9. American Heart, A., et al., *Diagnosis and management of the metabolic syndrome. An American Heart Association/National Heart, Lung, and Blood Institute Scientific Statement. Executive summary.* Cardiol Rev, 2005. **13**(6): p. 322-7.
10. Grundy, S.M., et al., *Clinical management of metabolic syndrome: report of the American Heart Association/National Heart, Lung, and Blood Institute/American Diabetes Association conference on scientific issues related to management.* Circulation, 2004. **109**(4): p. 551-6.
11. Lemieux, I., et al., *Hypertriglyceridemic waist: A marker of the atherogenic metabolic triad (hyperinsulinemia; hyperapolipoprotein B; small, dense LDL) in men?* Circulation, 2000. **102**(2): p. 179-84.
12. Carr, D.B., et al., *Intra-abdominal fat is a major determinant of the National Cholesterol Education Program Adult Treatment Panel III criteria for the metabolic syndrome.* Diabetes, 2004. **53**(8): p. 2087-94.
13. Park, Y.W., et al., *The metabolic syndrome: prevalence and associated risk factor findings in the US population from the Third National Health and Nutrition Examination Survey, 1988-1994.* Arch Intern Med, 2003. **163**(4): p. 427-36.
14. Ferrannini, E., et al., *Hyperinsulinaemia: the key feature of a cardiovascular and metabolic syndrome.* Diabetologia, 1991. **34**(6): p. 416-22.
15. Grundy, S.M., et al., *Definition of metabolic syndrome: Report of the National Heart, Lung, and Blood Institute/American Heart Association conference on scientific issues related to definition.* Circulation, 2004. **109**(3): p. 433-8.

16. Grundy, S.M., *Obesity, metabolic syndrome, and cardiovascular disease.* J Clin Endocrinol Metab, 2004. **89**(6): p. 2595-600.
17. Nakao, Y.M., et al., *Intra-abdominal fat area is a predictor for new onset of individual components of metabolic syndrome: MEtabolic syndRome and abdominaL ObesiTy (MERLOT study).* Proc Jpn Acad Ser B Phys Biol Sci, 2012. **88**(8): p. 454-61.
18. Phillips, L.K. and J.B. Prins, *The link between abdominal obesity and the metabolic syndrome.* Curr Hypertens Rep, 2008. **10**(2): p. 156-64.
19. He, H.B., et al., *[Relationship of different types of abdominal obesity to risk of metabolic syndrome].* Zhonghua Yi Xue Za Zhi, 2008. **88**(18): p. 1251-4.
20. Silva, V., K.R. Stanton, and A.J. Grande, *Harmonizing the diagnosis of metabolic syndrome--focusing on abdominal obesity.* Metab Syndr Relat Disord, 2013. **11**(2): p. 102-8.
21. Despres, J.P. and I. Lemieux, *Abdominal obesity and metabolic syndrome.* Nature, 2006. **444**(7121): p. 881-7.
22. Jensen, M.D., et al., *Influence of body fat distribution on free fatty acid metabolism in obesity.* J Clin Invest, 1989. **83**(4): p. 1168-73.
23. Boden, G., et al., *Effects of acute changes of plasma free fatty acids on intramyocellular fat content and insulin resistance in healthy subjects.* Diabetes, 2001. **50**(7): p. 1612-7.
24. Jensen, M.D., *Is visceral fat involved in the pathogenesis of the metabolic syndrome? Human model.* Obesity (Silver Spring), 2006. **14 Suppl 1**: p. 20S-24S.
25. Bergman, R.N., et al., *Why visceral fat is bad: mechanisms of the metabolic syndrome.* Obesity (Silver Spring), 2006. **14 Suppl 1**: p. 16S-19S.
26. Deslypere, J.P., L. Verdonck, and A. Vermeulen, *Fat tissue: a steroid reservoir and site of steroid metabolism.* J Clin Endocrinol Metab, 1985. **61**(3): p. 564-70.
27. Kershaw, E.E. and J.S. Flier, *Adipose tissue as an endocrine organ.* J Clin Endocrinol Metab, 2004. **89**(6): p. 2548-56.
28. Cote, M., et al., *Adiponectinemia in visceral obesity: impact on glucose tolerance and plasma lipoprotein and lipid levels in men.* J Clin Endocrinol Metab, 2005. **90**(3): p. 1434-9.
29. Ridker, P.M., et al., *C-reactive protein, the metabolic syndrome, and risk of incident cardiovascular events: an 8-year follow-up of 14 719 initially healthy American women.* Circulation, 2003. **107**(3): p. 391-7.
30. Xydakis, A.M., et al., *Adiponectin, inflammation, and the expression of the metabolic syndrome in obese individuals: the impact of rapid weight loss through caloric restriction.* J Clin Endocrinol Metab, 2004. **89**(6): p. 2697-703.
31. Hotamisligil, G.S., et al., *IRS-1-mediated inhibition of insulin receptor tyrosine kinase activity in TNF-alpha- and obesity-induced insulin resistance.* Science, 1996. **271**(5249): p. 665-8.

32. Kern, P.A., et al., *Adiponectin expression from human adipose tissue: relation to obesity, insulin resistance, and tumor necrosis factor-alpha expression.* Diabetes, 2003. **52**(7): p. 1779-85.
33. Hara, T., et al., *Decreased plasma adiponectin levels in young obese males.* J Atheroscler Thromb, 2003. **10**(4): p. 234-8.
34. You, T., et al., *Abdominal adipose tissue cytokine gene expression: relationship to obesity and metabolic risk factors.* Am J Physiol Endocrinol Metab, 2005. **288**(4): p. E741-7.
35. Biddinger, S.B. and C.R. Kahn, *From mice to men: insights into the insulin resistance syndromes.* Annu Rev Physiol, 2006. **68**: p. 123-58.
36. Matsumoto, M., et al., *Dual role of transcription factor FoxO1 in controlling hepatic insulin sensitivity and lipid metabolism.* J Clin Invest, 2006. **116**(9): p. 2464-72.
37. Brown, M.S. and J.L. Goldstein, *Selective versus total insulin resistance: a pathogenic paradox.* Cell Metab, 2008. **7**(2): p. 95-6.
38. Brown, M.S. and J.L. Goldstein, *The SREBP pathway: regulation of cholesterol metabolism by proteolysis of a membrane-bound transcription factor.* Cell, 1997. **89**(3): p. 331-40.
39. Horton, J.D., J.L. Goldstein, and M.S. Brown, *SREBPs: activators of the complete program of cholesterol and fatty acid synthesis in the liver.* J Clin Invest, 2002. **109**(9): p. 1125-31.
40. Shimomura, I., et al., *Decreased IRS-2 and increased SREBP-1c lead to mixed insulin resistance and sensitivity in livers of lipodystrophic and ob/ob mice.* Mol Cell, 2000. **6**(1): p. 77-86.
41. Kahn, B.B. and J.S. Flier, *Obesity and insulin resistance.* J Clin Invest, 2000. **106**(4): p. 473-81.
42. Gallagher, E.J., D. Leroith, and E. Karnieli, *Insulin resistance in obesity as the underlying cause for the metabolic syndrome.* Mt Sinai J Med, 2010. **77**(5): p. 511-23.
43. Pelleymounter, M.A., et al., *Effects of the obese gene product on body weight regulation in ob/ob mice.* Science, 1995. **269**(5223): p. 540-3.
44. Halaas, J.L., et al., *Weight-reducing effects of the plasma protein encoded by the obese gene.* Science, 1995. **269**(5223): p. 543-6.
45. Taylor, S.I., et al., *Mutations in the insulin receptor gene in genetic forms of insulin resistance.* Recent Prog Horm Res, 1990. **46**: p. 185-213; discussion 213-7.
46. Taylor, S.I., et al., *Mutations of the human insulin receptor gene.* Trends Endocrinol Metab, 1990. **1**(3): p. 134-9.
47. Taylor, S.I., et al., *Mutations in insulin-receptor gene in insulin-resistant patients.* Diabetes Care, 1990. **13**(3): p. 257-79.
48. Biddinger, S.B., et al., *Hepatic insulin resistance is sufficient to produce dyslipidemia and susceptibility to atherosclerosis.* Cell Metab, 2008. **7**(2): p. 125-34.

49. Haas, J.T. and S.B. Biddinger, *Dissecting the role of insulin resistance in the metabolic syndrome.* Curr Opin Lipidol, 2009. **20**(3): p. 206-10.
50. Grundy, S.M., et al., *Diagnosis and management of the metabolic syndrome: an American Heart Association/National Heart, Lung, and Blood Institute Scientific Statement.* Circulation, 2005. **112**(17): p. 2735-52.
51. Maruyama, C., K. Imamura, and T. Teramoto, *Assessment of LDL particle size by triglyceride/HDL-cholesterol ratio in non-diabetic, healthy subjects without prominent hyperlipidemia.* J Atheroscler Thromb, 2003. **10**(3): p. 186-91.
52. Solymoss, B.C., et al., *Incidence and clinical characteristics of the metabolic syndrome in patients with coronary artery disease.* Coron Artery Dis, 2003. **14**(3): p. 207-12.
53. Malik, S., et al., *Impact of the metabolic syndrome on mortality from coronary heart disease, cardiovascular disease, and all causes in United States adults.* Circulation, 2004. **110**(10): p. 1245-50.
54. Lakka, H.M., et al., *The metabolic syndrome and total and cardiovascular disease mortality in middle-aged men.* JAMA, 2002. **288**(21): p. 2709-16.
55. Isomaa, B., et al., *Cardiovascular morbidity and mortality associated with the metabolic syndrome.* Diabetes Care, 2001. **24**(4): p. 683-9.
56. Reaven, G., *The metabolic syndrome or the insulin resistance syndrome? Different names, different concepts, and different goals.* Endocrinol Metab Clin North Am, 2004. **33**(2): p. 283-303.
57. Stern, M.P., et al., *Does the metabolic syndrome improve identification of individuals at risk of type 2 diabetes and/or cardiovascular disease?* Diabetes Care, 2004. **27**(11): p. 2676-81.
58. Laaksonen, D.E., et al., *Metabolic syndrome and development of diabetes mellitus: application and validation of recently suggested definitions of the metabolic syndrome in a prospective cohort study.* Am J Epidemiol, 2002. **156**(11): p. 1070-7.
59. Hanson, R.L., et al., *Components of the "metabolic syndrome" and incidence of type 2 diabetes.* Diabetes, 2002. **51**(10): p. 3120-7.
60. Nesto, R.W., *Correlation between cardiovascular disease and diabetes mellitus: current concepts.* Am J Med, 2004. **116 Suppl 5A**: p. 11S-22S.
61. Bjornsson, E., *The clinical aspects of non-alcoholic fatty liver disease.* Minerva Gastroenterol Dietol, 2008. **54**(1): p. 7-18.
62. Choudhury, J. and A.J. Sanyal, *Clinical aspects of fatty liver disease.* Semin Liver Dis, 2004. **24**(4): p. 349-62.
63. Boppidi, H. and S.R. Daram, *Nonalcoholic fatty liver disease: hepatic manifestation of obesity and the metabolic syndrome.* Postgrad Med, 2008. **120**(2): p. E01-7.
64. Kim, C.H. and Z.M. Younossi, *Nonalcoholic fatty liver disease: a manifestation of the metabolic syndrome.* Cleve Clin J Med, 2008. **75**(10): p. 721-8.

65. Grundy, S.M., *Cholesterol gallstones: a fellow traveler with metabolic syndrome?* Am J Clin Nutr, 2004. **80**(1): p. 1-2.
66. Volzke, H., et al., *Hepatic steatosis is associated with an increased risk of carotid atherosclerosis.* World J Gastroenterol, 2005. **11**(12): p. 1848-53.
67. Villanova, N., et al., *Endothelial dysfunction and cardiovascular risk profile in nonalcoholic fatty liver disease.* Hepatology, 2005. **42**(2): p. 473-80.
68. Cohen, J.C., J.D. Horton, and H.H. Hobbs, *Human fatty liver disease: old questions and new insights.* Science, 2011. **332**(6037): p. 1519-23.
69. McCullough, A.J., *Epidemiology of the metabolic syndrome in the USA.* J Dig Dis, 2011. **12**(5): p. 333-40.
70. Review, T., et al., *World Gastroenterology Organisation global guidelines: Nonalcoholic fatty liver disease and nonalcoholic steatohepatitis.* J Clin Gastroenterol, 2014. **48**(6): p. 467-73.
71. Kotronen, A., et al., *Liver fat in the metabolic syndrome.* J Clin Endocrinol Metab, 2007. **92**(9): p. 3490-7.
72. Hamaguchi, M., et al., *The metabolic syndrome as a predictor of nonalcoholic fatty liver disease.* Ann Intern Med, 2005. **143**(10): p. 722-8.
73. Hsiao, P.J., et al., *Significant correlations between severe fatty liver and risk factors for metabolic syndrome.* J Gastroenterol Hepatol, 2007. **22**(12): p. 2118-23.
74. Weiss, R., *Fat distribution and storage: how much, where, and how?* Eur J Endocrinol, 2007. **157 Suppl 1**: p. S39-45.
75. Donnelly, K.L., et al., *Sources of fatty acids stored in liver and secreted via lipoproteins in patients with nonalcoholic fatty liver disease.* J Clin Invest, 2005. **115**(5): p. 1343-51.
76. Sparks, J.D. and C.E. Sparks, *Insulin regulation of triacylglycerol-rich lipoprotein synthesis and secretion.* Biochim Biophys Acta, 1994. **1215**(1-2): p. 9-32.
77. Cummings, M.H., et al., *Acute hyperinsulinemia decreases the hepatic secretion of very-low-density lipoprotein apolipoprotein B-100 in NIDDM.* Diabetes, 1995. **44**(9): p. 1059-65.
78. Day, C.P. and O.F. James, *Steatohepatitis: a tale of two "hits"?* Gastroenterology, 1998. **114**(4): p. 842-5.
79. Ma, X. and Z. Li, *Pathogenesis of nonalcoholic steatohepatitis (NASH).* Chin J Dig Dis, 2006. **7**(1): p. 7-11.
80. Perkins, J.D., *Innate immunity involved in the pathogenesis of nonalcoholic steatohepatitis.* Liver Transpl, 2006. **12**(10): p. 1553-4.
81. Park, S.H., *[Nonalcoholic steatohepatitis: pathogenesis and treatment].* Korean J Hepatol, 2008. **14**(1): p. 12-27.
82. Tsochatzis, E.A., G.V. Papatheodoridis, and A.J. Archimandritis, *Adipokines in nonalcoholic steatohepatitis: from pathogenesis to implications in diagnosis and therapy.* Mediators Inflamm, 2009. **2009**: p. 831670.

83. Neuschwander-Tetri, B.A., *Hepatic lipotoxicity and the pathogenesis of nonalcoholic steatohepatitis: the central role of nontriglyceride fatty acid metabolites.* Hepatology, 2010. **52**(2): p. 774-88.
84. Rolo, A.P., J.S. Teodoro, and C.M. Palmeira, *Role of oxidative stress in the pathogenesis of nonalcoholic steatohepatitis.* Free Radic Biol Med, 2012. **52**(1): p. 59-69.
85. Rinella, M.E., et al., *Dysregulation of the unfolded protein response in db/db mice with diet-induced steatohepatitis.* Hepatology, 2011. **54**(5): p. 1600-9.
86. Puri, P., et al., *Activation and dysregulation of the unfolded protein response in nonalcoholic fatty liver disease.* Gastroenterology, 2008. **134**(2): p. 568-76.
87. Ron, D. and P. Walter, *Signal integration in the endoplasmic reticulum unfolded protein response.* Nat Rev Mol Cell Biol, 2007. **8**(7): p. 519-29.
88. Haze, K., et al., *Identification of the G13 (cAMP-response-element-binding protein-related protein) gene product related to activating transcription factor 6 as a transcriptional activator of the mammalian unfolded protein response.* Biochem J, 2001. **355**(Pt 1): p. 19-28.
89. Harding, H.P., Y. Zhang, and D. Ron, *Protein translation and folding are coupled by an endoplasmic-reticulum-resident kinase.* Nature, 1999. **397**(6716): p. 271-4.
90. Cox, J.S., C.E. Shamu, and P. Walter, *Transcriptional induction of genes encoding endoplasmic reticulum resident proteins requires a transmembrane protein kinase.* Cell, 1993. **73**(6): p. 1197-206.
91. Harding, H.P., et al., *Perk is essential for translational regulation and cell survival during the unfolded protein response.* Mol Cell, 2000. **5**(5): p. 897-904.
92. Harding, H.P., et al., *Regulated translation initiation controls stress-induced gene expression in mammalian cells.* Mol Cell, 2000. **6**(5): p. 1099-108.
93. Calfon, M., et al., *IRE1 couples endoplasmic reticulum load to secretory capacity by processing the XBP-1 mRNA.* Nature, 2002. **415**(6867): p. 92-6.
94. Yoshida, H., et al., *XBP1 mRNA is induced by ATF6 and spliced by IRE1 in response to ER stress to produce a highly active transcription factor.* Cell, 2001. **107**(7): p. 881-91.
95. Yoshida, H., et al., *ATF6 activated by proteolysis binds in the presence of NF-Y (CBF) directly to the cis-acting element responsible for the mammalian unfolded protein response.* Mol Cell Biol, 2000. **20**(18): p. 6755-67.
96. Ozcan, U., et al., *Endoplasmic reticulum stress links obesity, insulin action, and type 2 diabetes.* Science, 2004. **306**(5695): p. 457-61.
97. Rahman, S.M., et al., *CCAAT/enhancing binding protein beta deletion in mice attenuates inflammation, endoplasmic reticulum stress, and lipid accumulation in diet-induced nonalcoholic steatohepatitis.* Hepatology, 2007. **45**(5): p. 1108-17.
98. Yang, L., et al., *Endoplasmic reticulum stress, hepatocyte CD1d and NKT cell abnormalities in murine fatty livers.* Lab Invest, 2007. **87**(9): p. 927-37.

99. Wang, D., Y. Wei, and M.J. Pagliassotti, *Saturated fatty acids promote endoplasmic reticulum stress and liver injury in rats with hepatic steatosis.* Endocrinology, 2006. **147**(2): p. 943-51.
100. Gregor, M.F., et al., *Endoplasmic reticulum stress is reduced in tissues of obese subjects after weight loss.* Diabetes, 2009. **58**(3): p. 693-700.
101. Yamamoto, K., et al., *Induction of liver steatosis and lipid droplet formation in ATF6alpha-knockout mice burdened with pharmacological endoplasmic reticulum stress.* Mol Biol Cell, 2010. **21**(17): p. 2975-86.
102. Zeng, L., et al., *ATF6 modulates SREBP2-mediated lipogenesis.* EMBO J, 2004. **23**(4): p. 950-8.
103. Lee, A.H., et al., *Regulation of hepatic lipogenesis by the transcription factor XBP1.* Science, 2008. **320**(5882): p. 1492-6.
104. Wang, S., et al., *IRE1alpha-XBP1s induces PDI expression to increase MTP activity for hepatic VLDL assembly and lipid homeostasis.* Cell Metab, 2012. **16**(4): p. 473-86.
105. Wang, C., et al., *ATF4 regulates lipid metabolism and thermogenesis.* Cell Res, 2010. **20**(2): p. 174-84.
106. Seo, J., et al., *Atf4 regulates obesity, glucose homeostasis, and energy expenditure.* Diabetes, 2009. **58**(11): p. 2565-73.
107. Bobrovnikova-Marjon, E., et al., *PERK-dependent regulation of lipogenesis during mouse mammary gland development and adipocyte differentiation.* Proc Natl Acad Sci U S A, 2008. **105**(42): p. 16314-9.
108. Oyadomari, S., et al., *Dephosphorylation of translation initiation factor 2alpha enhances glucose tolerance and attenuates hepatosteatosis in mice.* Cell Metab, 2008. **7**(6): p. 520-32.
109. Zhang, W., et al., *ER stress potentiates insulin resistance through PERK-mediated FOXO phosphorylation.* Genes Dev, 2013. **27**(4): p. 441-9.
110. Zhang, X.Q., et al., *Role of endoplasmic reticulum stress in the pathogenesis of nonalcoholic fatty liver disease.* World J Gastroenterol, 2014. **20**(7): p. 1768-76.
111. Ozcan, U., et al., *Chemical chaperones reduce ER stress and restore glucose homeostasis in a mouse model of type 2 diabetes.* Science, 2006. **313**(5790): p. 1137-40.
112. Kammoun, H.L., et al., *GRP78 expression inhibits insulin and ER stress-induced SREBP-1c activation and reduces hepatic steatosis in mice.* J Clin Invest, 2009. **119**(5): p. 1201-15.
113. Puri, P., et al., *A lipidomic analysis of nonalcoholic fatty liver disease.* Hepatology, 2007. **46**(4): p. 1081-90.
114. Caballero, F., et al., *Enhanced free cholesterol, SREBP-2 and StAR expression in human NASH.* J Hepatol, 2009. **50**(4): p. 789-96.
115. Angelin, B., *1994 Mack-Forster Award Lecture. Review. Studies on the regulation of hepatic cholesterol metabolism in humans.* Eur J Clin Invest, 1995. **25**(4): p. 215-24.

116. Havel, R.J., *Receptor and non-receptor mediated uptake of chylomicron remnants by the liver.* Atherosclerosis, 1998. **141 Suppl 1**: p. S1-7.
117. Savard, C., et al., *Synergistic interaction of dietary cholesterol and dietary fat in inducing experimental steatohepatitis.* Hepatology, 2013. **57**(1): p. 81-92.
118. Subramanian, S., et al., *Dietary cholesterol exacerbates hepatic steatosis and inflammation in obese LDL receptor-deficient mice.* J Lipid Res, 2011. **52**(9): p. 1626-35.
119. Espenshade, P.J. and A.L. Hughes, *Regulation of sterol synthesis in eukaryotes.* Annu Rev Genet, 2007. **41**: p. 401-27.
120. Glomset, J.A., *The plasma lecithins:cholesterol acyltransferase reaction.* J Lipid Res, 1968. **9**(2): p. 155-67.
121. Schwarz, M., et al., *Alternate pathways of bile acid synthesis in the cholesterol 7alpha-hydroxylase knockout mouse are not upregulated by either cholesterol or cholestyramine feeding.* J Lipid Res, 2001. **42**(10): p. 1594-603.
122. Bjorkhem, I., et al., *Differences in the regulation of the classical and the alternative pathway for bile acid synthesis in human liver. No coordinate regulation of CYP7A1 and CYP27A1.* J Biol Chem, 2002. **277**(30): p. 26804-7.
123. Javitt, N.B., *Cholesterol, hydroxycholesterols, and bile acids.* Biochem Biophys Res Commun, 2002. **292**(5): p. 1147-53.
124. Van Rooyen, D.M., et al., *Hepatic free cholesterol accumulates in obese, diabetic mice and causes nonalcoholic steatohepatitis.* Gastroenterology, 2011. **141**(4): p. 1393-403, 1403 e1-5.
125. Luong, D.Q., R. Oster, and A.P. Ashraf, *Metformin treatment improves weight and dyslipidemia in children with metabolic syndrome.* J Pediatr Endocrinol Metab, 2015. **28**(5-6): p. 649-55.
126. Ladeiras-Lopes, R., et al., *Novel therapeutic targets of metformin: metabolic syndrome and cardiovascular disease.* Expert Opin Ther Targets, 2015. **19**(7): p. 869-77.
127. Derosa, G., et al., *Thiazolidinedione effects on blood pressure in diabetic patients with metabolic syndrome treated with glimepiride.* Hypertens Res, 2005. **28**(11): p. 917-24.
128. Cabre, A., et al., *Fatty acid binding protein 4 is increased in metabolic syndrome and with thiazolidinedione treatment in diabetic patients.* Atherosclerosis, 2007. **195**(1): p. e150-8.
129. Geurin, M.D. and L. St Anna, *Thiazolidinedione therapy for managing metabolic syndrome.* Am Fam Physician, 2010. **82**(12): p. 1553-4.
130. Mazza, A., et al., *The role of metformin in the management of NAFLD.* Exp Diabetes Res, 2012. **2012**: p. 716404.
131. Hyogo, H., et al., *Efficacy of atorvastatin for the treatment of nonalcoholic steatohepatitis with dyslipidemia.* Metabolism, 2008. **57**(12): p. 1711-8.
132. Athyros, V.G., et al., *Effect of multifactorial treatment on non-alcoholic fatty liver disease in metabolic syndrome: a randomised study.* Curr Med Res Opin, 2006. **22**(5): p. 873-83.

133. Garcia-Calvo, M., et al., *The target of ezetimibe is Niemann-Pick C1-Like 1 (NPC1L1).* Proc Natl Acad Sci U S A, 2005. **102**(23): p. 8132-7.
134. Altmann, S.W., et al., *Niemann-Pick C1 Like 1 protein is critical for intestinal cholesterol absorption.* Science, 2004. **303**(5661): p. 1201-4.
135. Park, H., et al., *Efficacy of long-term ezetimibe therapy in patients with nonalcoholic fatty liver disease.* Journal of Gastroenterology, 2011. **46**(1): p. 101-107.
136. Fukuda, M., et al., *Ezetimibe Ameliorates Cardiovascular Complications and Hepatic Steatosis in Obese and Type 2 Diabetic db/db Mice.* Journal of Pharmacology and Experimental Therapeutics, 2010. **335**(1): p. 70-75.
137. Zheng, S., et al., *Ezetimibe improves high fat and cholesterol diet-induced non-alcoholic fatty liver disease in mice.* Eur J Pharmacol, 2008. **584**(1): p. 118-24.
138. Deushi, M., et al., *Ezetimibe improves liver steatosis and insulin resistance in obese rat model of metabolic syndrome.* FEBS Lett, 2007. **581**(29): p. 5664-70.
139. Yoneda, M., et al., *Efficacy of ezetimibe for the treatment of non-alcoholic steatohepatitis: An open-label, pilot study.* Hepatol Res, 2010. **40**(6): p. 566-73.
140. Chan, D.C., et al., *Effect of Ezetimibe on Hepatic Fat, Inflammatory Markers, and Apolipoprotein B-100 Kinetics in Insulin-Resistant Obese Subjects on a Weight Loss Diet.* Diabetes Care, 2010. **33**(5): p. 1134-1139.
141. Enjoji, M., et al., *NPC1L1 inhibitor ezetimibe is a reliable therapeutic agent for non-obese patients with nonalcoholic fatty liver disease.* Lipids Health Dis, 2010. **9**: p. 29.
142. Wang, H.H., et al., *Effect of ezetimibe on the prevention and dissolution of cholesterol gallstones.* Gastroenterology, 2008. **134**(7): p. 2101-10.
143. Smith, S.C., Jr., *Review of recent clinical trials of lipid lowering in coronary artery disease.* Am J Cardiol, 1997. **80**(8B): p. 10H-13H.
144. Spady, D.K., *Reverse cholesterol transport and atherosclerosis regression.* Circulation, 1999. **100**(6): p. 576-8.
145. Baigent, C., et al., *Efficacy and safety of cholesterol-lowering treatment: prospective meta-analysis of data from 90,056 participants in 14 randomised trials of statins.* Lancet, 2005. **366**(9493): p. 1267-78.
146. Barter, P., et al., *HDL cholesterol, very low levels of LDL cholesterol, and cardiovascular events.* N Engl J Med, 2007. **357**(13): p. 1301-10.
147. Heinecke, J.W., *The not-so-simple HDL story: A new era for quantifying HDL and cardiovascular risk?* Nat Med, 2012. **18**(9): p. 1346-7.
148. Berge, K.E., et al., *Accumulation of dietary cholesterol in sitosterolemia caused by mutations in adjacent ABC transporters.* Science, 2000. **290**(5497): p. 1771-5.
149. Sumi, K., et al., *Cooperative Interaction between Hepatocyte Nuclear Factor 4{alpha} and GATA Transcription Factors Regulates ATP-Binding Cassette Sterol Transporters ABCG5 and ABCG8.* Mol Cell Biol, 2007. **27**(12): p. 4248-60.

150. Freeman, L.A., et al., *The orphan nuclear receptor LRH-1 activates the ABCG5/ABCG8 intergenic promoter.* J Lipid Res, 2004. **45**(7): p. 1197-206.
151. Bonde, Y., et al., *Stimulation of murine biliary cholesterol secretion by thyroid hormone is dependent on a functional ABCG5/G8 complex.* Hepatology, 2012. **56**(5): p. 1828-37.
152. Sabeva, N.S., J. Liu, and G.A. Graf, *The ABCG5 ABCG8 sterol transporter and phytosterols: implications for cardiometabolic disease.* Curr Opin Endocrinol Diabetes Obes, 2009. **16**(2): p. 172-7.
153. Back, S.S., et al., *Cooperative transcriptional activation of ATP-binding cassette sterol transporters ABCG5 and ABCG8 genes by nuclear receptors including Liver-X-Receptor.* BMB Rep, 2013. **46**(6): p. 322-7.
154. Graf, G.A., et al., *ABCG5 and ABCG8 are obligate heterodimers for protein trafficking and biliary cholesterol excretion.* J Biol Chem, 2003. **278**(48): p. 48275-82.
155. Graf, G.A., et al., *Coexpression of ATP-binding cassette proteins ABCG5 and ABCG8 permits their transport to the apical surface.* J Clin Invest, 2002. **110**(5): p. 659-69.
156. Okiyoneda, T., et al., *Calreticulin facilitates the cell surface expression of ABCG5/G8.* Biochem Biophys Res Commun, 2006. **347**(1): p. 67-75.
157. Graf, G.A., J.C. Cohen, and H.H. Hobbs, *Missense mutations in ABCG5 and ABCG8 disrupt heterodimerization and trafficking.* J Biol Chem, 2004. **279**(23): p. 24881-8.
158. Vrins, C., et al., *The sterol transporting heterodimer ABCG5/ABCG8 requires bile salts to mediate cholesterol efflux.* FEBS Lett, 2007. **581**(24): p. 4616-20.
159. Nguyen, T.M., et al., *ACAT2 and ABCG5/G8 are both required for efficient cholesterol absorption in mice: evidence from thoracic lymph duct cannulation.* J Lipid Res, 2012. **53**(8): p. 1598-609.
160. Salen, G., E.H. Ahrens, Jr., and S.M. Grundy, *Metabolism of beta-sitosterol in man.* J Clin Invest, 1970. **49**(5): p. 952-67.
161. Neil, H.A., G.W. Meijer, and L.S. Roe, *Randomised controlled trial of use by hypercholesterolaemic patients of a vegetable oil sterol-enriched fat spread.* Atherosclerosis, 2001. **156**(2): p. 329-37.
162. Volger, O.L., et al., *Dietary vegetable oil and wood derived plant stanol esters reduce atherosclerotic lesion size and severity in apoE*3-Leiden transgenic mice.* Atherosclerosis, 2001. **157**(2): p. 375-81.
163. Whittaker, M.H., *Effects of dietary phytosterols on cholesterol metabolism and atherosclerosis: clinical and experimental evidence.* Am J Med, 2000. **109**(7): p. 600-1.
164. Lutjohann, D., et al., *Sterol absorption and sterol balance in phytosterolemia evaluated by deuterium-labeled sterols: effect of sitostanol treatment.* J Lipid Res, 1995. **36**(8): p. 1763-73.

165. Su, K., et al., *The ABCG5 ABCG8 Sterol Transporter Opposes the Development of Fatty Liver Disease and Loss of Glycemic Control Independently of Phytosterol Accumulation.* J Biol Chem, 2012. **287**(34): p. 28564-75.
166. Sabeva, N.S., E.J. Rouse, and G.A. Graf, *Defects in the leptin axis reduce abundance of the ABCG5-ABCG8 sterol transporter in liver.* J Biol Chem, 2007. **282**(31): p. 22397-405.
167. Su, K., et al., *Acceleration of biliary cholesterol secretion restores glycemic control and alleviates hypertriglyceridemia in obese db/db mice.* Arterioscler Thromb Vasc Biol, 2014. **34**(1): p. 26-33.
168. Basso, F., et al., *Hepatic ABCG5/G8 overexpression reduces apoB-lipoproteins and atherosclerosis when cholesterol absorption is inhibited.* J Lipid Res, 2007. **48**(1): p. 114-26.
169. Wilund, K.R., et al., *High-level expression of ABCG5 and ABCG8 attenuates diet-induced hypercholesterolemia and atherosclerosis in Ldlr-/-mice.* J Lipid Res, 2004. **45**(8): p. 1429-1436.
170. Bouchard, G., et al., *Cholesterol gallstone formation in overweight mice establishes that obesity per se is not linked directly to cholelithiasis risk.* J Lipid Res, 2002. **43**(7): p. 1105-13.
171. Graewin, S.J., et al., *Leptin Regulates Gallbladder Genes Related to Gallstone Pathogenesis in Leptin-Deficient Mice.* Journal of the American College of Surgeons, 2008. **206**(3): p. 503-510.
172. Graewin, S.J., et al., *Leptin-resistant obese mice do not form biliary crystals on a high cholesterol diet.* J Surg Res, 2004. **122**(2): p. 145-9.
173. Tran, K.Q., et al., *Leptin-resistant obese mice have paradoxically low biliary cholesterol saturation.* Surgery, 2003. **134**(2): p. 372-7.
174. Hyogo, H., et al., *Leptin promotes biliary cholesterol elimination during weight loss in ob/ob mice by regulating the enterohepatic circulation of bile salts.* J Biol Chem, 2002. **277**(37): p. 34117-24.
175. Hyogo, H., S. Roy, and D.E. Cohen, *Restoration of gallstone susceptibility by leptin in C57BL/6J ob/ob mice.* J Lipid Res, 2003. **44**(6): p. 1232-40.
176. Goldblatt, M.I., et al., *Decreased gallbladder response in leptin-deficient obese mice.* J Gastrointest Surg, 2002. **6**(3): p. 438-42; discussion 443-4.
177. Ishibashi, S., et al., *Disruption of cholesterol 7alpha-hydroxylase gene in mice. I. Postnatal lethality reversed by bile acid and vitamin supplementation.* J Biol Chem, 1996. **271**(30): p. 18017-23.
178. Schwarz, M., et al., *Disruption of cholesterol 7alpha-hydroxylase gene in mice. II. Bile acid deficiency is overcome by induction of oxysterol 7alpha-hydroxylase.* J Biol Chem, 1996. **271**(30): p. 18024-31.
179. Kalaany, N.Y. and D.J. Mangelsdorf, *LXRS and FXR: the yin and yang of cholesterol and fat metabolism.* Annu Rev Physiol, 2006. **68**: p. 159-91.
180. De Fabiani, E., et al., *The negative effects of bile acids and tumor necrosis factor-alpha on the transcription of cholesterol 7alpha-hydroxylase gene (CYP7A1) converge to hepatic nuclear factor-4: a novel mechanism of feedback regulation of*

bile acid synthesis mediated by nuclear receptors. J Biol Chem, 2001. **276**(33): p. 30708-16.
181. Lu, T.T., et al., *Molecular basis for feedback regulation of bile acid synthesis by nuclear receptors.* Mol Cell, 2000. **6**(3): p. 507-15.
182. Goodwin, B., et al., *A regulatory cascade of the nuclear receptors FXR, SHP-1, and LRH-1 represses bile acid biosynthesis.* Mol Cell, 2000. **6**(3): p. 517-26.
183. Jones, S., *Mini-review: endocrine actions of fibroblast growth factor 19.* Mol Pharm, 2008. **5**(1): p. 42-8.
184. Owen, B.M., D.J. Mangelsdorf, and S.A. Kliewer, *Tissue-specific actions of the metabolic hormones FGF15/19 and FGF21.* Trends Endocrinol Metab, 2015. **26**(1): p. 22-9.
185. Potthoff, M.J., S.A. Kliewer, and D.J. Mangelsdorf, *Endocrine fibroblast growth factors 15/19 and 21: from feast to famine.* Genes Dev, 2012. **26**(4): p. 312-24.
186. Inagaki, T., et al., *Fibroblast growth factor 15 functions as an enterohepatic signal to regulate bile acid homeostasis.* Cell Metab, 2005. **2**(4): p. 217-25.
187. Choi, M., et al., *Identification of a hormonal basis for gallbladder filling.* Nat Med, 2006. **12**(11): p. 1253-5.
188. Yu, C., et al., *Elevated cholesterol metabolism and bile acid synthesis in mice lacking membrane tyrosine kinase receptor FGFR4.* J Biol Chem, 2000. **275**(20): p. 15482-9.
189. Ito, S., et al., *Impaired negative feedback suppression of bile acid synthesis in mice lacking betaKlotho.* J Clin Invest, 2005. **115**(8): p. 2202-8.
190. Yamazaki, Y., et al., *Involvement of a cyclic adenosine monophosphate-dependent signal in the diet-induced canalicular trafficking of adenosine triphosphate-binding cassette transporter g5/g8.* Hepatology, 2015.
191. Kidambi, S. and S.B. Patel, *Sitosterolaemia: pathophysiology, clinical presentation and laboratory diagnosis.* J Clin Pathol, 2008. **61**(5): p. 588-94.
192. Su, K., et al., *Acceleration of biliary cholesterol secretion restores glycemic control and alleviates hypertriglyceridemia in obese, db/db mice.* Arterioscler Thromb Vasc Biol, 2013. **34**(1): p. 26-33.
193. Biddinger, S.B., et al., *Hepatic insulin resistance directly promotes formation of cholesterol gallstones.* Nat Med, 2008. **14**(7): p. 778-82.
194. Rudkowska, I. and P.J. Jones, *Polymorphisms in ABCG5/G8 transporters linked to hypercholesterolemia and gallstone disease.* Nutr Rev, 2008. **66**(6): p. 343-8.
195. Kok, T., et al., *Induction of hepatic ABC transporter expression is part of the PPARalpha-mediated fasting response in the mouse.* Gastroenterology, 2003. **124**(1): p. 160-71.
196. Oude Elferink, R.P., et al., *Uncoupling of biliary phospholipid and cholesterol secretion in mice with reduced expression of mdr2 P-glycoprotein.* J Lipid Res, 1996. **37**(5): p. 1065-75.

197. Dikkers, A., et al., *Scavenger receptor BI and ABCG5/G8 differentially impact biliary sterol secretion and reverse cholesterol transport in mice.* Hepatology, 2013. **58**(1): p. 293-303.
198. Xie, Q., et al., *Effect of tauroursodeoxycholic acid on endoplasmic reticulum stress-induced caspase-12 activation.* Hepatology, 2002. **36**(3): p. 592-601.
199. Benz, C., et al., *Effect of tauroursodeoxycholic acid on bile-acid-induced apoptosis and cytolysis in rat hepatocytes.* J Hepatol, 1998. **28**(1): p. 99-106.
200. Benz, C., et al., *Effect of tauroursodeoxycholic acid on bile acid-induced apoptosis in primary human hepatocytes.* Eur J Clin Invest, 2000. **30**(3): p. 203-9.
201. Cohen, P., et al., *Selective deletion of leptin receptor in neurons leads to obesity.* J Clin Invest, 2001. **108**(8): p. 1113-21.
202. Takanabe, R., et al., *Up-regulated expression of microRNA-143 in association with obesity in adipose tissue of mice fed high-fat diet.* Biochem Biophys Res Commun, 2008. **376**(4): p. 728-32.
203. Gao, X., et al., *Vagus nerve contributes to the development of steatohepatitis and obesity in phosphatidylethanolamine N-methyltransferase deficient mice.* J Hepatol, 2014.
204. Lautenbach, A., et al., *Human obesity reduces the number of hepatic leptin receptor (ob-R) expressing NK cells.* Endocr Res, 2011. **36**(4): p. 158-66.
205. Koch, L., et al., *Central insulin action regulates peripheral glucose and fat metabolism in mice.* J Clin Invest, 2008. **118**(6): p. 2132-47.
206. Kozarsky, K.F., et al., *Overexpression of the HDL receptor SR-BI alters plasma HDL and bile cholesterol levels.* Nature, 1997. **387**(6631): p. 414-7.
207. Wiersma, H., et al., *Hepatic SR-BI, not endothelial lipase, expression determines biliary cholesterol secretion in mice.* J Lipid Res, 2009. **50**(8): p. 1571-80.
208. Banni, S., et al., *Vagus nerve stimulation reduces body weight and fat mass in rats.* PLoS One, 2012. **7**(9): p. e44813.
209. German, J., et al., *Hypothalamic leptin signaling regulates hepatic insulin sensitivity via a neurocircuit involving the vagus nerve.* Endocrinology, 2009. **150**(10): p. 4502-11.
210. Li, X., et al., *Intracerebroventricular leptin infusion improves glucose homeostasis in lean type 2 diabetic MKR mice via hepatic vagal and non-vagal mechanisms.* PLoS One, 2011. **6**(2): p. e17058.
211. Li, Y., et al., *Hepatic overexpression of SIRT1 in mice attenuates endoplasmic reticulum stress and insulin resistance in the liver.* The FASEB Journal, 2011. **25**(5): p. 1664-1679.
212. Escolà-Gil, J.C., et al., *The Cholesterol Content of Western Diets Plays a Major Role in the Paradoxical Increase in High-Density Lipoprotein Cholesterol and Upregulates the Macrophage Reverse Cholesterol Transport Pathway.* Arteriosclerosis, Thrombosis, and Vascular Biology, 2011. **31**(11): p. 2493-2499.

213. Gustavsson, C., et al., *Cocoa butter and safflower oil elicit different effects on hepatic gene expression and lipid metabolism in rats.* Lipids, 2009. **44**(11): p. 1011-27.
214. Hager, L., et al., *Lecithin:cholesterol acyltransferase deficiency protects against cholesterol-induced hepatic endoplasmic reticulum stress in mice.* J Biol Chem, 2012. **287**(24): p. 20755-68.
215. Feng, B., et al., *The endoplasmic reticulum is the site of cholesterol-induced cytotoxicity in macrophages.* Nat Cell Biol, 2003. **5**(9): p. 781-92.
216. Rohrl, C., et al., *Endoplasmic reticulum stress impairs cholesterol efflux and synthesis in hepatic cells.* J Lipid Res, 2014. **55**(1): p. 94-103.
217. Davis, H.R., Jr., et al., *Niemann-Pick C1 Like 1 (NPC1L1) is the intestinal phytosterol and cholesterol transporter and a key modulator of whole-body cholesterol homeostasis.* J Biol Chem, 2004. **279**(32): p. 33586-92.
218. Tsuchida, T., et al., *Ursodeoxycholic acid improves insulin sensitivity and hepatic steatosis by inducing the excretion of hepatic lipids in high-fat diet-fed KK-Ay mice.* Metabolism, 2012. **61**(7): p. 944-53.
219. Rayner, K.J., et al., *Inhibition of miR-33a/b in non-human primates raises plasma HDL and lowers VLDL triglycerides.* Nature, 2011. **478**(7369): p. 404-7.
220. Yu, L., et al., *Ezetimibe normalizes metabolic defects in mice lacking ABCG5 and ABCG8.* J Lipid Res, 2005. **46**(8): p. 1739-44.
221. Cliffe, L.J., et al., *Accelerated intestinal epithelial cell turnover: a new mechanism of parasite expulsion.* Science, 2005. **308**(5727): p. 1463-5.
222. Talalay, P., *Enzymic analysis of steroid hormones.* Methods Biochem Anal, 1960. **8**: p. 119-43.
223. Wang, J., et al., *Relative Roles of ABCG5/ABCG8 in Liver and Intestine.* J Lipid Res, 2014.
224. McDonald, J.G., et al., *A comprehensive method for extraction and quantitative analysis of sterols and secosteroids from human plasma.* J Lipid Res, 2012. **53**(7): p. 1399-409.
225. Honda, A., et al., *Highly sensitive and specific analysis of sterol profiles in biological samples by HPLC-ESI-MS/MS.* J Steroid Biochem Mol Biol, 2010. **121**(3-5): p. 556-64.
226. Kempen, H.J., et al., *Serum lathosterol concentration is an indicator of whole-body cholesterol synthesis in humans.* J Lipid Res, 1988. **29**(9): p. 1149-55.
227. van der Veen, J.N., et al., *Activation of the liver X receptor stimulates trans-intestinal excretion of plasma cholesterol.* J Biol Chem, 2009. **284**(29): p. 19211-9.
228. Brunham, L.R., et al., *Intestinal ABCA1 directly contributes to HDL biogenesis in vivo.* J Clin Invest, 2006. **116**(4): p. 1052-62.
229. Ohashi, R., et al., *Reverse cholesterol transport and cholesterol efflux in atherosclerosis.* QJM, 2005. **98**(12): p. 845-56.
230. Amaral, J.D., et al., *Bile acids: regulation of apoptosis by ursodeoxycholic acid.* J Lipid Res, 2009. **50**(9): p. 1721-34.

231. Angulo, P., *Use of ursodeoxycholic acid in patients with liver disease.* Curr Gastroenterol Rep, 2002. **4**(1): p. 37-44.
232. Lindor, K.D., et al., *Ursodeoxycholic acid for treatment of nonalcoholic steatohepatitis: results of a randomized trial.* Hepatology, 2004. **39**(3): p. 770-8.
233. Dufour, J.F., et al., *Randomized placebo-controlled trial of ursodeoxycholic acid with vitamin E in nonalcoholic steatohepatitis.* Clinical Gastroenterology and Hepatology, 2006. **4**(12): p. 1537-1543.
234. Ratziu, V., et al., *A randomized controlled trial of high-dose ursodesoxycholic acid for nonalcoholic steatohepatitis.* J Hepatol, 2011. **54**(5): p. 1011-9.
235. Adams, L.A., et al., *A pilot trial of high-dose ursodeoxycholic acid in nonalcoholic steatohepatitis.* Hepatol Int, 2010. **4**(3): p. 628-33.
236. Yoneda, M., et al., *Efficacy of ezetimibe for the treatment of non-alcoholic steatohepatitis: An open-label, pilot study.* Hepatology Research, 2010. **40**(6): p. 566-573.
237. Kir, S., et al., *FGF19 as a postprandial, insulin-independent activator of hepatic protein and glycogen synthesis.* Science, 2011. **331**(6024): p. 1621-4.
238. Beuers, U., *beta1 integrin is a long-sought sensor for tauroursodeoxycholic acid.* Hepatology, 2013. **57**(3): p. 867-9.
239. Gohlke, H., et al., *alpha5 beta1-integrins are sensors for tauroursodeoxycholic acid in hepatocytes.* Hepatology, 2013. **57**(3): p. 1117-29.
240. Tomlinson, E., et al., *Transgenic mice expressing human fibroblast growth factor-19 display increased metabolic rate and decreased adiposity.* Endocrinology, 2002. **143**(5): p. 1741-7.
241. Fu, L., et al., *Fibroblast growth factor 19 increases metabolic rate and reverses dietary and leptin-deficient diabetes.* Endocrinology, 2004. **145**(6): p. 2594-603.
242. Shin, D.J. and T.F. Osborne, *FGF15/FGFR4 integrates growth factor signaling with hepatic bile acid metabolism and insulin action.* J Biol Chem, 2009. **284**(17): p. 11110-20.
243. Holt, J.A., et al., *Definition of a novel growth factor-dependent signal cascade for the suppression of bile acid biosynthesis.* Genes Dev, 2003. **17**(13): p. 1581-91.
244. Wang, Y., et al., *The combination of ezetimibe and ursodiol promotes fecal sterol excretion and reveals a G5G8-independent pathway for cholesterol elimination.* J Lipid Res, 2015. **56**(4): p. 810-20.
245. Lew, J.L., et al., *The farnesoid X receptor controls gene expression in a ligand- and promoter-selective fashion.* J Biol Chem, 2004. **279**(10): p. 8856-61.
246. Campana, G., et al., *Regulation of ileal bile acid-binding protein expression in Caco-2 cells by ursodeoxycholic acid: role of the farnesoid X receptor.* Biochem Pharmacol, 2005. **69**(12): p. 1755-63.
247. Rao, A., et al., *The organic solute transporter alpha-beta, Ostalpha-Ostbeta, is essential for intestinal bile acid transport and homeostasis.* Proc Natl Acad Sci U S A, 2008. **105**(10): p. 3891-6.

248. Dawson, P.A., et al., *Targeted deletion of the ileal bile acid transporter eliminates enterohepatic cycling of bile acids in mice.* J Biol Chem, 2003. **278**(36): p. 33920-7.
249. Liu, J., et al., *The absence of ABCD2 reveals a novel role for peroxisomes in metabolic responses to dietary lipids.* J. Lipid Research, 2012. **53**(6): p. 1071-1079.
250. Miao, J., et al., *Bile acid signaling pathways increase stability of Small Heterodimer Partner (SHP) by inhibiting ubiquitin-proteasomal degradation.* Genes Dev, 2009. **23**(8): p. 986-96.
251. Wang, L., et al., *Redundant pathways for negative feedback regulation of bile acid production.* Dev Cell, 2002. **2**(6): p. 721-31.
252. Kerr, T.A., et al., *Loss of nuclear receptor SHP impairs but does not eliminate negative feedback regulation of bile acid synthesis.* Dev Cell, 2002. **2**(6): p. 713-20.
253. Potthoff, M.J., et al., *FGF15/19 regulates hepatic glucose metabolism by inhibiting the CREB-PGC-1alpha pathway.* Cell Metab, 2011. **13**(6): p. 729-38.
254. Bhatnagar, S., H.A. Damron, and F.B. Hillgartner, *Fibroblast growth factor-19, a novel factor that inhibits hepatic fatty acid synthesis.* J Biol Chem, 2009. **284**(15): p. 10023-33.
255. Watanabe, M., et al., *Bile acids lower triglyceride levels via a pathway involving FXR, SHP, and SREBP-1c.* J Clin Invest, 2004. **113**(10): p. 1408-18.
256. Ho, H.K., et al., *Fibroblast growth factor receptor 4 regulates proliferation, anti-apoptosis and alpha-fetoprotein secretion during hepatocellular carcinoma progression and represents a potential target for therapeutic intervention.* J Hepatol, 2009. **50**(1): p. 118-27.
257. Nicholes, K., et al., *A mouse model of hepatocellular carcinoma: ectopic expression of fibroblast growth factor 19 in skeletal muscle of transgenic mice.* Am J Pathol, 2002. **160**(6): p. 2295-307.
258. Luo, J., et al., *A nontumorigenic variant of FGF19 treats cholestatic liver diseases.* Sci Transl Med, 2014. **6**(247): p. 247ra100.
259. Zhou, M., et al., *Separating Tumorigenicity from Bile Acid Regulatory Activity for Endocrine Hormone FGF19.* Cancer Res, 2014. **74**(12): p. 3306-16.

VITA

PERSONAL INFORMATION

Name: Yuhuan Wang

P.O.B: Yantai, P.R.C

EDUCATION:

2010-2015 PhD, Department of Pharmaceutical Sciences, University of Kentucky

2005-2009 BS in Pharmaceutics, China Pharmaceutical University

PUBLICATIONS:

1. Wang Y, Su K, Sabeva NS, Ji A, van der Westhuyzen DR, Foufelle F, Gao X, Graf GA. GRP78 rescues the ABCG5 ABCG8 sterol transporter in db/db mice (In press; Metabolism).
2. Wang Y, Liu X, Pijut SS, Li J, Horn J, Bradford EM, Leggas M, Barrett TA, Graf GA. The combination of ezetimibe and ursodiol promotes fecal sterol excretion and reveals a G5G8-independent pathway for cholesterol elimination. J Lipid Res. 2015 Apr; 56(4):810-20.
3. Pijut SS, Corbett DE, Wang Y, Li J, Graf GA. Effect of peripheral circadian dysfunction on metabolic disease in respones to a diabetogenic diet (Under review at Am J Physiol Endocrinol Metab).
4. Su K, Sabeva NS, Wang Y, Liu,X, Lester JD, Liu J, Liang S, Graf GA. Acceleration of biliary cholesterol secretion restores glycemic control and alleviates hypertriglyceridemia in obese db/db mice. Arterioscler Thromb

Vasc Biol. 2014 Jan; 34 (1): 26-33.

5. Salous AK, Panchatcharam M, Sunkara M, Mueller P, Dong A, Wang Y, Graf GA, Smyth SS, Morris AJ. Mechanism of rapid elimination of lysophosphatidic acid and related lipids from the circulation of mice. J Lipid Res. 2013 Oct; 54(10): 2775-84.
6. Su K, Sabeva NS, Liu J, Wang Y, Bhatnagar S, van der Westhuyzen DR, Graf GA. The ABCG5 ABCG8 sterol transporter opposes the development of fatty liver disease and loss of glycemic control independent of phytosterol accumulation. J Biol Chem. 2012 Aug 17; 287(34): 28564-75.
7. Yang L, Qian Z, Ji H, Yang R, Wang Y, Xi L, Sheng L, Zhao B, Zhang X. Inhibitory effect on protein kinase Ctheta by Crocetin attenuates palmitate-induced insulin insensitivity in 3T3-L1 adipocytes. Eur J Pharmacol. 2010 Sep 10; 642(1-3): 47-55.

HONORS AND AWARDS:

1. Research publication highlight recognized by UK College of Pharmacy "The combination of ezetimibe and ursodiol promotes fecal sterol excretion and reveals a G5G8-independent pathway for cholesterol elimination." (2015)
2. Research highlighted as journal news by ASBMB Today. "Two drugs are better than one- A two-pronged approach to increasing cholesterol elimination." (2015)
3. First place in the poster presentation competition at the 2014 Drug Discovery & Development Symposium. (2014)
4. Outstanding poster presentation award at The 23nd South East Lipid Research Conference. (2014)
5. Third place in poster presentation competition at UK College of Pharmacy Rho Chi Research Day. (2014)

6. Research publication highlight recognized by UK College of Pharmacy "Acceleration of biliary cholesterol secretion restores glycemic control and alleviates hypertriglyceridemia in obese db/db mice." Kai Su, Nadezhda S. Sabeva, Yuhuan Wang, Xiaoxi Liu, Joshua D. Lester, Jingjing Liu, Shuang Liang, Gregory A. Graf. Arterioscler Thromb Vasc Biol. 2014 Jan; 34(1):26-33. doi: 10.1161. (2014)
7. First place in the poster presentation competition at Barnstable Brown Obesity and Diabetes Research. (2012)

ORAL/POSTER PRESENTATIONS:

1. GRP78 rescues the ABCG5 ABCG8 sterol transporter in db/db mice. (Poster presentation at the Arteriosclerosis, Thrombosis and Vascular Biology/Peripheral Vascular Disease 2015 Scientific Sessions, San Francisco, CA, USA, 2015)
2. The Combination of Ezetimibe and Ursodiol Promotes Fecal Sterol Excretion and Reveals a G5G8-independent Pathway for Cholesterol Elimination. (Oral presentation at the 17th Annual Gill Heart Institue Cardiovascular Research Day, Lexington, KY, USA, 2014).
3. The combination of ezetimibe and ursodiol cooperatively promotes fecal sterol excretion and reveals a G5G8-independent pathway for cholesterol elimination. (Poster presentation at the 23nd South East Lipid Research Conference, Callaway Gardens, Pine Mountain, Georgia, USA, 2014)
4. The combination of ezetimibe and ursodiol cooperatively promotes fecal sterol excretion and reveals a G5G8-independent pathway for cholesterol elimination. (Poster presentation at Gordon Research Conference on Lipoprotein Metabolism, Waterville Valley Resort, NH, USA, 2014)
5. An Urso-EZ combination therapy that simultaneously increases biliary

secretion and reduces cholesterol absorption actively promotes cholesterol elimination in mice. (Poster presentation at Rho Chi Research Day, Lexington, KY, USA, 2014)

6. Alleviation of endoplasmic reticulum (ER) stress rescues the ABCG5 ABCG8 cholesterol transporters in obese, insulin resistant db/db mice. (Poster presentation at Barnstable Brown Obesity and Diabetes Research Day, Lexington, KY, USA; ASBMB Special Symposium Frontiers in Lipid Biology, Banff Alberta, Canada, 2012)